



Universitetet
i Stavanger

Faculty of Science and Technology

MASTER THESIS

Study program/ Specialization: M.Sc., Petroleum Technology - Drilling	Spring semester, 2018 Restricted
Author: Andreas Holme (Author's signature)
Faculty supervisor: Helge Hodne Equinor supervisor: Janne Synnøve Vølstad	
Title of thesis: <i>“Design of Johan Sverdrup water injectors – unlocking the 9 5/8” liner cement job”</i> Tittel på oppgaven: <i>“Design av Johan Sverdrup vanninjektorer – avdekke sementjobben på 9 5/8” liner”</i>	
Credits (ECTS): 30	
Key words: - Injection - Drilling 12 ¼” - Running Liner - Cementing - Image log	Pages: 133 + Attachments: 6 Stavanger, 14.06.2018

Abstract

For the injection wells on Johan Sverdrup, cementing operations concerning the 9 5/8" liners are extraordinarily critical. Complications like equipment malfunction, losses, and lost rotation, both during circulation and displacement, have caused several time-consuming unplanned operations. Consequently, adding incident-related expenditures, which could have been avoided.

The objective of this thesis is to shed light on the underlying causes threatening the achievement of a good, isolating cement behind the liner. In order to accomplish such a task, historical data from all the injection wells have been analyzed in an attempt to uncover the root causes. During this investigation, data from image logs, real-time logs and drilling parameters have been studied. As a result, it became evident that considerable alterations in rock composition between the templates were present. Consequently, the different formations had to be investigated separately, while comparison between the templates should only be performed with great care.

Firstly, an investigation of the cement height at lost rotation was carried out. Interesting results were obtained, which strongly implies the necessity for rotation during cementing. In addition, good cement was identified with astonishingly low displacement rates while performing rotation. Furthermore, successful alterations were implemented in order to improve cement bonding in high-permeable reservoir zone.

Secondly, the results acquired from the cementing operations suggested that an investigation of the drilling phase was required. Irregular borehole geometry and unstable formations causing over-gauged hole sections during drilling was uncovered in the previously determined intervals of interest from the cement operations. Additionally, it is believed that several of these undesirable hole geometries could have been avoided through optimized operational practice.

Also, liner runs through the problematic formations were investigated, in addition to the occasional wiper trip. Here, major obstruction was seen for many of the wells, however, the location of the restrictions varied for the different templates.

Finally, mitigating actions were proposed for each of the abovementioned phases. Namely, drilling, liner running and cementing. The actions incorporated learnings from the previous injection wells, implementation of new tools and technology, in addition to operational improvements.

Preface

First, I wish to express our forthright appreciation to the professionals in Johan Sverdrup's planning department, where I have been provided valuable guidance throughout the entire period of writing this thesis. During the months I spent at Equinor, I was always met by helpful and encouraging employees.

I would also like to thank Equinor as an organization for the great opportunity to work with such an exciting topic. Gaining valuable insight through working with one of history's largest discoveries on the Norwegian Continental Shelf.

Furthermore, I would like to express gratitude towards my supervisors at Equinor, namely Janne Synnøve Vølstad and Joar Grimsrud, in addition to my university supervisor, Helge Hodne. During the writing of this thesis I have been in contact with several professionals originating from various disciplines and companies. Within Equinor, I would especially like to thank Brice Fortier for his guidance on image logs, Liv Omdal for sharing her knowledge on injection well barriers, and finally Kristi Elin Larsen, Sumit Neogi and Brit Selvikvåg for giving me valuable insight in the geology of Johan Sverdrup.

Fortunately, I was also given the opportunity to travel offshore during the drilling of G-2. This was an unforgettable and exceptionally educative experience. In that regard, I would like to thank drilling engineer Olav Helgeland for sharing his knowledge and showing me around the rig.

This thesis concludes my five-year educational journey at the University of Stavanger. I would like to thank lecturers and fellow students for contributing to an exciting and highly educational chapter of my life.

Table of Contents

ABSTRACT	III
PREFACE.....	V
TABLE OF CONTENTS	VII
LIST OF FIGURES	IX
LIST OF TABLES.....	XIII
1 INTRODUCTION.....	1
2 THE JOHAN SVERDRUP FIELD	3
2.1 INTRODUCTION.....	3
2.2 FIELD DESCRIPTION.....	4
2.3 FIELD DEVELOPMENT	4
2.4 GEOLOGY	6
2.4.1 <i>General geology</i>	6
2.4.2 <i>Injection well geology</i>	7
3 THEORY.....	13
3.1 PRIMARY CEMENTING.....	13
3.2 CEMENTING FLUIDS.....	14
3.2.1 <i>Low viscous mud</i>	14
3.2.2 <i>Spacer</i>	14
3.2.3 <i>Cement</i>	15
3.3 PARAMETERS AFFECTING CEMENT PLACEMENT	17
3.3.1 <i>Mud conditioning</i>	17
3.3.2 <i>Mud removal</i>	18
3.3.3 <i>Eccentricity</i>	19
3.3.4 <i>Casing movement</i>	21
3.3.5 <i>Displacement rate</i>	24
3.4 DRILLING.....	25
3.4.1 <i>Bottom hole pressure (BHP)</i>	25
3.4.2 <i>Well inclination, Azimuth and Dogleg Severity (DLS)</i>	27
3.4.3 <i>Vibrations</i>	28
3.4.4 <i>BHA composition</i>	29
3.4.5 <i>Drilling parameters and hole quality</i>	30
3.4.6 <i>Hole cleaning</i>	31

3.4.7	<i>Drillbit</i>	32
3.5	LINER	33
3.6	LOGGING.....	35
3.6.1	<i>Caliper log</i>	35
3.6.2	<i>Image log</i>	35
3.6.3	<i>Gamma Ray log</i>	36
3.6.4	<i>Density-Neutron log</i>	37
4	INJECTION WELLS	39
4.1	JOHAN SVERDRUP INJECTION WELLS	40
4.2	REGULATIONS	42
4.3	BARRIERS	44
5	RESULTS	49
5.1	CEMENTING.....	49
5.1.1	<i>Introduction</i>	49
5.1.2	<i>Results</i>	50
5.2	DRILLING.....	55
5.2.1	<i>Introduction</i>	55
5.2.2	<i>Results</i>	58
5.3	WIPER TRIP	93
5.4	RUNNING LINER	95
5.4.1	<i>Introduction</i>	95
5.4.2	<i>Results</i>	97
6	SUMMARY AND DISCUSSION	105
6.1	CEMENT.....	105
6.2	DRILLING.....	106
6.3	RUNNING LINER.....	108
6.4	PROPOSED SOLUTIONS	110
7	CONCLUSION.....	113
	REFERENCES	115
	ABBREVIATIONS.....	119
	APPENDIX A – EQUINOR’S INTERNAL GUIDELINES.....	121

List of Figures

FIGURE 1: MAP SHOWING THE LOCATIONS OF ALDOUS AND AVALDSNES. [1]	3
FIGURE 2: MAP OVER JOHAN SVERDRUP CONTAINING THE DIFFERENT GEOLOGICAL AREAS. [8]	5
FIGURE 3: REMAINING OIL RESERVES ON THE NCS AS OF JUNE 2018 [9]	6
FIGURE 4: CROSS-SECTION NW TO SE OF JOHAN SVERDRUP FIELD. STRATIGRAPHIC GROUPS ARE OUTLINED. [8].....	7
FIGURE 5: CORE PHOTO OF LOWER AASGARD FM. A HARD LIMESTONE STRINGER (A) AND LIME-RICH MARL (B) ARE PRESENT.	9
FIGURE 6: CORE PHOTO OF DRAUPNE FM. 2 SHALE (A), OMISSION ZONE (B) AND DRAUPNE FM. 1 (C).....	11
FIGURE 7: ILLUSTRATION OF THE POSITIONS OF LEAD AND TAIL CEMENT IN THE ANNULAR SPACE. [20]	17
FIGURE 8: DIFFERENT RHEOLOGICAL MODELS. PRESENTED WITH SHEAR STRESS VS. SHEAR RATE. HERSHEY-BULKLEY FLUIDS EXHIBIT BOTH YIELD STRESS AND NON-LINEAR RELATIONSHIP BETWEEN SHEAR STRESS AND SHEAR RATE. [15]	20
FIGURE 9: VELOCITY PROFILE AS A FUNCTION OF ECCENTRICITY [22]	21
FIGURE 10: ILLUSTRATIONS OF WHIRLING MOTIONS AND LATERAL MOVEMENT DURING RECIPROICATION. [15]	22
FIGURE 11: ANNULAR FLOW PATTERNS CAUSED BY SECONDARY MOVEMENTS FROM ROTATION. [15].....	22
FIGURE 12: 3D SIMULATION OF CEMENT DISPLACEMENT IN ANNULUS WITH 70% ECCENTRICITY AND 20 RPM. THE FIGURE SHOWS A FAIRLY CONTINUOUS DISPLACEMENT INTERFACE. [30].....	23
FIGURE 13: STRESSES-DIRECTION OF THE STRESSES ACTING ON THE BOREHOLE WALL. [35].....	26
FIGURE 14: SKETCH ILLUSTRATING BREAKOUT AND DRILLING- INDUCED FRACTURE. [38]	27
FIGURE 15: EFFECTIVE BOREHOLE DIAMETER (RED DASHED CIRCLE) ILLUSTRATED FOR A HOLE CONTAINING SPIRAL GEOMETRY OVER A GIVEN LENGTH. THE DASHED GREY CIRCLES INDICATE THE OFF-CENTER POSITIONS OF THE BIT DUE TO LATERAL VIBRATIONS DURING A DRILLED INTERVAL. THE BLACK SOLID LINE ILLUSTRATES THE IN-GAUGE DIAMETER/BIT DIAMETER.	28
FIGURE 16: SCHEMATIC OF STANDARD LINER EQUIPMENT NEEDED TO RUN AND CEMENT THE LINER. [48]	34
FIGURE 17: ILLUSTRATING THE MEASUREMENTS 360 DEGREES AROUND THE BOREHOLE, WHERE THE TOP SIDE IS SITUATED AT 0° AND 360°, WHILE THE LOW SIDE IS SITUATED AT THE CENTER, NAMELY 180°. THE 2D-IMAGE (RIGHT) COULD BE WRAPPED INTO A 3D IMAGE OF THE WELLBORE (LEFT). [52].....	36
FIGURE 18: PRODUCTION WELLS, INJECTION WELLS AND TOTAL WELLS REPORTED WITH INTEGRITY FAILURE, ISSUE OR UNCERTAINTY IN THIS SURVEY. [35]	39
FIGURE 19: MAP SHOWING THE LOCATION OF THE JOHAN SVERDRUP INJECTION WELLS, AND THEIR RESPECTIVE TEMPLATES (BLACK TRIANGLES).	40
FIGURE 20: WATER INJECTOR DESIGN ON JOHAN SVERDRUP	41
FIGURE 21: WELL BARRIER SCHEMATIC OF AN INJECTION/DISPOSAL WELL WITH INJECTION PRESSURES ABOVE MINIMUM IN-SITU STRESS (MINIMUM HORIZONTAL STRESS, Σ_{MIN}).	43
FIGURE 22: WELL BARRIER SCHEMATIC OF THE BARRIER IN PLACE TOWARDS INJECTION PRESSURE, WHERE THE PRESSURE IS ABOVE MINIMUM HORIZONTAL STRESS OF THE CAP ROCK. EXAMPLE FROM G-3.....	45
FIGURE 23: WELL BARRIER SCHEMATIC OF THE BARRIERS IN PLACE TOWARDS RESERVOIR PRESSURE, WHERE THE PRESSURE IS BELOW MINIMUM HORIZONTAL STRESS OF THE CAP ROCK. EXAMPLE FROM F-14.	46
FIGURE 24: WELL BARRIER SCHEMATIC OF THE BARRIERS IN PLACE TOWARDS INJECTION PRESSURE, WHERE THE PRESSURE IS BELOW MINIMUM HORIZONTAL STRESS OF THE CAP ROCK. THIS IS AN EXAMPLE OF AN INJECTION WELL WHERE THE PRODUCTION PACKER IS PLACED ABOVE THE RESERVOIR, I.E. NOT A DEEP SET PACKER. EXAMPLE FROM G-2.	47

FIGURE 25: WELL BARRIER SCHEMATIC OF THE BARRIERS IN PLACE TOWARDS RESERVOIR PRESSURE, WHERE THE PRESSURE IS BELOW MINIMUM HORIZONTAL STRESS OF THE CAP ROCK. THIS IS AN EXAMPLE OF AN INJECTION WELL WHERE THE PRODUCTION PACKER IS PLACED ABOVE THE RESERVOIR, I.E. NOT A DEEP-SET PACKER. EXAMPLE FROM G-2.....	47
FIGURE 26: THEORETICAL TOP OF CEMENT AT LOST ROTATION VERSUS THE TOP OF CONTINUOUS CEMENT FROM THE LOGS.....	53
FIGURE 27: DIFFERENCE BETWEEN THE TOP OF CONTINUOUS GOOD CEMENT ON THE LOGS AND THE THEORETICAL TOP OF CEMENT AT LOST ROTATION.	54
FIGURE 28: GOOD, ISOLATING CEMENT ABOVE AND BELOW TOP RESERVOIR (TOP DRAUPNE FM. 2).....	54
FIGURE 29: REAL-TIME LOG FOR E-1. ILLUSTRATING HOW THE DIFFERENT MAXIMUM AND MINIMUM VALUES WERE OBTAINED.	55
FIGURE 30: INCLINATION AT TD FOR THE 12 1/4" SECTION OF THE JOHAN SVERDRUP INJECTOR WELLS.....	56
FIGURE 31: LENGTH OF THE 12 1/4" SECTIONS ON THE JOHAN SVERDRUP INJECTORS. LENGTHS ARE GIVEN IN MEASURED DEPTH. ..	57
FIGURE 32: DRILLED LENGTH OF SOLA FOR THE DIFFERENT WELLS ON JOHAN SVERDRUP. LENGTH OF SOLA FOR THE E-WELLS SHOWN INSIDE CIRCLE.....	58
FIGURE 33: REAL-TIME CALIPER LOGS FOR F-14 (LEFT) AND G-4 T2 (RIGHT). SOLA FM. IS SITUATED WITHIN THE DASHED LINES. THE LEFT AXES ARE GIVEN IN METERS.	59
FIGURE 34: MAXIMUM AND MINIMUM ROP FOR THE DIFFERENT INJECTION WELLS WHEN DRILLING SOLA FM.	59
FIGURE 35: MAXIMUM AND MINIMUM WOB FOR THE DIFFERENT INJECTION WELLS WHILE DRILLING SOLA FM.....	60
FIGURE 36: MAXIMUM AND MINIMUM FLOW RATE FOR THE DIFFERENT INJECTION WELLS WHEN DRILLING SOLA FM.	60
FIGURE 37: MAXIMUM AND MINIMUM ROTATION FOR THE INJECTION WELLS WHEN DRILLING SOLA FM. THE BLUE LINE SHOWS THE LINEAR TREND FOR THE RPM MIN VALUES.	61
FIGURE 38: IMAGE LOG FROM THE DRILLING OF F-14, CONTAINING VARIOUS MEASUREMENTS.	62
FIGURE 39: IMAGE LOG FROM THE DRILLING OF G-4 T2, CONTAINING VARIOUS MEASUREMENTS.	63
FIGURE 40: MAXIMUM AND MINIMUM TORQUE VALUES FOR THE INJECTION WELLS WHEN DRILLING SOLA FM.	64
FIGURE 41: MAXIMUM AND MINIMUM VALUES FOR LATERAL VIBRATIONS FOR THE INJECTION WELLS WHEN DRILLING SOLA FM.	65
FIGURE 42: DRILLED LENGTH OF AASGARD FOR THE DIFFERENT INJECTION WELLS. LENGTH OF AASGARD FOR THE G-WELLS ARE SHOWN INSIDE THE CIRCLE.	65
FIGURE 43: REAL-TIME CALIPER LOGS FOR F-14, F-13, E-2, G-4 AND G-4 T2 (FROM LEFT TO RIGHT). AASGARD FM. IS SITUATED WITHIN THE DASHED LINES. THE LEFT AXES ARE GIVEN IN METERS.	66
FIGURE 44: MAXIMUM AND MINIMUM ROP FOR THE INJECTION WELLS WHEN DRILLING AASGARD FM.	67
FIGURE 45: MAXIMUM AND MINIMUM WOB FOR THE INJECTION WELLS WHEN DRILLING AASGARD FM.	67
FIGURE 46: MAXIMUM AND MINIMUM FLOW RATE FOR THE INJECTION WELLS WHEN DRILLING AASGARD FM.....	68
FIGURE 47: MAXIMUM AND MINIMUM ROTATION FOR THE INJECTION WELLS WHEN DRILLING AASGARD FM.	69
FIGURE 48: IMAGE LOG FROM THE DRILLING OF F-11, CONTAINING VARIOUS MEASUREMENTS.	70
FIGURE 49: IMAGE LOG FROM THE DRILLING OF AASGARD FOR F-14. FEATURES REGARDING SPIRAL GEOMETRY IN THE BOREHOLE ARE MARKED WITH RED LINES ON THE PEF LOG.	71
FIGURE 50: MAXIMUM AND MINIMUM TORQUE FOR THE INJECTOR WELLS WHEN DRILLING AASGARD FM.	72
FIGURE 51: IMAGE LOG FROM THE DRILLING OF G-4 T2, CONTAINING VARIOUS MEASUREMENTS.	73
FIGURE 52: IMAGE LOG FROM THE DRILLING OF G-3, CONTAINING VARIOUS MEASUREMENTS.....	75
FIGURE 53: MAXIMUM AND MINIMUM STICK SLIP FOR THE INJECTION WELLS WHEN DRILLING AASGARD FM.....	76
FIGURE 54: MAXIMUM AND MINIMUM LATERAL VIBRATIONS FOR THE INJECTION WELLS WHEN DRILLING AASGARD FM.	77

FIGURE 55: DRILLED LENGTH OF DRAUPNE FM. 2 FOR THE DIFFERENT INJECTION WELLS.	78
FIGURE 56: REAL-TIME CALIPER LOGS FOR F-14 (LEFT) AND G-4 T2 (RIGHT). SOLA FM. IS SITUATED WITHIN THE DASHED LINES. THE LEFT AXES ARE GIVEN IN METERS.	79
FIGURE 57: MAXIMUM AND MINIMUM ROP FOR THE INJECTION WELLS WHEN DRILLING DRAUPNE FM. 2.	80
FIGURE 58: MAXIMUM AND MINIMUM WOB FOR THE INJECTION WELLS WHEN DRILLING DRAUPNE FM. 2.	80
FIGURE 59: MAXIMUM AND MINIMUM FLOW RATE FOR THE INJECTION WELLS WHEN DRILLING DRAUPNE FM. 2.	81
FIGURE 60: MAXIMUM AND MINIMUM ROTATION FOR THE INJECTION WELLS WHEN DRILLING DRAUPNE FM. 2.	82
FIGURE 61: IMAGE LOG FROM THE DRILLING OF F-11, CONTAINING VARIOUS MEASUREMENTS.	83
FIGURE 62: DRAUPNE FM. 2 HOT SHALE DRILLED BY PILOT WELL U-1 B AT 80°. THE FIGURE ILLUSTRATED THE GAMMA RAY, RESISTIVITY, DENSITY IMAGE, CALIPER IMAGE AND 3D CALIPER IMAGE LOGS (FROM LEFT TO RIGHT) FROM DRILLING, FIRST RE-LOG (17.5 HOURS) AND SECOND RE-LOG (30 HOURS). DETERIORATION OF THE BOREHOLE AFTER 17.5 HOURS IS EVIDENT. HOWEVER, IT DOES NOT SEEM TO WORSEN FROM 17.5 TO 30 HOURS.	84
FIGURE 63: IMAGE LOG FROM THE DRILLING OF E-1, CONTAINING VARIOUS MEASUREMENTS. INTERESTING FEATURES WHICH MAY INDICATE IRREGULAR HOLE GEOMETRY ARE MARKED WITHIN THE BLACK SQUARES.	85
FIGURE 64: IMAGE LOG FROM THE DRILLING OF E-3, CONTAINING VARIOUS MEASUREMENTS.	86
FIGURE 65: MAXIMUM AND MINIMUM DLS FOR THE INJECTION WELLS WHEN DRILLING DRAUPNE FM. 2.	86
FIGURE 66: MAXIMUM AND MINIMUM STICK SLIP VALUES FOR THE INJECTION WELLS WHEN DRILLING DRAUPNE FM. 2.	87
FIGURE 67: TOTAL AMOUNT OF B/U CIRCULATED FOR THE INJECTION WELLS.	88
FIGURE 68: FLOW RATE AND ROTATION FOR THE INJECTION WELLS WHEN CIRCULATING B/U AT TD.	89
FIGURE 69: FLOW RATE AND ROTATION FOR THE INJECTION WELLS WHEN CIRCULATING B/U ABOVE TD.	89
FIGURE 70: REAL-TIME LOG FOR F-12 WHEN DRILLING STRINGERS IN AASGARD FM.	90
FIGURE 71: REAL-TIME LOG FOR G-4 WHEN DRILLING STRINGER IN AASGARD FM.	91
FIGURE 72: REAL-TIME LOG FOR G-4 T2 WHEN DRILLING STRINGERS IN SOLA/AASGARD FM.	92
FIGURE 73: AMOUNT OF B/U DURING WIPER TRIP FOR THE INJECTION WELLS.	94
FIGURE 74: FLOW RATE AND ROTATION FOR THE INJECTION WELLS WHEN CIRCULATING AT TD DURING WIPER TRIP.	94
FIGURE 75: LENGTH OF LINERS USED ON THE DIFFERENT INJECTION WELLS.	95
FIGURE 76: ILLUSTRATING THE DISTANCE THE LINER WAS WORKED DOWN AND THE CORRESPONDING MAXIMUM WEIGHT APPLIED IN SOLA FOR THE F-WELLS.	97
FIGURE 77: ILLUSTRATING THE DISTANCE THE LINER WAS WORKED DOWN AND THE CORRESPONDING MAXIMUM WEIGHT APPLIED IN SOLA FOR THE G-WELLS.	98
FIGURE 78: ILLUSTRATING THE DISTANCE THE LINER WAS WORKED DOWN AND THE CORRESPONDING MAXIMUM WEIGHT APPLIED IN DRAUPNE 2 FOR THE G-WELLS.	100
FIGURE 79: TORQUE VALUES FOR ROTATION OF LINER AT TD WITH 20 RPM, BEFORE SETTING LINER HANGER SLIPS.	102
FIGURE 80: TIME FROM DRILLING TO RUNNING LINER IN SOLA FM. FOR THE INJECTION WELLS, INCLUDING THE 12 ¼" SECTION LENGTHS.	103
FIGURE 81: TIME FROM DRILLING TO RUNNING LINER IN AASGARD FM. FOR THE INJECTION WELLS.	103
FIGURE 82: TIME FROM DRILLING TO RUNNING LINER IN DRAUPNE FM. 2 FOR THE INJECTION WELLS.	104

List of Tables

TABLE 1: TABLE SHOWING THE ADVANTAGES AND DISADVANTAGES OF IMPLEMENTING A HIGH MUD WEIGHT PHILOSOPHY. [35] 25

TABLE 2: VOLUMES AND DENSITIES OF THE CEMENT USED ON THE DIFFERENT INJECTION WELLS. 49

TABLE 3: OVERVIEW OF DISPLACEMENT RATE AND ROTATION WHEN DISPLACING CEMENT IN ANNULUS, INCLUDING WELLS WITH LOST ROTATION DURING DISPLACEMENT. 51

TABLE 4: LENGTH OF CEMENT AND DEPTH OF TOP CEMENT AT LOST ROTATION. INCLUDING THE CORRESPONDING FORMATION. 52

TABLE 5: OVERVIEW OF THE MUD PROPERTIES FOR ALL INJECTOR WELLS. 57

1 Introduction

In order to utilize this enormous oil field's full potential, injection wells need to be present to provide sufficient pressure support during production. At its peak, Johan Sverdrup will constitute 25% of Norwegian petroleum production. A vital part of being able to achieve these colossal rates is to obtain a continuous isolating cement outside the 9 5/8" liner to act as a barrier against both injection and reservoir pressures. If this criterion is not met, either injection pressures must be reduced, which eventually negatively affects production rates, or a side track must be made.

During drilling and cementing of the injection wells on Johan Sverdrup, several obstacles have emerged. Lost rotation during cementing, lost circulation, major obstruction during liner running and tool failure has caused time-consuming unplanned operations such as cutting, fishing, and pulling liner, in addition to a side track. Obviously, it is in Equinor's best interest that mitigating actions are performed to reduce the probability of such incidents.

First, chapter 2 will cover general information regarding the field, such as discovery, location, development, and reservoir properties. In addition, geology is presented, both for the field in general and for the injection wells.

Furthermore, all injection wells drilled on Johan Sverdrup have been studied during the creation of this thesis. In order to obtain a comprehensive understanding as to how the liner cement could be compromised; drilling, liner running, and cementing operations were investigated. The objective of this thesis is to uncover the underlying causes for obtaining poor liner cement by examining data related to all the beforementioned phases. Supporting theory regarding this investigation is presented in chapter 3. An introduction to injection wells is presented in chapter 4, where both internal and external regulations are covered. Also, barriers related to injection are illustrated and explained.

Initially, the cement jobs were studied in an attempt to uncover the reason for lost rotation and pack-off tendencies during displacement. Secondly, a handful of formations were carefully selected due to their troublesome behavior during drilling, liner running and cementing. Furthermore, each of these formations have been studied and analyzed separately for both drilling and liner running, in addition to the occasional wiper trip. These results will be presented in chapter 5. Finally, in chapter 6 and 7, valuable results will be discussed and mitigating actions will be proposed.

2 The Johan Sverdrup Field

2.1 Introduction

The Johan Sverdrup field consists of two discoveries within two different production licenses, namely Avaldsnes and Aldous. Avaldsnes was discovered by Lundin Norway AS in July 2010 by well 16/2-6, with a primary goal to determine the presence of hydrocarbons in Upper Jurassic formation. A 17-meter oil column was detected in Draupne and Hugin in the Upper to Middle Jurassic formations. Aldous, which is divided into Aldous Major South and Aldous Major North, were discovered in August 2011 and September 2011, respectively. Aldous Major South was found by well 16/2-8, which was drilled to a depth of 2083 meters and encountered an oil column of 65 meters. Aldous Major North is a minor field located by the well 16/2-9S, which was drilled to a depth of 2047 meter by Lundin to confirm extension of the Aldous Major South. A map of Aldous and Avaldsnes is presented in Figure 1 [1].

Later, in early 2012, exploration activities revealed that the two discoveries constitute one connected field. The field turned out to be the fifth largest discovery on the Norwegian Continental Shelf (NCS), with a remarkable resource estimate between 2,1 – 3,1 billion barrels of oil equivalents (per February 2018).

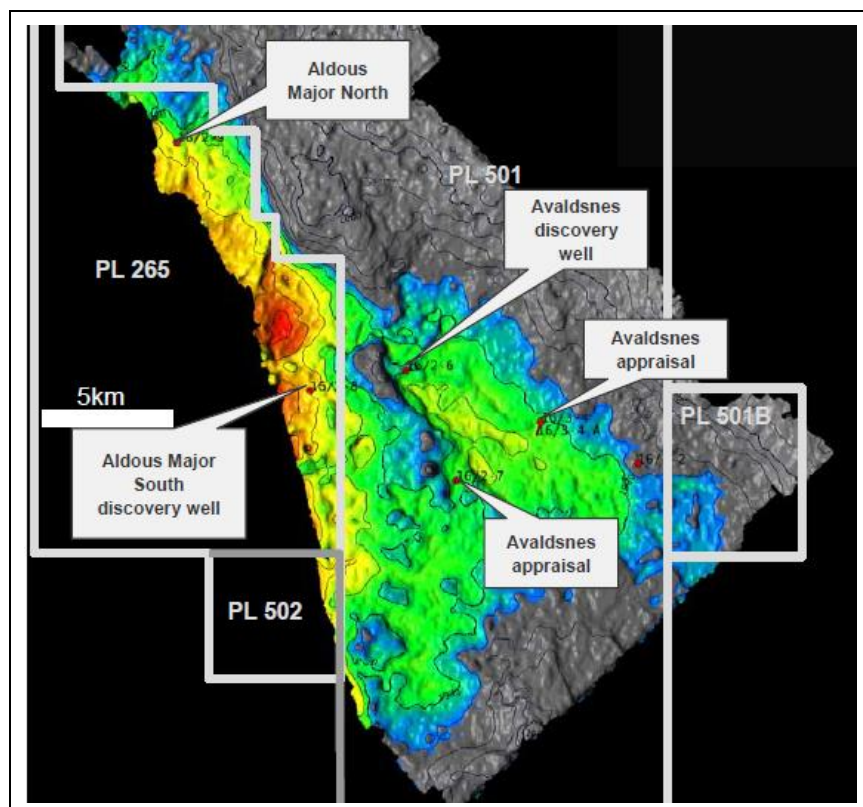


Figure 1: Map showing the locations of Aldous and Avaldsnes. [1]

2.2 Field description

The field is located 160 kilometers west of Stavanger on the Utsira High in the North Sea, 40 kilometers south of the Grane field and 65 kilometers northeast of the Sleipner field. The water depth is 110-120 meters, with a reservoir apex at approximately 1800 meters below the sea floor. The area of the field is 200 square kilometers, and the main reservoir has a temperature around 75,5 °C and 83,5 °C [2].

The majority of resources are in Upper Jurassic Draupne sandstone (Viking group), which has a homogeneous distribution of grains and an astonishingly high permeability (multi-Darcy). Including a porosity of 25-30%, this yields excellent reservoir properties. Besides the Draupne sandstone, there are detected oil in Staffjord and Vestland Groups, as well as in Zechstein carbonates. During the first phase of production, the Upper Jurassic sandstone are being produced.

The oil is strongly undersaturated with low gas-oil-ratio (~40 Sm³/Sm³) and moderate density (~800 kg/m³) and viscosity (~2 cP). The reservoir contains a hydrostatic pressure approximately equal to 180 bars [3].

2.3 Field development

The Plan for Development and Operation (PDO) concerning phase 1 of Johan Sverdrup, was approved during the second quarter of 2015. Following this go-ahead, the pre-drilling campaign for phase 1 started 1st of March 2016, and as of May 2018, there have been drilled eight production wells, six pilot wells and ten injection wells (per June 2018). Phase 1 includes a field center with four platforms: Drilling, riser, living quarter and process platform, and three water injection templates (F-, E- and G-template) connected to the field center via umbilical and flowlines. Oil and gas will be transported via pipeline to shore, where oil is transported to the Mongstad terminal in Hordaland and gas to the Kårstø processing plant in Rogaland, all via Statpipe. Main power is provided from shore. Estimated production start is expected to be by the end of 2019, with a production of 440 000 barrels per day. As of February 2018, the break-even price is expected to be below 15 USD per barrel [4] [5].

Furthermore, another processing platform will be added to the field during the second phase of development. The objective of this phase is to develop the satellite areas: Avaldsnes, Kvitsøy and Geitungen (shown in Figure 2) for processing and export. During phase 2 development, 28

new wells are expected to be drilled. Production start is estimated to 2022, with a predicted break-even of under 20 USD per barrel for phase 1 and phase 2 combined [6] [7].

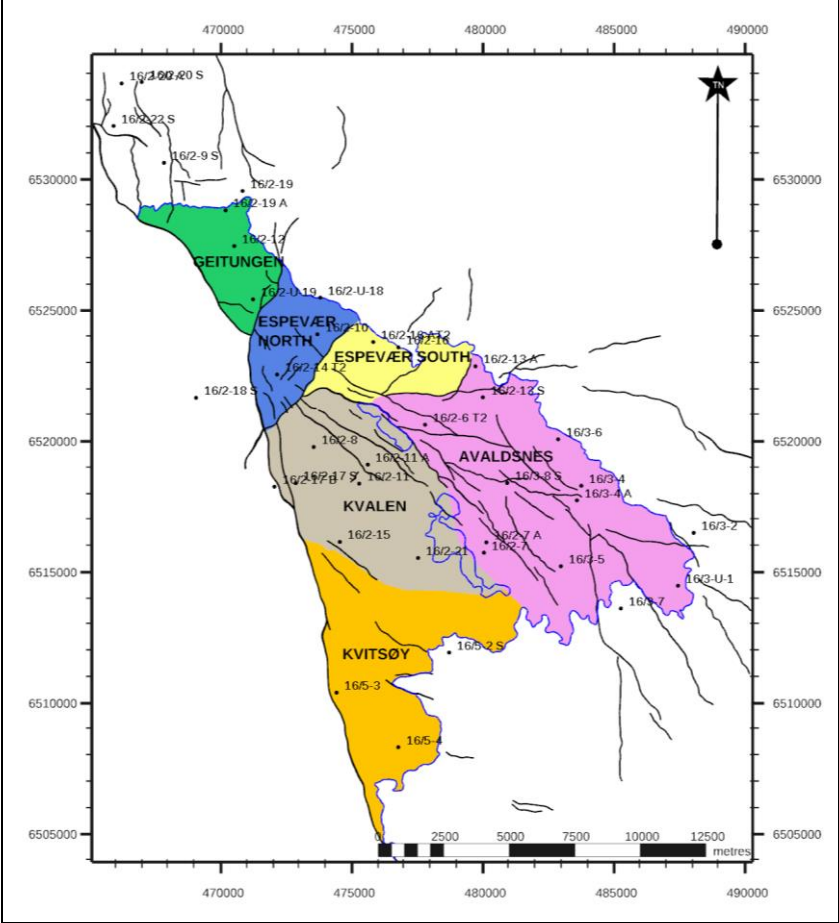


Figure 2: Map over Johan Sverdrup containing the different geological areas. [8]

The drainage strategy of Johan Sverdrup includes seawater injection from injection wells mainly positioned near the oil-water zone, usually 5-10 km away from the production wells. The purpose of these injection wells is to maintain reservoir pressure, which is obtained by full voidage replacement of oil with injected water from day one. Regarding other reservoir management strategies, the production wells are going to be horizontal and placed structurally high, in addition to be completed with gas lift. The producers are expected to produce significant amounts of water after some time, which is solved by full re-injection of produced water (PWRI).

Furthermore, Johan Sverdrup is recognized as the fifth largest oil field in the NCSs history, in terms of resource estimate. However, in terms of remaining oil reserves, Johan Sverdrup is by

far the largest on the NCS today, as shown in Figure 3. During peak production, this giant oil field will constitute 25% of all Norwegian petroleum production [9].

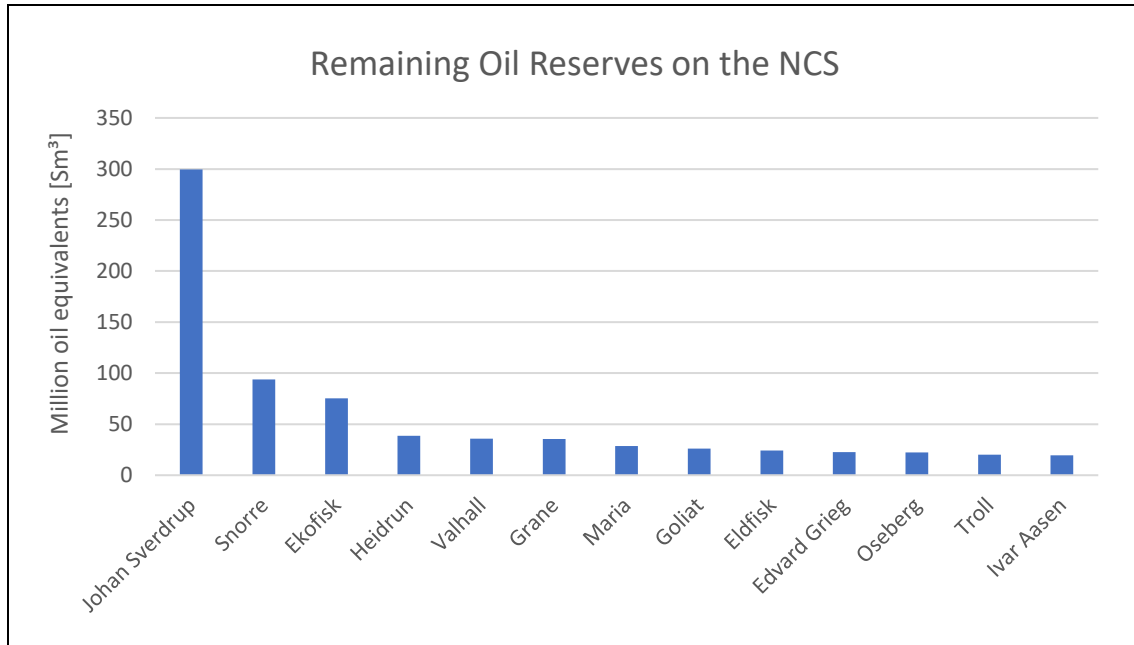


Figure 3: Remaining Oil Reserves on the NCS as of June 2018 [9]

2.4 Geology

Both general geology and injection well specific geology will be discussed in this subchapter.

2.4.1 General geology

As previously mentioned, the main reservoir is located in the Upper Jurassic Draupne sandstone defined within the Viking Gp. This Draupne sandstone extends over the majority of the field, except in some wells which are located in the northern part of Geitungen Terrace and Utsira High. Regarding the depositional system, the sandstone is believed to be fan deltas building out from the Utsira High into a shallow marine setting.

In most of Espevær High, in addition to certain parts of Avaldsnes and Geitungen, shown in Figure 4, the Viking Gp. (containing Draupne) lies unconformably on top of sandstones and mudstones of Statfjord Gp. (Upper Triassic–Lower Jurassic). Statfjord, in turn, rests on the conglomeratic- and sandstone-rich Hegre Gp. (Triassic) which overlies the Zechstein Gp. (Permian). For the east side of Avaldsnes High, on the other hand, the main reservoir (Draupne) is in direct contact with the basement rock.

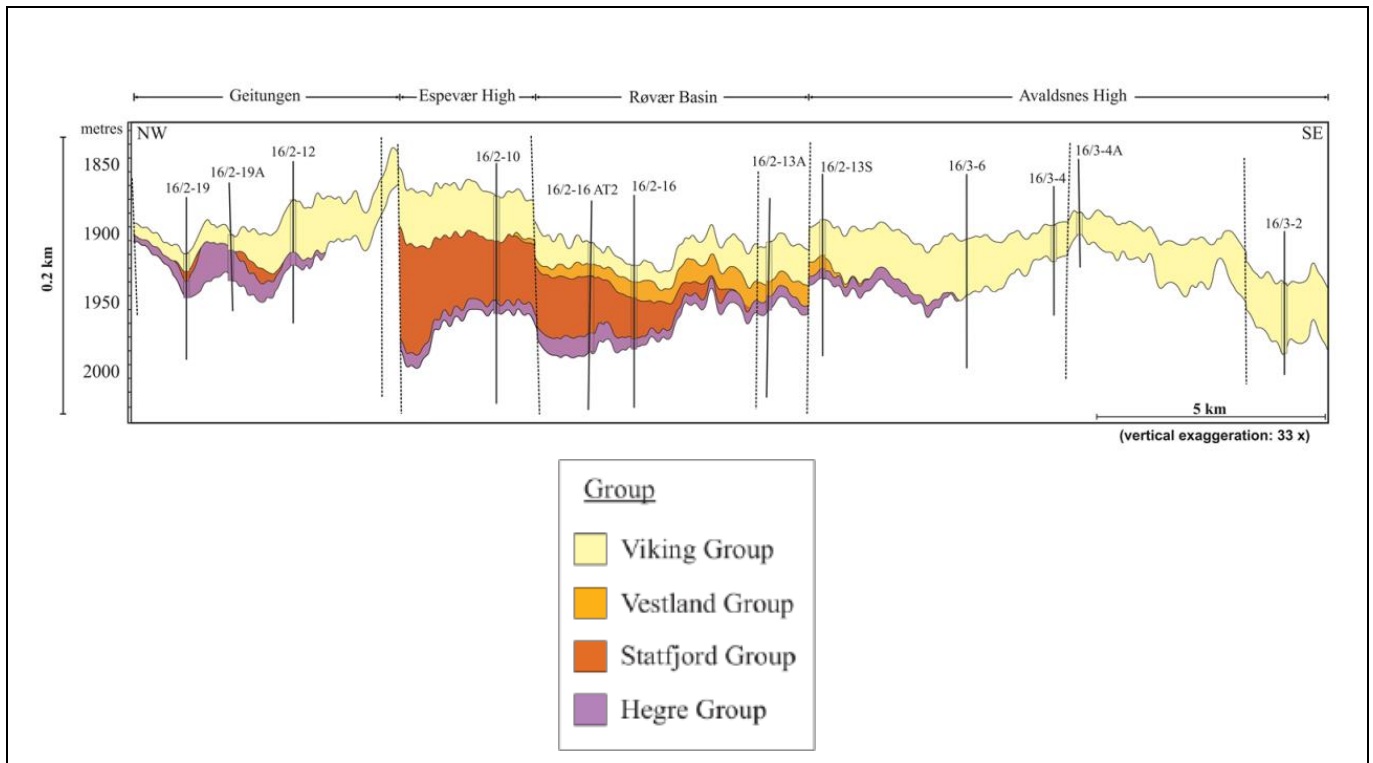


Figure 4: Cross-section NW to SE of Johan Sverdrup field. Stratigraphic groups are outlined. [8]

2.4.2 Injection well geology

The 12 ¼” sections for the injection wells, which are the main concern for this thesis, exposes the Shetland Gp., Cromer Knoll Gp. and Viking Gp.

The Late Cretaceous to Early Paleogene Shetland Gp. is mainly limestone/chalk and marls, and comprises the Ekofisk, Tor, Hod, Blodøks and Svarte formations. The chalk formations are known to be stable and have been used for longer transport sections, however they may also reduce the rate of penetration (ROP) significantly. In addition, high strength chalk formations may also increase the vibrations during drilling, which is partly due to the high friction coefficient in chalk [10].

The Early Cretaceous Cromer Knoll Gp. comprises Rødby Fm., Sola Fm. and Aasgard Fm. The first and latter formations are mainly marls and interbedded chalk/limestone (stringers) with occasional claystone. The Sola formation, on the other hand, is known to be unstable and mainly composed of claystone. High angles versus well instability has been one of the main challenges regarding the Cromer Knoll Gp. due to the heterolithic qualities of the lithology in Cromer Knoll, there is always a risk of hanging up on shoulders and wash outs [11].

The reservoir section in the Viking Group comprises Draupne Fm. 2 and Draupne Fm. 1. Draupne 1 Fm. is mainly high permeable sandstone throughout the field, opposed to Draupne 2 Fm. which changes composition between the different injection wells.

Furthermore, through the drilling of the Johan Sverdrup injectors, three of the abovementioned formations stood out as especially problematic. In the following sub-chapters, these formations and their related problems will be characterized in greater detail. The formations are presented in descending order from shallowest to deepest.

2.4.2.1 Sola Fm.

As previously mentioned, Sola is regarded as a weak formation. It is composed of mainly claystone, with the occasional introduction of marl and/or calcite stringers. The formation has yielded stability issues on offset fields but did not show similar problems during the pre-drilling of eight wells in the field center, including angles up to 86 degrees.

Some variations may be observed between the different templates. For the F-template wells, Sola is mainly claystone with marl, for the E- and G-wells calcite is introduced in the form of calcareous claystone and thin layers of limestone/chalk, respectively.

Due to the weak claystone composition of Sola Fm., the F-template experienced stability issues both during and after drilling. This will be discussed later.

2.4.2.2 Aasgard Fm.

The Aasgard Fm. is a heterogenous unit composed of interbedded marlstones and lime-mudstones. One black claystone layer occurs. The top boundary is represented by a prominent lithological change from the carbonaceous claystones of the Sola Fm., corresponding to a marked increase in sonic, resistivity and density logs. The base records another major lithological change to the organic-rich Draupne shales, Draupne spiculites or to the omission interval, and corresponds to a large sonic, neutron and density decrease, and to a gamma ray spike. The Aasgard Fm. is present across the entire field, with observed thicknesses ranging from approximately 3 m to 48 m with a general thinning towards the west.

Figure 5 shows a core photo of lower Aasgard, where a limestone stringer (A) and lime-rich marl (B) is present.

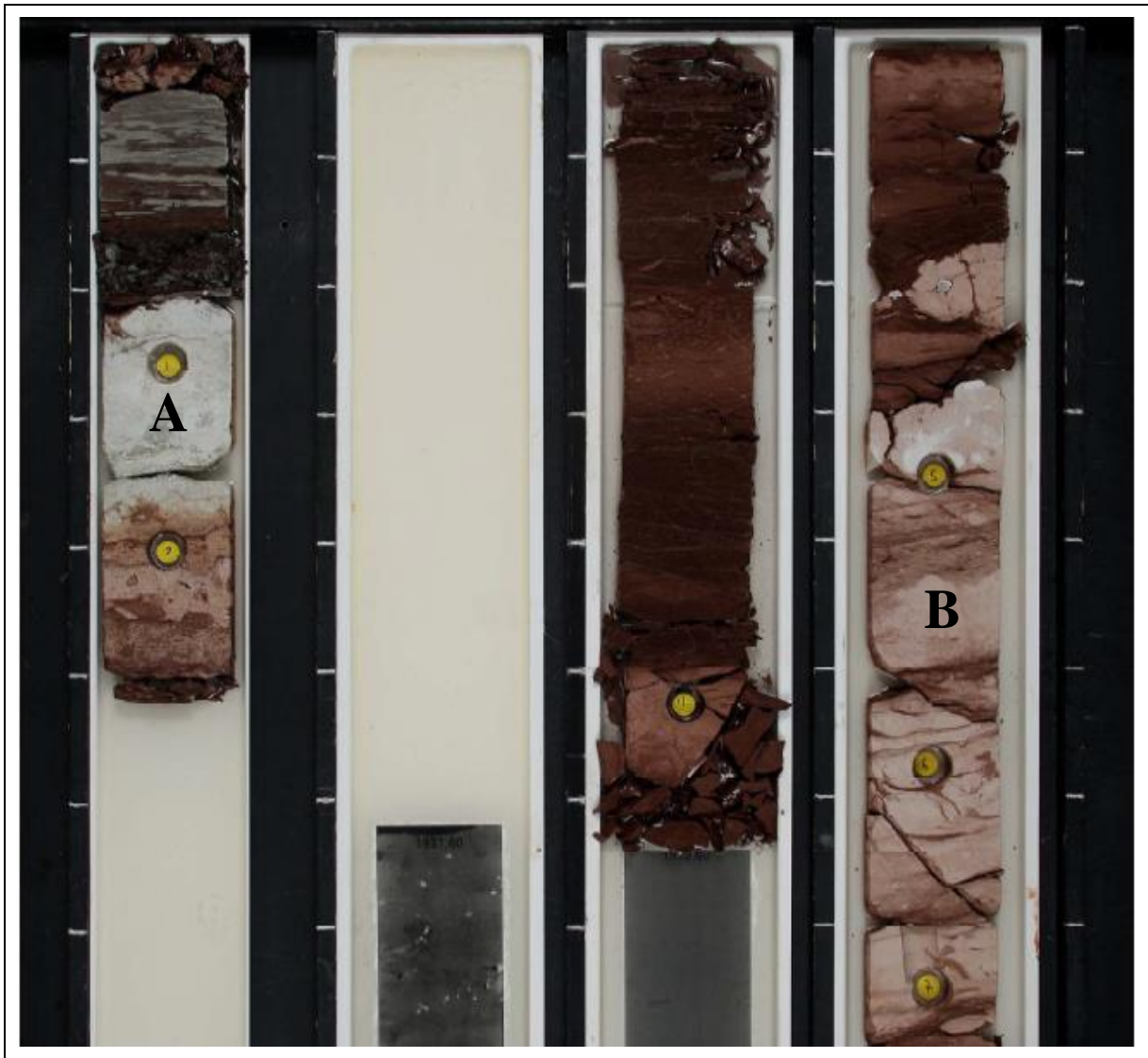


Figure 5: Core photo of lower Aasgard Fm. A hard limestone stringer (A) and lime-rich marl (B) are present.

2.4.2.3 Draupne

Draupne Fm. is divided into two stratigraphic intervals, namely Draupne Fm. 1 and Draupne Fm. 2. Draupne Fm. 1 lies underneath Draupne Fm. 2 and is fairly consistent in terms of composition: Multi-Darcy sandstone, with possible highly calcite cemented zones and loosely consolidated sand. The hard calcite cemented zones are most evident at the base of Draupne Fm. 1.

The Draupne 2, however, comprise different rock types including shales, spiculites and sandy siltstones (omission interval). Which rock type succeeding the Aasgard Fm. varies across the field. The different rock types are presented below.

The Draupne shales comprise dark grey and black mudstones. The shales are internally subdivided into the informal Draupne “not hot” shale and Draupne “hot” shales. The upwards vertical transition from the Draupne “not hot” shale to the Draupne “hot” shale is indicated by an increase in gamma ray values which reflects an increase in organic carbon content. The Draupne shales are not present in all sectors of the field. Draupne “hot shale” is present in the G-template area, but absent in both the E- and F-template areas.

The Draupne spiculites are a biogenic rock mainly composed of sponges with spicules composed of opaline silica. During diagenesis the spicules become unstable, dissolve and precipitate as chalcedony cement. The spiculites occur directly below the Aasgard Fm. in the E- and F-template areas.

Fieldwide, the omission interval overlies the Draupne Fm. 1 sandstone reservoir. This interval comprises dark green-grey, poorly sorted silty sandstones, with scattered belemnite fragments, phosphatic clasts, glauconite grains and carbonate cement. This section might be very hard and could create problems if there are weak formations present in Draupne Fm. 2. The omission interval is recognized from logs by a large spike on the gamma ray log, most likely due to presence of abundant glauconite. The omission interval is overlain by the Draupne “hot” shales in the G-template area and spiculites in the E-template and F-template areas.

In Figure 6, one can observe Draupne Fm. 2 shale, omission zone and Draupne Fm. 1. For the G-wells, problems have occurred related to Draupne shale, due to its weak, laminated structure. In addition, Draupne “hot” shale is believed to possess time-dependent behavior. During the drilling of pilot well U-1 B, it was observed that the hot shale part of Draupne Fm. 2 may be subject to time-dependent shear failure (break-out). This is based on taking gradual weight and meeting restriction when running in hole 17.5 hours after drilling, in addition to an over-gauged borehole on the caliper logs (during first re-log) [12] [13]. Another theory is based on fluid penetration in microcracks in the layering of the formation near the wellbore, which is breaking loose the laminations. Consequently, the fragments accumulate on the low side of the well. In this case, an increase in mud weight could accelerate this process [14]. At the time of writing this thesis, the properties and time-dependent mechanisms of the organic rich Draupne “hot” shale is not completely understood.

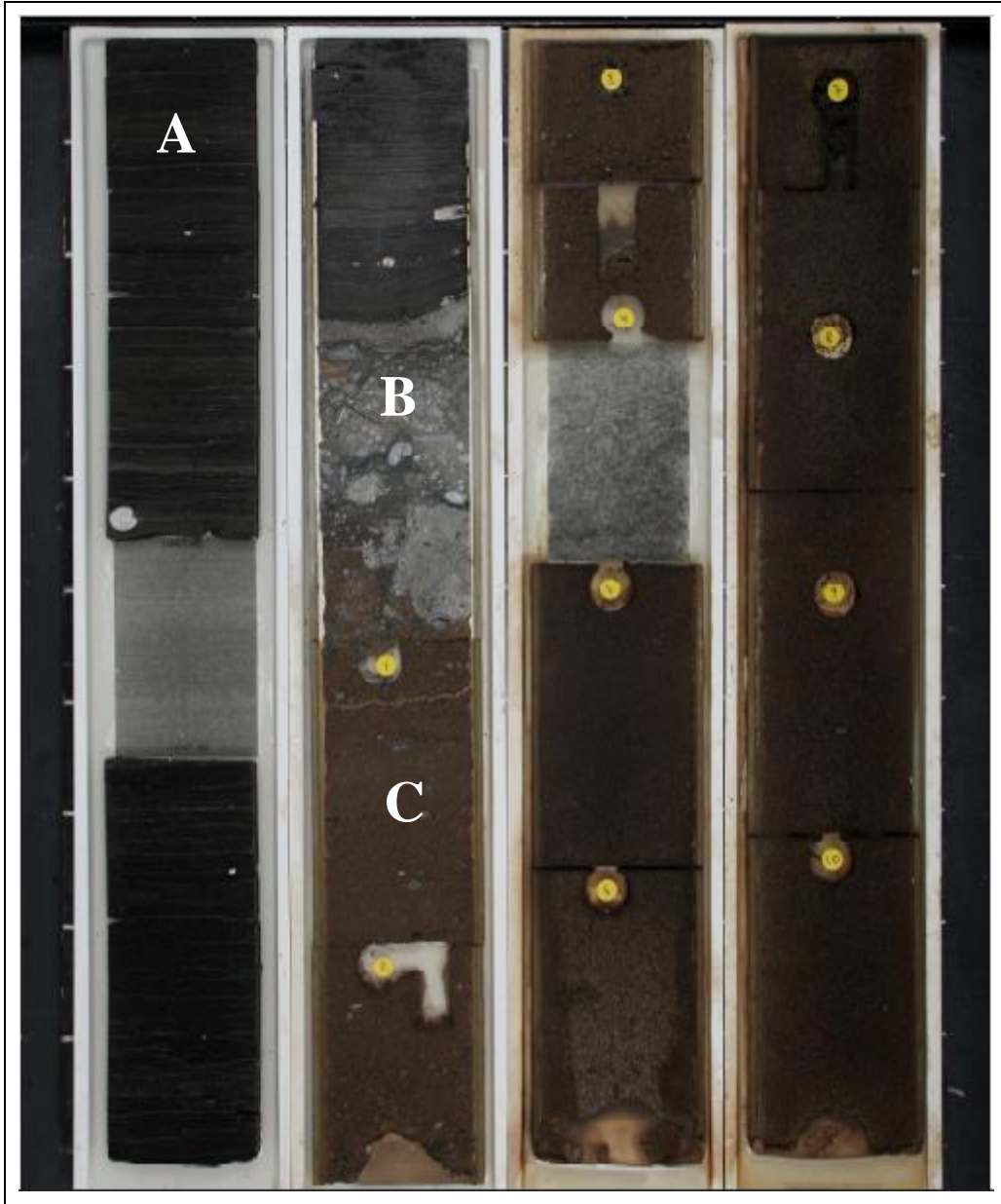


Figure 6: Core photo of Draupne Fm. 2 shale (A), omission zone (B) and Draupne Fm. 1 (C).

3 Theory

3.1 Primary Cementing

Primary cementing is the process of placing cement in the annulus between the casing and the formations exposed to the wellbore. The main objectives of primary cementing are:

- Zonal isolation
- Protection against corrosion and erosion
- Casing anchor (axial support)
- Support borehole walls

The foremost goal of primary cementing has always been to provide zonal isolation in oil, water and gas wells. To be able to achieve this, a hydraulic seal needs to be in place. This seal is created at the casing – cement interface, as well as at the cement – formation interface. At the same time, one must prevent the generation of fluid channels in the cement sheath.

Therefore, one must carefully consider any parameter that may affect the integrity of the cement sheath and the quality of isolation during the well's productive lifetime and after abandonment [15] [16].

As mentioned, the cement sheath should also anchor and support the casing string and protect the casing against corrosion by formation fluids. Uncemented casings are prone to rapid corrosion, e.g. if exposed to hot formation brines and H₂S. Also, casing string could be exposed to eroding environments, such as production fluid carrying unconsolidated formation sand. Lateral loads acting on a poorly cemented casing, could result in buckling or collapse due to overloading at critical points. Contrarily, a properly cemented casing obtains a uniformly distributed load along the casing wall, approximately equal to the overburden pressure [15].

The engineer must consider data from various sources to optimize the parameters of the cement job according to well conditions. Every cementing operation has specific objectives combining technical and economic considerations, along with local regulations. To fulfill the objective of a cementing operation, one must first consider three essential types of well data:

- Depth and dimensional data
- Wellbore environment – including drilling fluid design and pressure regime
- Temperature regime

These data dictate the character of the displacement and the cement properties. The pore and fracture gradients, along with the annular configuration, are essential in determining the flow regime. This is because they restrict the rheology and density of the fluids, consequently affecting the pump rates. Wellbore conditions also indicate whether special materials must be considered, due to the presence of salt, gas, or other conditions. All these factors, including temperature and pressure effects, dictate the selection of additives controlling flow and setting behavior [15].

3.2 Cementing Fluids

Since cement slurries are usually incompatible with most drilling fluids, alternative fluids such as spacers, low viscous mud and/or chemical washes are pumped prior to the cement to prepare the annular space for an optimal cement job. Together, these fluids contribute to clean the borehole, remove drilling mud and thereby minimize cement contamination. Generally, the fluids are pumped in an ascending order according to their density and viscosity to provide the most efficient displacement of the different fluids, this is called the density and rheology hierarchy [15].

3.2.1 Low viscous mud

The low viscous mud is the first fluid to be pumped after the liner has reached target depth (TD) and the mud has been properly conditioned. The purpose of the low viscous mud is to dilute the drilling fluid for easier displacement and to erode filter cake due to its turbulent flow regime. The volume of low viscous mud should be large in order to be effective. [17]

A low viscous OBM of 1.20–1.25 s.g. was used on all of the injector wells on Johan Sverdrup.

3.2.2 Spacer

Spacers are pre-flushes with meticulously designed densities and rheological properties. The spacer will be injected ahead of the cement, but behind the low viscosity mud. Furthermore, the main objective of the spacer is to prepare the liner/casing and the formation for the cementing operation. A spacer could be constructed to satisfy various needs, for example: reactive spacers can provide increased assistance regarding the removal of drilling mud and weighted spacers

can contribute to well control. The interfaces between mud/spacer and spacer/cement must be compatible. The effectiveness of a spacer is highly reliable on the following parameters:

- Flow rate
- Contact time
- Fluid properties

The flow rate will affect the flow regime of the spacer as it is displaced in the annulus. Due to their relatively high viscosity, spacers will most often be displaced in a laminar flow regime. However, their composition can be altered to reduce viscosity without compromising stability, allowing for a turbulent flow regime. A rule of thumb in the industry is to obtain a contact time (between the formation/casing and the spacer) of 10 minutes in order for the spacer to be efficient [15].

SealBond spacer by Baker Hughes were used on all the injector wells on Johan Sverdrup. The SealBond spacer helps mitigate lost circulation issues while cementing, in addition to minimize induced losses. Also, the spacer forms a seal to minimize filtrate invasion into the formation [18].

Equinor's guidelines for cementing, GL3519, states that a volume of 12-15 m³ is usually sufficient for mud removal purposes for a 9 5/8" liner [17].

3.2.3 Cement

Portland cement is by far the most important binding material in terms of produced quantity and is used in nearly all well cementing operations. It is a common example of a hydraulic cement: sets and develops compressive strength as a result of hydration, which is a chemical reaction between water and the compounds in the cement. Portland cement has a uniform, predictable and relatively rapid development of strength. In addition, Portland cement possesses low permeability and low solubility in water, making it suitable for achieving and maintaining zonal isolation [15].

The properties of Portland cement often have to be altered in order to meet the demands of a particular well. These modifications are obtained through adding chemical compounds most commonly referred to as additives. There are eight major additives:

- Accelerators:
 - Reduce setting time
 - Increase rate of compressive strength development
- Retarders
 - Delay setting time of cement
- Extenders
 - Lower the density of a cement system
 - Reduce quantity of cement per unit volume of set product
- Weighting agents
 - Increase the density of a cement system
- Dispersants
 - Reduce the viscosity of a cement slurry
- Fluid-loss control agents
 - Controls leakage of the aqueous phase of the cement to the formation
- Lost-circulation control agents
 - Controls loss of cement slurry to the formation (weak or vugular formation)
- Specialty additives
 - E.g. fibers, antifoam agents, flexible particles, etc.

3.2.3.1 Lead and Tail cement

Oftentimes, one batch of cement with similar properties is sufficient for primary cementing operations. However, sometimes formation properties suggest that a separation into two different cement slurries is beneficial, namely lead and tail cement (Figure 7). These two slurries possess different properties, such as density, setting time and/or strength. Conventional use of lead and tail cement consists of a lighter lead cement to ensure that the total hydrostatic pressure of the cement column does not exceed the fracture pressure of the formation at any point along the cement interval. Also, the heavier tail cement provides extra support around the casing shoe.

However, problems could emerge if the setting time of the lead slurry is less than for the tail slurry, when cementing a zone of inflow. This will result in the hydrostatic pressure exerted by the lead slurry being partially lost before the tail slurry has set, creating an underbalance in the well. Consequently, in a worst-case scenario, pressurized formation fluids may enter the well

and create migration routes through the still deformable gelled lead slurry and further up the wellbore [19]. In less severe cases, the tail slurry may be compromised and observed as patchy on the cement logs. Therefore, a lead slurry with added retarder could mitigate these problems, making the slurry able to maintain hydrostatic pressure on the tail cement until it attains enough strength to prevent annular fluid migration.

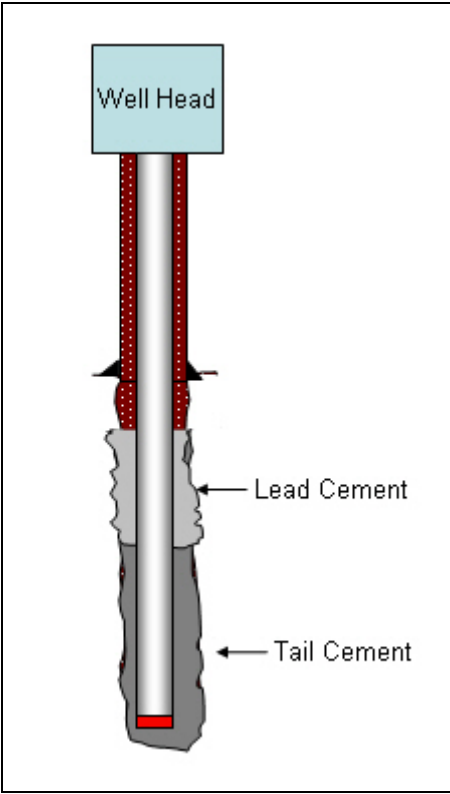


Figure 7: Illustration of the positions of lead and tail cement in the annular space. [20]

3.3 Parameters Affecting Cement Placement

There is an abundance of factors that comes into play when dealing with the process of preparing a well for cement displacement. Some of the most essential factors are described in the following sub-chapters.

3.3.1 Mud conditioning

The objective of drilling mud is to promote optimal drilling operations and transport cuttings in the annulus to surface. Although, mud is not always optimized for use during displacement, completion, or logging. Therefore, mud conditioning is introduced. Before cement is placed in the well, two mud properties can be altered: mud density and rheology. Generally, it is

beneficial to reduce the mud density, plastic viscosity (PV), yield stress and gel strength, without compromising well control. This will reduce the driving forces needed for mud displacement and increase mud mobility. Of course, these steps are only taken when sufficient cuttings have been removed from the wellbore, since reducing these parameters will yield unsuited conditions for cuttings transport [15].

When the mud is clean, its rheology can be modified by adding e.g. water, base oil or dispersants. Subsequently, sufficient circulation of the mud is needed for the rheological properties of the mud to fall within the desired range. Also, moving the string while conditioning helps to get rid of the gelled mud and keep cuttings suspended. In horizontal sections, high rotational speed is especially favorable. More information regarding casing movement is presented in section 3.3.4.1.

Furthermore, the mud should be circulated when the casing is in place, preferably by ramping up the flow in small to moderate steps. This is done due to gelled mud in the borehole, which has been developed during the static period between tripping drill pipe and running casing. In addition, circulation of mud is preferable because it:

- Erodes hydrated or gelled mud that may be trapped in washouts, borehole wall of permeable formation or on the narrow side of the casing.
- Aids in detecting gas flow into the well.
- Homogenizes the mud after treatment of surface.
- Due to thixotropy, reduces PV and yield stress.

Sadly, operators often circulate a minimum to condition the mud, which in turn could compromise their cement job due to a substantial amount of cuttings left in hole.

During the casing run, gelled mud or cuttings may be scraped off into the mud, causing fluctuating pressures or even pack-offs when circulation is resumed. Preventive action should be taken by also circulating at intermediate depths, preferably in competent formations [15].

3.3.2 Mud removal

Mud removal has been a subject of severe interest for many years because of its correlation with zonal isolation and cement quality. For the primary cementing to achieve its main objective: zonal isolation, the drilling mud and pre-flushes must be fully removed from both the casing and formation in the annulus. If not removed, the residual mud could leave mud

channels or layers of mud on the walls across zones. This will eventually lead to interzonal communication [15].

Furthermore, during the cementing operation, the main objectives for the cementing engineer regarding mud removal are casing centralization, selecting the fluid sequence, volume pumped, and properties of the fluids. Usually, these are the only parameters the engineer can control. Moreover, to achieve removal of mud in the annulus, a low viscosity fluid and a spacer is often used. The low viscosity fluid generates a turbulent flow regime when pumped at high rates and will consequently erode the filter cake. After, a spacer will displace the low viscosity fluid, to prepare for the displacement of cement [15].

As the complexity of wells increase due to the demand for locating new fields or increase recovery, the mud removal process becomes even more troublesome. Managing the fluid displacements in highly deviated, high pressure, high temperature wells, often presents complex and unfamiliar challenges.

3.3.3 Eccentricity

When the inner pipe of an annulus is not centered, situations where the flow regime may be laminar on the narrow side and turbulent on the wide side may occur. This is due to the fact that the velocity distribution around the annulus is distorted and the flow choose the path of least resistance, namely the wider side.

Pipe standoff ratio is a term used in the industry (see Equation 1), which is defined API Spec 10D (2002) as:

$$R_{STO} = [(1 - \epsilon) \times 100] \quad (1)$$

where,

ϵ , eccentricity
 R_{STO} , stand-off ratio

Eccentricity, ϵ , is defined as the ratio of the distance between the centers of the cylinders to their radial differences. Consequently, higher R_{STO} means less eccentricity, e.g. 100% standoff yields a concentric pipe. API defines the minimum standoff at 67%, but states that it is merely to specify minimum performance requirements that centralizers shall meet. The effect of

eccentricity on fluid velocity is shown in Figure 9, which clearly shows the negative effect in form of a significant reduction of velocity on the narrow side. The figure presents a Herschel-Bulkley fluid, which means it exhibits a yield stress. In addition to yield stress, these fluids are thixotropic, meaning they exhibit time-dependent changes in rheology, as seen in Figure 8. Some cement, for instance Portland, could be accurately characterized by this rheological model [21].

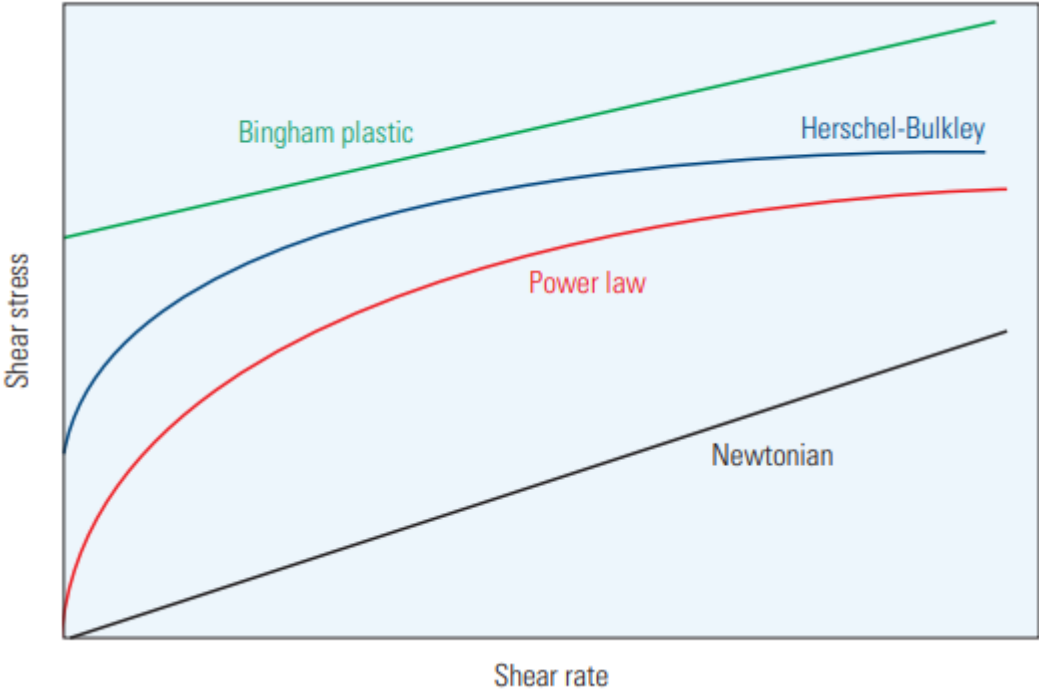


Figure 8: Different rheological models. Presented with shear stress vs. shear rate. Herschel-Bulkley fluids exhibit both yield stress and non-linear relationship between shear stress and shear rate. [15]

For non-Newtonian fluids with yield stress, the fluid flow on the narrow side could become static as the eccentricity increases, also seen in Figure 9. This is a direct result of the shear stress in the fluid being lower than the fluid yield stress. This is solved by increasing the flow rate, creating turbulent flow (if possible). Regarding fluids not exhibiting yield stress, the flow will decrease as eccentricity increases, but would not reach zero (unless eccentricity reaches 1) [22].

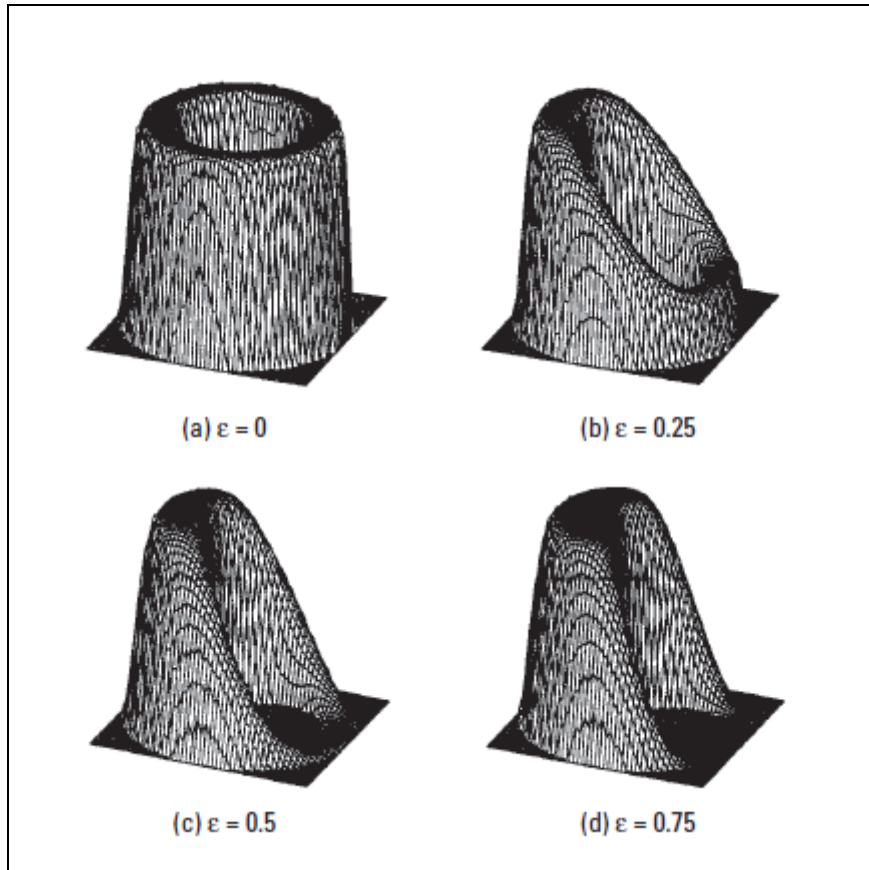


Figure 9: Velocity profile as a function of eccentricity [22]

3.3.4 Casing movement

Rotation of the casing promotes cuttings transport in deviated wells [23]. One could also expect positive effect of rotation regarding mud circulation and displacement during cement jobs. The two basic pipe movements are rotation and reciprocation along their axes. Furthermore, secondary movements may contribute to an even greater effect on mud circulation and displacement efficiency. These secondary movements consist of (illustrated in Figure 10 and Figure 11):

- Orbital or whirling movement
- Lateral movement in inclined wells when reciprocating
- Taylor vortices, which increase shear stress at the wall

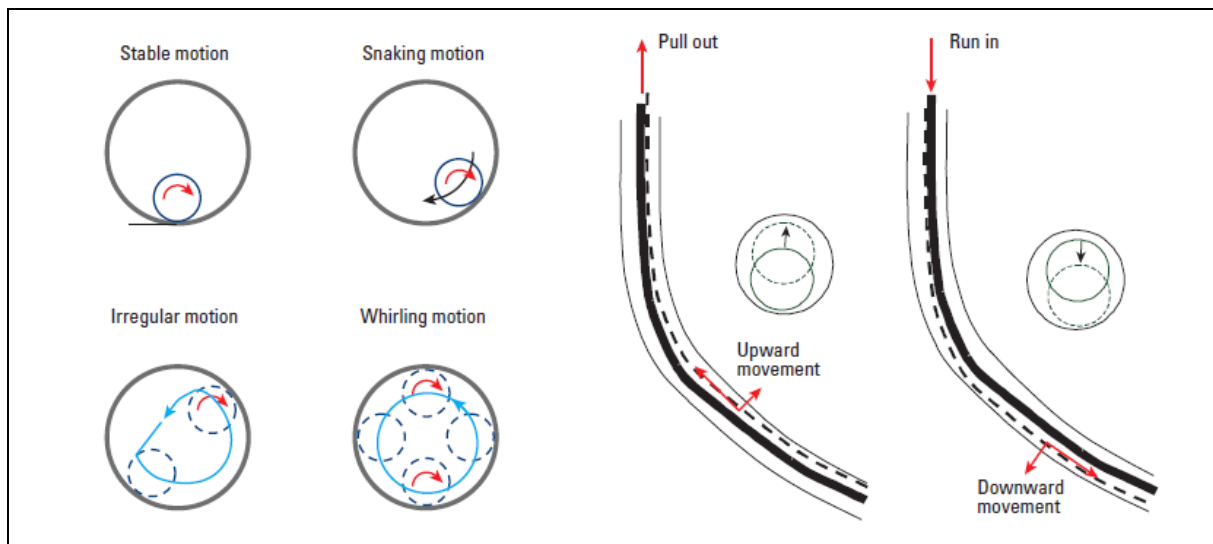


Figure 10: Illustrations of whirling motions and lateral movement during reciprocation. [15]

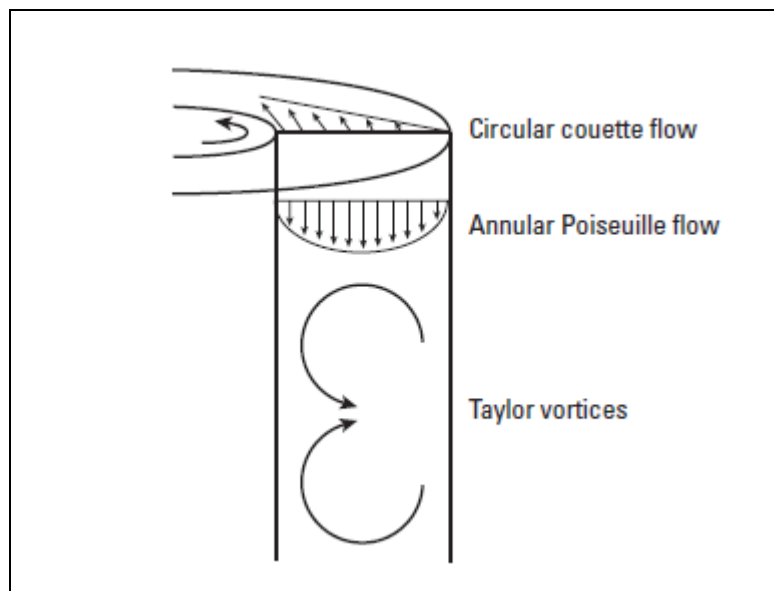


Figure 11: Annular flow patterns caused by secondary movements from rotation. [15]

Circulation efficiencies derived from numerical models concerning non-Newtonian fluids in laminar flow show that pipe movement partially counteract the detrimental effect of pipe eccentricity [24] [25].

3.3.4.1 Rotation during cementing

While satisfying the industries demand for longer-reaching wells and operations in harsher conditions, the liner systems now require high performance in tension, compression and rotatability, to be able to position the liner at TD. As the length of the deviated wells increase,

so does the torque and drag forces, which might sometimes be too high to allow for liner rotation. Historical issues regarding cemented liners are associated with liner top integrity, packer/hanger pre-set or failure to set, cement integrity and shoe integrity [26]. Unsatisfying bonding of cement demands remedial operations for squeeze cementing the liner top or adding a liner top packer to tie back the liner. These remedial actions lead to increased rig time, thus increasing overall costs [27].

Studies have shown that rotation during cementing improves the cement quality [27] [28] [29]. Insufficient mud removal is one of the major reasons for poor cement quality, which liner rotation mitigates. In an eccentric annulus, the mud will choose the path of least resistance, which will be on the wide side. This will cause the mud on the narrow side to experience a reduced flow rate, which may allow the mud to develop gel strength. Rotation will help to break this gelled mud and force fluids to flow more evenly around the borehole [17]. This phenomenon has also been confirmed by the use of computational fluid dynamics (CFD), which creates a three-dimensional image of the behavior of the cement/spacer/mud interfaces [30]. This is illustrated in Figure 12.

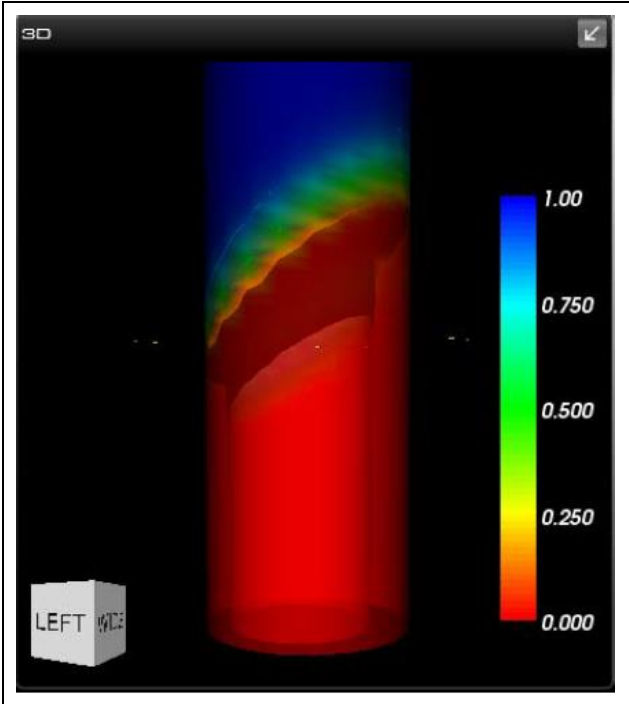


Figure 12: 3D simulation of cement displacement in annulus with 70% eccentricity and 20 rpm. The figure shows a fairly continuous displacement interface. [30]

Equinor’s guidelines for cementing, GL3519, states that rotation of liners during cementing should always be planned for to improve cement quality when zonal isolation is required. A rotation of 20 revolutions per minute is recommended for any liner size.

3.3.5 Displacement rate

The displacement rate is a vital operational parameter during cementing. Optimized displacement rates enable the cement to reduce channeling and sufficiently fill the annulus. Previous studies have shown that displacement efficiency increases with increasing flow rate [31] [32].

In Equinor's guidelines for cementing, namely "GL3519 – Well Cementing", it is stated that the displacement rate should be as high as possible without losing returns. It also states that pressure and return data should be closely monitored as the spacer and cement enters the open hole, since the cement and spacer will expose the formation to a higher pressure due to their density and rheological profile. Although a steady linear pressure is expected during displacement, pack-off tendencies are often experienced if the cement and/or spacer starts to lift accumulated cuttings in the annulus [17].

Moreover, in such a pack-off and/or loss situation, it is recommended to reduce the displacement rate to the maximum loss free rate provided it is higher than the recommended minimum rate for that particular job. When experiencing total losses, it is recommended to increase from a minimum acceptable rate to planned displacement rate from when spacer enters open hole. According to the guidelines, the preferable range for displacement rate for a 9 5/8" casing in a 12 1/4" hole is 1200–2000 liter/minute [17].

3.4 Drilling

There are several factors that could cause wellbore instability and render a borehole of poor quality, which will subsequently create problems during the casing running and cementing. Many of these factors are controllable and will later be analyzed for the 12 ¼” section on the Johan Sverdrup injectors, namely in section 5.2. The following sub-chapters will address some of these factors.

3.4.1 Bottom hole pressure (BHP)

The supporting pressure provided by dynamic (ECD) or static mud during drilling, will determine the stress concentration in the near wellbore vicinity. The pressure exerted on the formation can be altered through a change in mud weight, in order to balance the rock stresses. The choice of mud weight is a highly debated subject. Several studies are stating that an increase in mud weight will improve hole stability by providing increased support to the borehole walls [33] [34], where it is advised to drill with the highest mud weight possible. However, when maximizing mud weight, one will also increase the risk of lost returns, differential-pressure sticking, destabilization of naturally fractured formations and reduced drill rate. Both advantages and disadvantages by increasing the mud weight are shown in Table 1 [35].

Table 1: Table showing the advantages and disadvantages of implementing a high mud weight philosophy. [35]

Element	Advantage	Debatable	Disadvantage
Reduce borehole collapse	X		
Reduce fill	X	X	
Reduce pressure variations	X		
Reduce washout	X	X	
Reduce tight hole	X	X	
Reduce clay swelling	X	X	
Increase differential sticking		X	X
Increase lost circulation			X
Reduced drilling rate		X	X
Expensive mud			X
Poor pore pressure estimation		X	X

If the mud weight is too low, it is certain that the borehole wall will eventually give in because of lacking radial stress (σ_r), which is exerted by the drilling fluid. At low borehole pressures, the tangential stress (σ_θ) becomes larger. Figure 13 illustrates in which direction the different stresses act. The following equations (2 and 3) describes the relationships between downhole stresses [35]:

Radial stress:
$$\sigma_r = P_w \tag{4}$$

Tangential stress:
$$\sigma_\theta = 2\sigma_a - P_w \tag{5}$$

where,

- σ_a , vertical stress (or axial stress)
- σ_r , radial stress
- σ_θ , tangential stress (or hoop stress)
- P_w , pressure in the well exerted by the drilling fluid

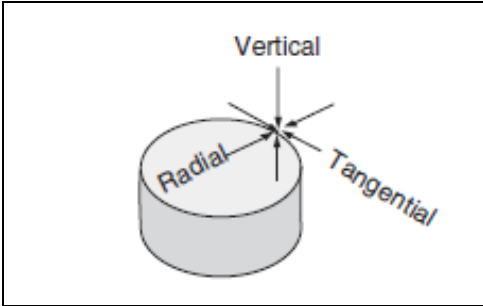


Figure 13: Stresses-direction of the stresses acting on the borehole wall. [35]

Borehole breakouts occur when the stresses around the borehole (tangential stress) exceeds the compressive strength of the formation. The enlargement is generated by the growth of intersecting conjugate shear planes, eventually causing parts of the formation around the borehole to spall off. The greatest concentration of stress around the borehole is found in the direction of the minimum horizontal stress, σ_{min} . Consequently, the breakout is oriented parallel to the minimum horizontal stress of the rock. [36] [37] [38].

Drilling-induced fractures, however, appear when the tangential stress is less than the tensile strength of the rock. This will happen when radial stresses increase (e.g. increase in MW), as can be observed from equation 3. These fractured are then oriented parallel to the maximum

horizontal stress. Both breakouts and drilling-induced fractures are illustrated in Figure 14. [36] [37] [38].

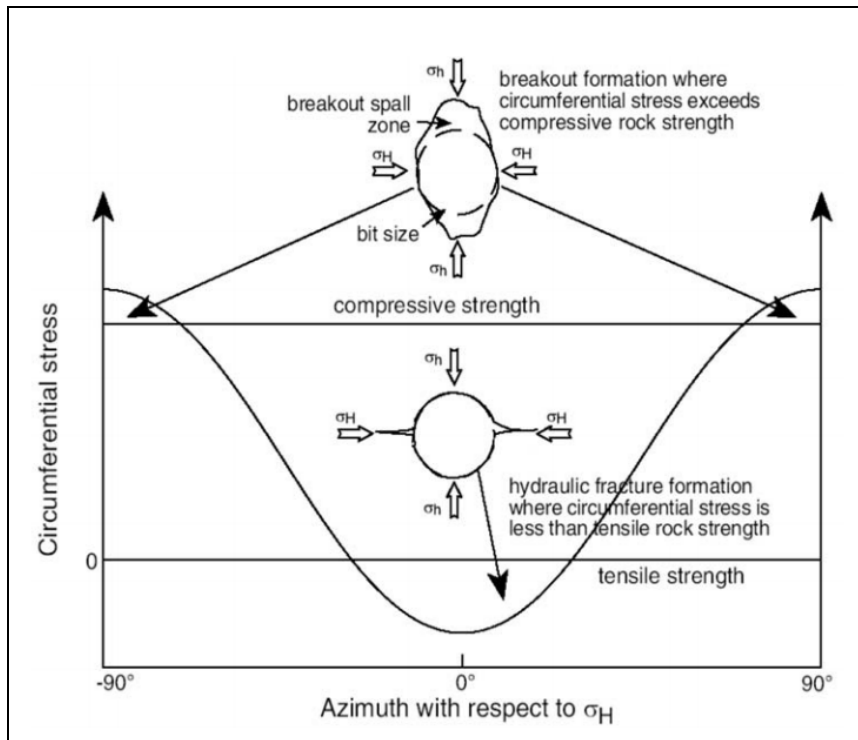


Figure 14: Sketch illustrating breakout and drilling-induced fracture. [38]

Breakouts occur when the circumferential (tangential) stresses exceed the compressive strength of the rock. Thus, breakouts are oriented parallel to σ_{min} . Similarly, drilling-induced fractures occur where the circumferential stresses are less than the tensile strength of the rock. Thus, drilling-induced fractures are oriented parallel to σ_{max} . [38]

3.4.2 Well inclination, Azimuth and Dogleg Severity (DLS)

Well inclination and azimuth with respect to the principal in-situ stresses can be an important factor concerning the risk of collapse and/or fracturing of the formation. Also, well inclination affects the ability to clean the hole properly, which will be more thoroughly discussed in section 3.4.6.

Dogleg severity (DLS) is defined as change in degrees per 30 meters of wellbore length and is a measurement of how rapid the well trajectory changes. High dogleg could cause undesirable wellbore geometry because of local inclination anomalies. Therefore, creating contact points exposed to high forces when running in hole (RIH) or pulling out of hole (POOH). Consequently, increasing the torque and drag forces, or worst case: creating an unbreachable obstruction in the well path. High local doglegs can occur at interfaces between hard and soft formations, e.g. entering or exiting a stringer. If the bit hits the stringer at a low angle of attack, or if the stringer is exited into soft formation while high WOB is maintained. Doglegs, together

with spiral geometry and multiple washouts, render a convoluted path for the casing when it is run downhole, often resulting in increased rig time or even stuck casing [15].

3.4.3 Vibrations

Drillstring vibration could be separated into three primary vibration modes: axial, torsional, and lateral, where lateral vibration appears to be the most destructive. Drillstring vibrations can enlarge the borehole under certain circumstances, where the physical deterioration of formation occurs due to forces acting from the drillstring, especially BHA components, as it vibrates down hole. Lateral vibrations induce irregular hole geometry, which is due to lateral motion enabling side-cutting at the bit. This phenomenon may cause spiraling hole shape, enlarged hole and difficulty steering the bit in the wanted direction [33] [39]. Spiraling hole geometry, if severe, will decrease the effective drift diameter of the borehole significantly. Hence, yielding the well unsuited for liner running. This is illustrated in Figure 15.

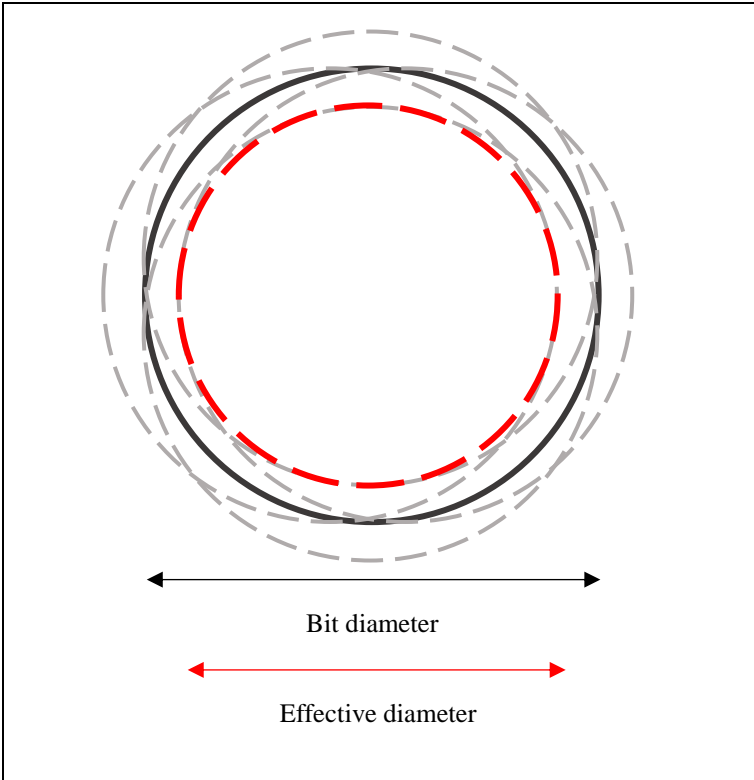


Figure 15: Effective borehole diameter (red dashed circle) illustrated for a hole containing spiral geometry over a given length. The dashed grey circles indicate the off-center positions of the bit due to lateral vibrations during a drilled interval. The black solid line illustrates the in-gauge diameter/bit diameter.

Elevated friction between the borehole wall and the drillstring in a deviated well will lead to less energy reaching the bit. This will again lead to the string being held up at different locations along the wellbore, and consequently torsional vibrations arise. In extreme cases, rotation for the whole drillstring could cease momentarily. This will cause the string to store high torque-loads and suddenly release the energy, making the drill pipe spin freely at high speeds. Consequently, the bit and BHA will accelerate and decelerate leading to unstable progress. This phenomenon is called stick slip. Furthermore, in addition to WOB and RPM, wellbore tortuosity also affects the magnitude of torsional vibrations, e.g. high local DLS tend to induce friction between the borehole and the drillstring [39] [40].

Stick-slip mitigation are available through various BHA tools, which will be discussed in section 3.4.4 below. In addition, software like SoftSpeed II by NOV could be employed. This particular software modifies the top drive controller to cure and prevent stick-slip. The system automatically identifies and mitigates stick-slip by varying the top drive RPM accordingly, consequently improving drilling performance. The SoftSpeed package features stick-slip indication, oscillation prevention and dampening, estimation of bit rotation speed and an automatic analyzer providing optimal parameters. Benefits using SoftSpeed has been verified on former Equinor wells, namely Oseberg and Peregrino. Here, BHA failure was caused by excessive lateral vibration and stick-slip, thus, BHA runs were performed. After implementing SoftSpeed, both stick slip and vibrations decreased, consequently eliminating the unplanned trips [41].

3.4.4 BHA composition

Awareness regarding BHA design could vastly improve the quality of the wellbore, due to minimizing shock and vibrations during drilling. Vital BHA components such as bit, stabilizers and reamers should be reviewed in terms of their functionality, in addition to interaction with the formation.

Roller stabilizers have been proved efficient regarding the improvement of borehole quality. Where their most well-known feature is to reduce the impact of whirl-induced patterns [39]. A comprehensive study was performed by S. F. Sowers and F. E. Dupriest on the impact of using roller stabilizers to mitigate bit and BHA vibrations. The study implied that torque generated

from solid-body stabilizers might be enough to generate detrimental vibrations such as stick slip. By replacing the conventional stabilizers with roller stabilizers at contact points possessing high lateral load, the capacity of torque development was greatly reduced [42].

To further mitigate vibrations, an AST (Anti-Stall Tool) can be employed. The AST tool has an internal dampening device, which is absorbing the high torque loads to render a more even torque signature. This is done by continuously and automatically adjust the depth of cut from the bit, which is especially effective when drilling through interbedded formations [43].

3.4.5 Drilling parameters and hole quality

Improper values for ROP, WOB, flow rate and rotation often contribute to poor hole cleaning, increased torque and drag, over-gauged or washed out borehole, and imbalances in formation stresses.

Furthermore, indications of poor hole quality may be direct or in-direct. Direct indications could be seen on the real-time caliper log, such as over-gauged borehole. In addition, excessive volume of cuttings and/or cavings over the shakers could also indicate over-gauged hole. Indirect indicators could be [34]:

- High torque and drag
- Increased circulating pressures
- Stuck pipe
- Excessive drill string vibrations
- Excessive doglegs

Sometimes, it can be very difficult to eliminate the causes for poor hole quality, even though the cause is known. However, it is often possible to reduce the severity of the damage. As an example, Aasgard Fm. contains interbedded lithology composed of hard limestone stringer and relatively soft marl in between. When hitting these hard stringers, the ROP will decrease drastically and lateral vibrations may increase. If parameters like flow rate, rotation and WOB are not altered, this will most likely cause washout sections in the relatively weak formations above the stringer. Flow rate and rotation must be lowered in order to cause minimal forces acting on the formation surrounding the bit.

In addition, according to Equinor's best practices, high RPM may prevent the bit from locking to the rock. Consequently, if low stable torque and low ROP is seen when hitting hard formation, one should reduce the RPM to allow the bit to bite the formation properly. However, the combination of high WOB and low RPM may give high stick-slip levels and torsional bending. Therefore, operational optimization may be required to maintain a decent ROP when meeting stringers [44]. Sometimes, the reduction in ROP could be misinterpreted as hard formation. The actual reason could be hole enlargements, whirl, corkscrew geometry or excessive WOB causing too high depth of cut.

Drilling data from Aasgard Fm., along with other formations exposed in the Johan Sverdrup injectors, will be analyzed in section 5.2.

3.4.6 Hole cleaning

Hole cleaning is highly dependable on the flow and rotation during drilling, especially in deviated wells. Although high rotation is beneficial for transporting cuttings to surface and breaking potential cuttings accumulations in the well, it could also generate unwanted vibrations, which again could cause hole enlargement. Moreover, high flow rate is also beneficial regarding transport of cuttings to surface. A rise in flow rate will directly increase the velocity in the annulus. In addition to flow rate and rotation, reciprocating the string during circulation will cause mechanical agitation to aid in breaking loose potential gelled mud or cuttings beds that accumulate for inclined wells (65-90°) [33].

As previously mentioned, the factors that control cuttings transport change with the hole angle. In high angle wells, the lateral motion of cuttings and debris result in continuous deposition of a layer of material on the low side of the borehole. The bed gets higher as the ROP increases, which consequently reduces the area of flow. This, again, increases the risk of pack off or stuck pipe [33].

Research has been performed, where a full-scale flow loop experiment concluded that hole enlargement dominated the cuttings transport process. Pack offs were seen to appear in, and around, the over-gauged sections. Also, another interesting result was obtained: The enlarged borehole sections were almost impossible to clean up, even when the BHA was back-reamed through the over-gauged section. As the top of the BHA enters the enlarged area, the mass inside the enlarged holes might be mobilized due to the increasing velocity around the high-

diameter components of the BHA. Holes that were in-gauge, on the other hand, tend to clean up the cuttings beds around the BHA quickly [33].

According to a study performed by SPE, Cameron, and Halliburton, sufficient hole cleaning with a flow rate of 4100 LPM, in a 12 ¼’’ deviated hole (>80°), often require at least 4 B/U to clean up the well [45]. Furthermore, a minimum flow rate of ~3100 LPM to enable sufficient cuttings transport was proposed by Mims and Krepp in 2003. Also, minimum effective rotation of 120 RPM was suggested, with optimal values between 120-180 RPM. However, these values for flow rate and rotation needs to be increased for long deviated sections and/or high ROP [46].

Moreover, Equinor’s best practice suggests that if a negative hole cleaning trend is observed, e.g. excessive ECD or SPP, one should evaluate increasing flow rate, increasing RPM and/or reducing ROP. Recommended parameters in a 12 ¼’’ section is minimum 3000 LPM and 130 RPM, however, it is specified that higher flow and rotation is needed in long, deviated wells or high ROP intervals. Regarding hole cleaning at TD, one should evaluate to reduce the ROP for the last stand while keeping flow rate and rotation high. Aiming to circulate 1 B/U during drilling the last stand. When reaching TD, circulation with reciprocation of last stand is recommended, although it should be evaluated to pull into competent formation if weak rock is present. The amount of circulation depends on the cuttings load up, inclination and ROP, but for a highly deviated, high ROP well with potential high cuttings load up, a minimum of 3 B/U is recommended [47].

3.4.7 Drillbit

Poor choice of drillbit could lead to insufficient ROP, excessive vibrations and have detrimental effects on the borehole quality. Normally, wells are drilled by using either a PDC (polycrystalline diamond compact), roller cone or hybrid bit.

The choice of drillbit is especially critical when it comes to drilling hard interbedded formations. An overload could occur when breaking through interbedded layers with a significant contrast in hardness, resulting in cutter damage. This could be mitigated by using an AST, which is located on top of the BHA to balance the WOB from surface against the reactive torque from the bit [10].

Furthermore, the common approach to drill hard rock has been to use a heavier set and more aggressive PDC design to enhance both durability and efficiency. However, by adopting this

design, the compressive loads on the BHA increase. Consequently, generating side forces leading to greater friction, and ultimately inducing stick slip. This could be avoided by adopting an aggressive, but lighter set PDC, which would reduce the requirement for high WOB while maintaining progress. Reduction in WOB will directly affect the torsional vibrations, which will decrease [10].

There are many ways to make the bit more aggressive, such as larger cutter size, increase spacing between cutters or decrease the amount of cutters. According to Akutsu et al. [10], the most significant effects are seen when reducing cutter chamfer angle and cutter back rake angle.

3.5 Liner

A liner is a casing string that does not extend all the way up to the wellhead but is instead suspended of the inside of the previous casing. This solution will reduce costs related to the reduction in steel needed, although it will render the running operations more complex.

A liner is run on drillpipe with a specialized running tool allowing for running, setting and cementing during the same trip. An illustration of a conventional liner system is shown in Figure 16. The liner hanger is situated at the top of the liner, which anchors the liner to the previous casing via wedge slips. These can be set either hydraulically (hydrostatic pressure differential) or mechanically (drillpipe rotation). In addition, a packer element is employed to seal off the annular space after cementing. Furthermore, landing collar, float collar and float shoe make up the shoe track, located at the bottom of the liner. The landing collar acts as a stopper plate, where the wiper plug comes to a halt. The float collar is made up of a short length of casing with an internal check valve, where the main purpose is to prevent flowback of cement slurry at the end of a cement job when the pumping is stopped. Similarly, the float shoe also contains a check valve to prevent back-flow, meaning that there are two barriers against reverse flow during cementing operations. In addition, a profiled structure is located at the end of float shoe, guiding the liner towards the borehole center. This will reduce the probability of taking weight at washed out areas or ledges. Moreover, as for a regular casing, the liner also embodies centralizers (stand-off devices) to reduce stand-off and consequently obtain a more efficient cement displacement.

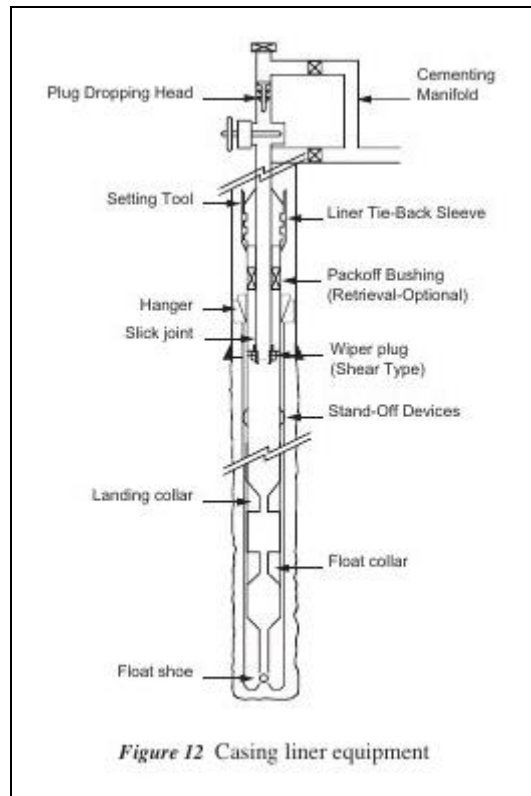


Figure 16: Schematic of standard liner equipment needed to run and cement the liner. [48]

Although prevalent, the conventional liner hangers encounter problems related to increased pressure loss in the liner hanger area when the hanger is set, in addition to slips pre-setting or failing to set. Increased pressure drop is due to the anchored slips, which provides a tortuous flow path for the mud when it is forced around the engaged slips, consequently increasing the ECD. Also, the conventional slips render an area especially prone to trapping of cuttings, fines and LCM materials. This could also affect the ECD and worst-case block off the annular space, resulting in a pack off [49]. This has also been indicated by a complex computational fluid dynamics (CFD) simulation with experimental validation, where it was observed that the flow path lines on both sides of the slips were prone to recirculation. This creates a hold-up of flow, consequently yielding higher pressure loss through the hanger area [50].

Furthermore, expandable liner hangers (ELH) could be employed to eliminate the risk of pack-off and elevated ECD. This is due to their design, which does not incorporate slips. Instead, the ELH system is anchored to the previous casing after cementing, by expanding the liner hanger body and provide metal-to-metal and/or elastomer-to-metal sealing. The hanger body is expanded by a high-diameter internal cone which is pressurized to force it down through the body and consequently expand the hanger. Moreover, since the ELH is not set until after the cement job, it has the ability to be reciprocated before and during cementing, something the

conventional liner hanger does not. Also, if sufficient circulation cannot be obtained at TD, the ELH could be retrieved with ease, as opposed to the conventional system, where the liner has to be cut and pulled if the slips are engaged. Furthermore, it has been shown that employing an expandable liner hanger system, could mitigate a lot of the problems related to cement placement in long, highly deviated wells [27].

3.6 Logging

Different logging tools have been used when drilling the Johan Sverdrup injection wells. The most essential logs used for interpretation of formation properties and borehole quality are presented below.

3.6.1 Caliper log

A caliper log is a diameter measurement of the borehole, along its depth. Caliper logs can either be acquired through wireline logging or logging while drilling (LWD). When employing wireline, the caliper tool is usually measuring the hole diameter with the aid of two or more expandable arms, with different phasing. The arms are able to move in and out and moves along with the borehole geometry as the logging tools is lowered into the well. This movement is transformed into an electric signal [15].

Open hole size can also be derived from LWD tools via acoustic, resistivity or nuclear measurements. These types of measurements are transmitted to the surface and can be displayed real-time.

3.6.2 Image log

Borehole imaging tools could be found both for wireline and LWD. However, both of them utilize variations in rock properties to produce an image of the borehole wall. LWD imaging, which are used for the injection wells, normally includes a lot of different measurements, e.g. gamma ray, neutron-density, resistivity, acoustic etc. Although these measurements appear to be at the exact time of drilling, one has to keep in mind that these measuring tools are situated several meters behind the bit. Consequently, there could be a delay of a few minutes to several hours, depending of the distance from the bit and drilling progress.

For the Johan Sverdrup injection wells, image logs were obtained with LithoTrak by Baker Hughes. The images were generated using both azimuthal sector density and photoelectric measurements, along with caliper measurements while drilling [51]. The image logs presented later in this thesis will contain density and photoelectric factor (PEF) imaging, with an approximate depth of investigation (DOI) of 2.5–4 inches and 1 inch, respectively. In addition, caliper, density-neutron, resistivity, ROP, WOB, inclination and azimuth values are presented alongside the images.

Values are measured in sectors around the whole circumference of the borehole, creating a 360-degree image. As one can observe from Figure 17, the 2D images of the borehole, can be wrapped to create a 3D visualization.

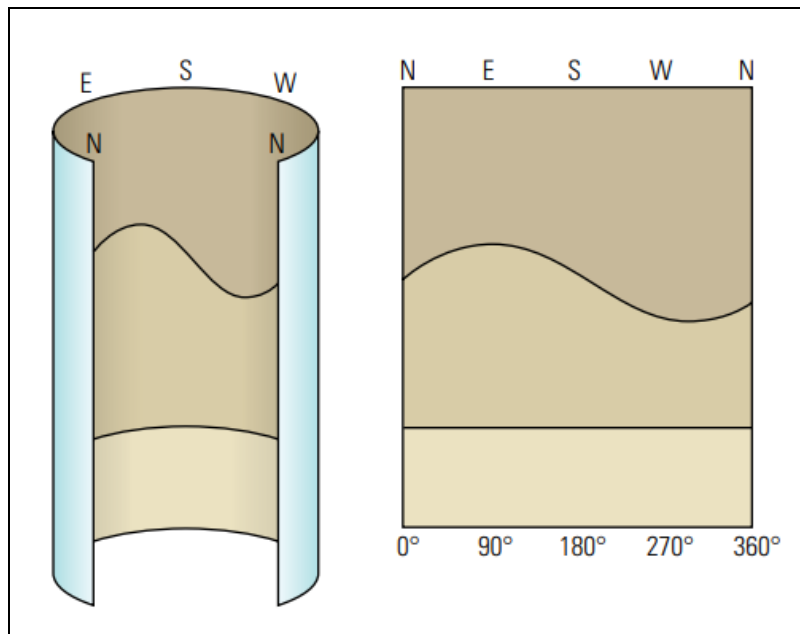


Figure 17: Illustrating the measurements 360 degrees around the borehole, where the top side is situated at 0° and 360° , while the low side is situated at the center, namely 180° . The 2D-image (right) could be wrapped into a 3D image of the wellbore (left). [52]

3.6.3 Gamma Ray log

The gamma ray (GR) log exploits the natural occurring radioactive materials such as uranium, thorium, potassium, radium and radon. There is a strong correlation between GR readings and radioactive isotope content of minerals, which is used to determine rock composition. Usually, high GR readings announces the presence of fine-grained deposits or clay-rich formations, e.g. mudstone, claystone or shale. These formations are responsible for most of the natural occurring radioactive readings, making GR suitable for identifying such formation. Uranium, Thorium and Potassium are found in these types of formation. A low GR reading, on the other hand, could indicate coarse-grained limestone or sandstone. The DOI of the gamma ray tool is usually a few inches [53].

3.6.4 Density-Neutron log

Both density and neutron logs are nuclear measurements. The neutron logging tool contains a neutron source, with a main purpose of emitting high energy neutrons directed towards the formation. When inside the formation, these neutrons undergo scattering and consequently losing energy and generating high energy GR. This scattering process develop most efficiently with hydrogen atoms. The occurring GR or low energy neutrons can be detected, and their count rate are correlated to the amount of hydrogen encountered in the formation. Naturally, if the formation contains large amounts of hydrogen, the neutrons are absorbed rapidly and slowed down over a short distance. Consequently, the count rate of low energy neutrons and GR count is low for the tool, yielding a positive reading for high-porosity formations. This is due to the presence of formation water or hydrocarbons inside the pores, rendering a higher hydrogen index (HI). Note that the HI is greater for hydrocarbons, than for formation water [54].

Similarly, density logging tools also contain a radioactive source, usually caesium-137 or cobalt-60, which emits gamma rays of medium energy. When the GR enters the formation, its scattered during interaction with the electrons in the atoms constituting the formation. Consequently, the energy of the GR is reduced after interaction with elections. In the energy of the GR is low enough when encountering an electron, photoelectric absorption may occur. The amount of GR reaching the detectors incorporated in the density tool is dependent on the electron-density of the formation. As a result, formations with high bulk density will attenuate the GR significantly, yielding low readings at the detectors. Similarly, low bulk density yields high readings [55].

The combination of the density and neutron logs are remarkably important for lithology identification. Since both measurements yields values for total porosity, they should overlie each other if plotted with compatible scales. However, it should be noted that these lines will only superimpose if exposed to limestone formations containing only fresh water. The separation of these two logs, relative to each other, can be used to interpret the measured lithology. E.g. clean sandstones will yield a negative separation (higher neutron values relative to density values) and shale will render a positive separation (higher density values relative to neutron values) [54].

4 Injection Wells

An injection well is a well where fluids are injected, rather than produced, where the primary objective commonly is to maintain reservoir pressure. Injected fluids may include fresh water, sea water, re-produced water, brine, gas, or water mixed with chemicals. Water-injection is common on offshore wells, where filtered and/or treated seawater is injected into a lower water-bearing section of the reservoir. This is regarded as an enhanced oil recovery (EOR) process.

There are several considerations that must be done when designing an injection well. Basically, fluid is injected with tremendous pressures, which must be transported from pump to reservoir while maintaining well integrity. Consequently, high quality, long lasting barriers must be in place. Furthermore, during a pilot survey of well integrity issues on the Norwegian Continental Shelf (NCS), it was found that 75 of 406 wells had integrity issues, where 27 of these were injection wells, as shown in Figure 18 [35].

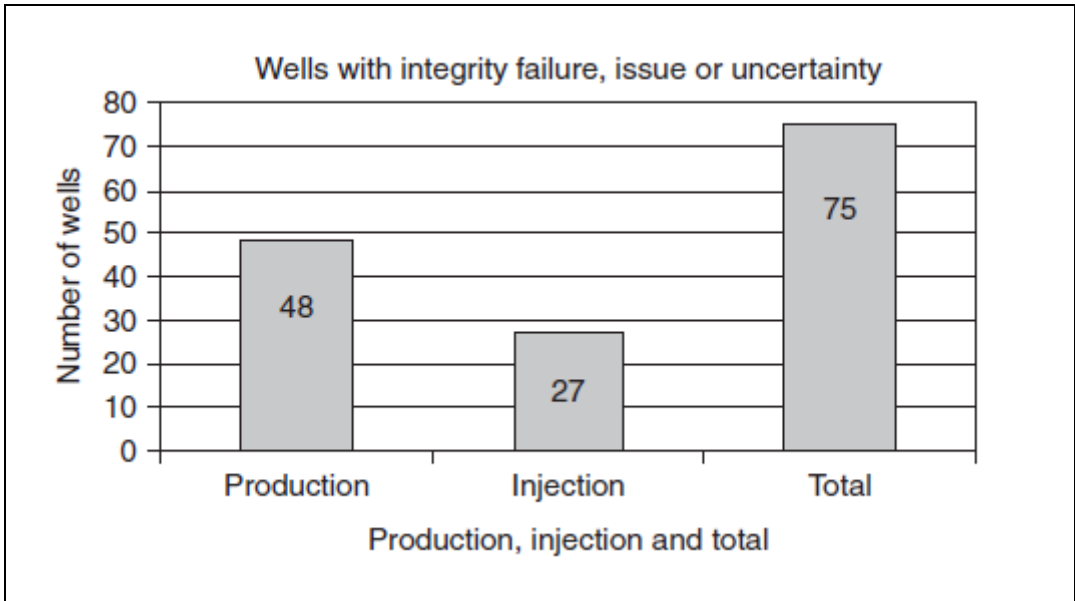


Figure 18: Production wells, injection wells and total wells reported with integrity failure, issue or uncertainty in this survey. [35]

Also, Water Alternating Gas (WAG) is a part of the recovery procedure. This is a method where water injection and gas injection are carried out alternately to yield better sweep efficiency and reduce gas channeling from injector well to production well [56].

Generally, the injectors are completed with a 6 5/8” or 5 1/2” standalone screen, including a swell packer above. Furthermore, above the swell packer follow an isolation packer and a production packer containing a pressure/temperature gauge (PPS gauge) in between. In most cases, both packers are placed below the top of the cap rock. This gauge is essential concerning verification of pressure containment, and consequently the integrity of the well as it starts to inject. This is verified by measuring the pressure in the annulus (though a couple of perforations, see Figure 20): if the pressure spikes during a pressure test or when injection is initiated, this would indicate a connective path between the injection point and the annulus below the cap rock. Therefore, the cement bonding in the annulus is insufficient to contain the given pressure, indicating a poor cement job.

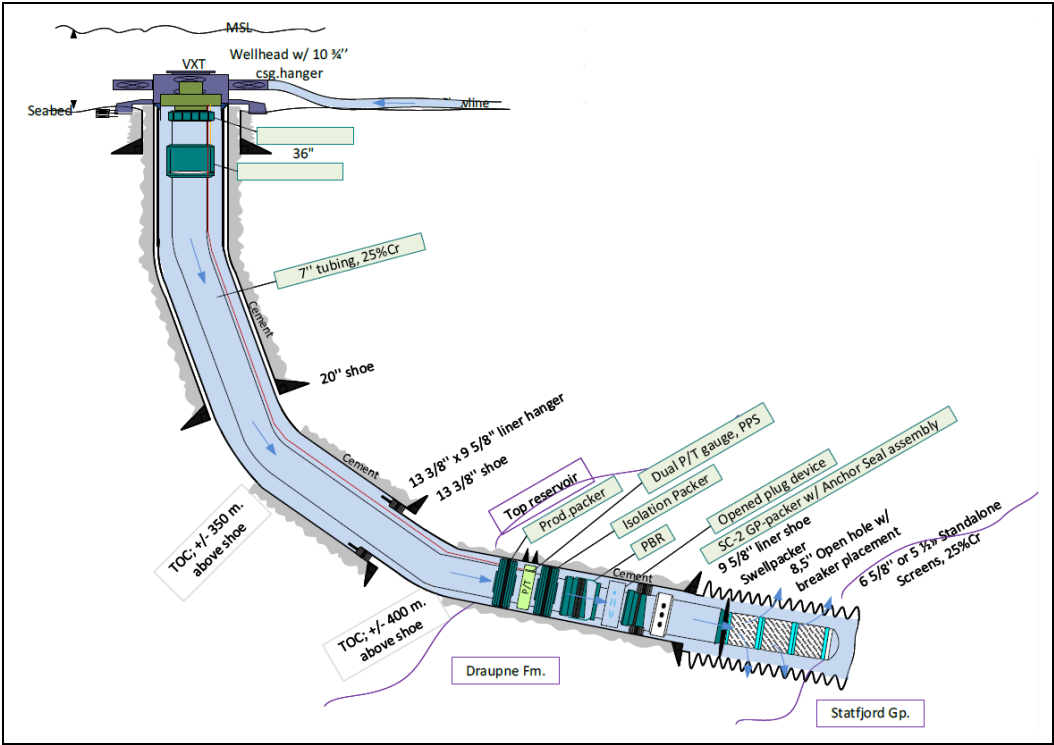


Figure 20: Water injector design on Johan Sverdrup

Additionally, after some time of injection, the pores in the reservoir will be partially plugged. This plugging will be most severe during PWRI, where the formation most likely will fracture. Therefore, a comprehensive study of the fracture propagation in the reservoir rock, Draupne and Statfjord, is necessary in order to indicate if the injection pressures will eventually cause fracturing in the cap rock and compromise the integrity of the reservoir.

4.2 Regulations

As previously mentioned, the primary cement on the 9 5/8” liner acts as a barrier towards injection pressures. Failure to meet the criteria for acceptable cement will result in lower injection rates than planned, due to not being able to inject with a pressure above the cap rock strength. Alternatively, one could try to obtain a better cement job by performing a side track.

For most of the injection wells the injection pressures will eventually exceed the fracture closure pressure of the cap rock. This pressure is equal to the minimum in-situ stress, since the pressure required to open a fracture is the same as the pressure needed to counteract the rock stress perpendicular to the surface [57]. The injection pressure could exceed the minimum in-situ stress of the cap rock during SW injection, although it is more likely to happen during PWRI. Cold water could mitigate the need for increased injection pressures due to minimizing the fraction injection pressure. This is related to a thermo-elastic stress reduction in the reservoir matrix [58]. According to NORSOK D-010 rev. 4, for wells injecting at a pressure greater than the fracture closure pressure at injection depth, the following applies [59]:

- *“The production packer should be set at a depth ensuring the injection or a casing leak below the production packer will not lead to fracturing of the cap rock or leak to shallower formation when applying maximum injection pressure)” (see Figure 21)*
- *“The casing/liner shall be logged and as a minimum have bonding from uppermost injection point (production packer) to 30 m MD above top reservoir.”*
- *“It shall be documented that injection will not result in a reservoir pressure exceeding the strength of the cap rock.”*

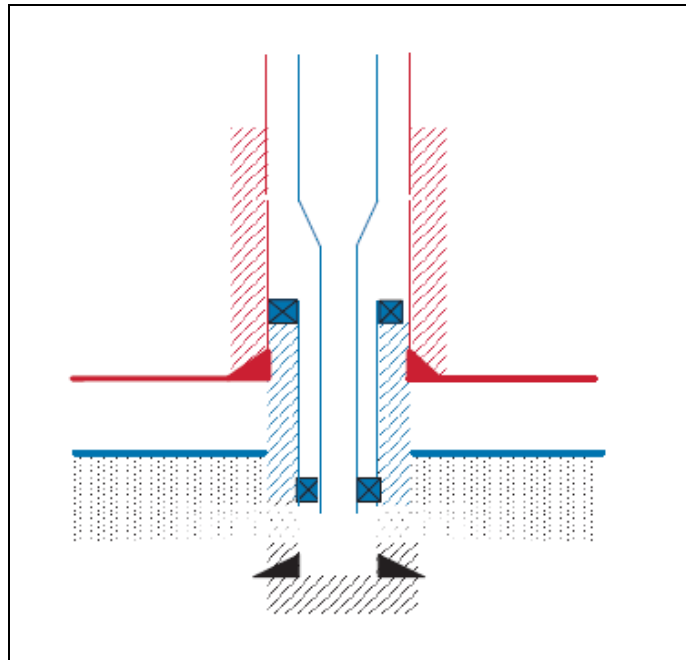


Figure 21: Well Barrier Schematic of an injection/disposal well with injection pressures above minimum in-situ stress (minimum horizontal stress, σ_{min}).

For Equinor’s internal regulations, injection with downhole pressure exceeding the stress in the cap rock shall only be done if the following conditions are fulfilled:

- *“The well shall have a deep-set production packer in the reservoir, cement behind liner/casing from injection point to caprock shall be verified sealing by a cement log, automatic choke control, and shall be placed outside manned high risk zones.”*
- *“Modelling work (using a Equinor approved 3D fracture simulator) shall show that there is no risk of vertical fracture growth from the injection interval up into the cap-rock.”*
- *“A dispensation shall be approved.”*

Equinor’s internal requirements state that a 30 m continuous logged cement interval, interpreted with high isolating potential, is required to qualify as a barrier. However, a dispensation can be made for a 30 m cumulative cement interpreted with “High isolating potential”, where the minimum continuous interval that can be considered as contributing to the 30 m cumulative total, is 10 m.

Furthermore, according to GL3507, “Well Integrity Guidelines – offshore operations”, the following applies for a single well injecting with higher pressure than the cap rock strength (σ_{\min}):

- *“Studies shall be conducted to determine the injection zones capacity for the injected fluid. The target reservoirs shall have sufficient permeability, thickness, and prevalence in order to ensure the integrity of the cap rock over the well life, and limitations on injection pressure shall be set.”*
- *“The cement shall provide hydraulic isolation from the upper most injection point (production packer) to a minimum of 50 m MD above the top reservoir verified by cement logs. Hydraulic cement isolation of the reservoir shall also be verified for nearby wells that can be exposed to the injection pressure due to risk of fracture propagation or leakage.”*
- *“It is accepted for a deep packer completion to only have one annular barrier (with formation integrity) towards injection pressure. Two annular barriers towards reservoir pressure shall be in place.”*

By examining both external and internal requirements, it is found that somewhat stricter demands are present for the internal guidelines. Here, it is advised to obtain 50 m MD cement above top reservoir, to act as a barrier against injection, as opposed to 30 m MD according to NORSOK. In addition, a deep-set packer is desired according internal regulations.

4.3 Barriers

As stated in section 4.2, the Equinor guidelines specify that for injection wells with a deep-set packer, only one barrier against injection pressure is sufficient, whereas two barriers shall be in place towards reservoir pressures. All injection wells except F-13 and G-2 has a deep-set packer, meaning that the production packer is set inside the reservoir. For F-13 and G-2, it is uncertain if the thickness of the reservoir is satisfactory regarding injecting with a pressure above σ_{\min} . A thin reservoir section will yield a shorter path from the uppermost injection point

(production packer) to the bottom of the cap rock and could potentially lead to out of zone injection (OOZI) after some time, according to Equinor's 3D fracture simulator.

For the wells containing a deep-set packer, Figure 22 illustrates the well barrier against injection pressures. Moreover, regarding the barriers against reservoir pressures, Figure 23 shows a well barrier schematic of the two barriers in place. By examining the two abovementioned figures, the demand for a continuous isolating barrier in the 9 5/8" liner cement is evident.

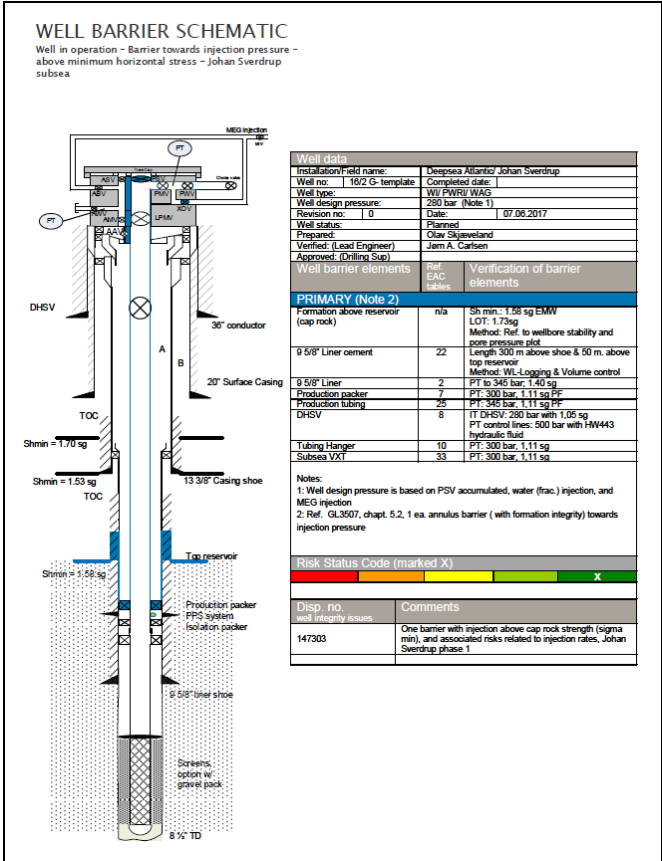


Figure 22: Well Barrier Schematic of the barrier in place towards injection pressure, where the pressure is above minimum horizontal stress of the cap rock. Example from G-3.

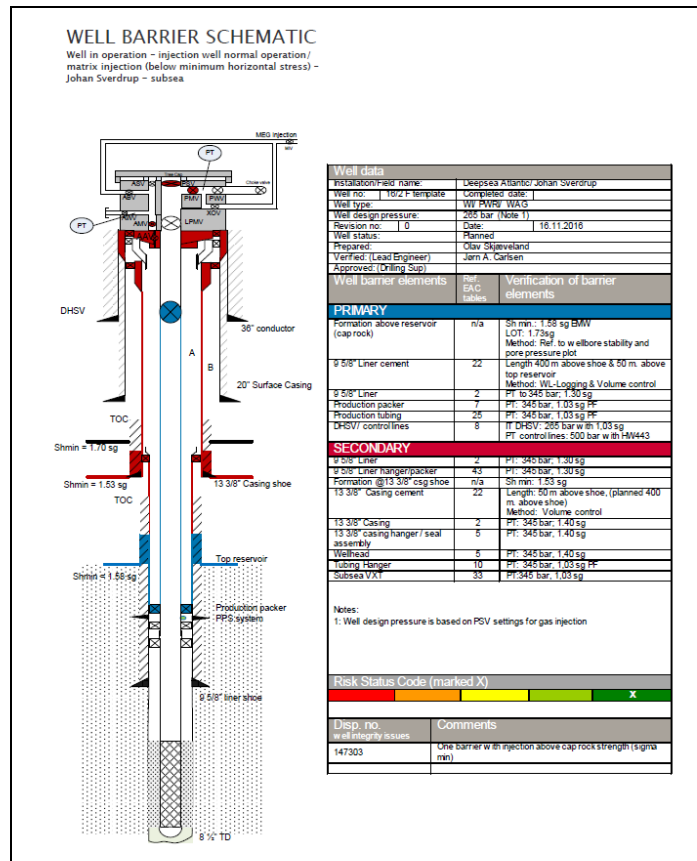


Figure 23: Well Barrier Schematic of the barriers in place towards reservoir pressure, where the pressure is below minimum horizontal stress of the cap rock. Example from F-14.

For injection wells without the possibility for a deep-set packer, namely F-13 and G-2, the barriers against injection pressures and reservoir pressures are illustrated in Figure 24 and Figure 25, respectively. Here, the guidelines state that there is a need for two barriers against both the injection pressures and the reservoir pressures. As one can observe from Figure 24, the 9 5/8" liner cement is an essential well barrier element for both the primary and secondary barriers. Consequently, there is a need for two intervals of minimum 30 m MD good isolating log-verified cement behind the liner for it to be able to act as a barrier toward injection pressures. Towards reservoir pressures (Figure 25), however, only one of the (minimum) 30 m MD intervals needs to be placed behind the 9 5/8" liner, where the other interval is placed behind the 13 3/8" casing.

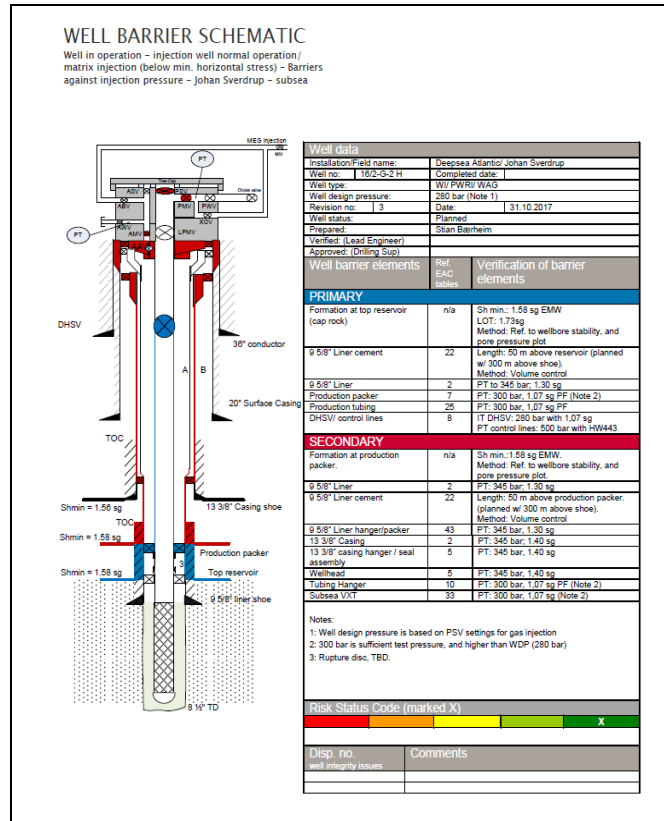


Figure 24: Well Barrier Schematic of the barriers in place towards injection pressure, where the pressure is below minimum horizontal stress of the cap rock. This is an example of an injection well where the production packer is placed above the reservoir, i.e. not a deep set packer. Example from G-2.

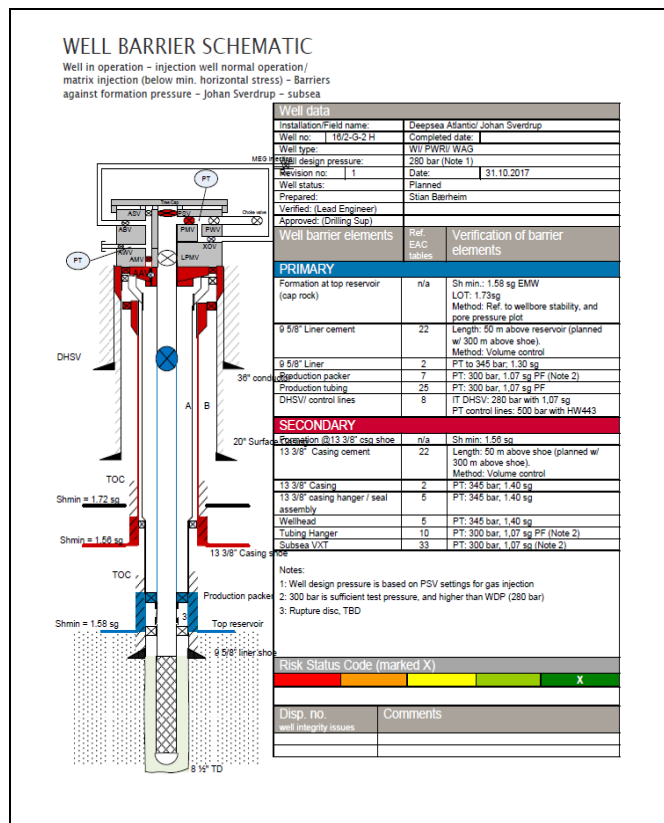


Figure 25: Well Barrier Schematic of the barriers in place towards reservoir pressure, where the pressure is below minimum horizontal stress of the cap rock. This is an example of an injection well where the production packer is placed above the reservoir, i.e. not a deep-set packer. Example from G-2.

5 Results

During the course of writing this thesis, all ten of the drilled injector wells on Johan Sverdrup were studied. The main objective is to unlock the 9 5/8” liner cement jobs performed on these wells; setting the scene for a major investigation of parameters affecting the cement job. Data collection and analysis were performed in order to investigate if there was any correlation of parameters for the wells featuring poor liner cement. Throughout this section, the figures and tables regarding the injection wells will be sorted in chronological order from left to right, where the first injection well to be drilled was F-11 and the last was G-2 (as of June 2018).

5.1 Cementing

5.1.1 Introduction

The injection wells on Johan Sverdrup were all cemented with Portland Class G cement, where half of the wells used both lead and tail cement. As one can observe in Table 2, the volumes pumped tend to be relatively equal, except for spacer volume on the E-wells, in addition to G-4 T2. For these wells, a longer contact time was obtained between the SealBond spacer and the formation/liner. A similar volume was planned for the other wells, but due to pack-off tendencies during circulation, the volumes were reduced. It was believed that the spacer was capable of mobilizing an increased amount of cuttings, which could make matters worse in terms of pack-off.

Table 2: Volumes and densities of the cement used on the different injection wells.

	F-11	F-14	F-12	F-13	E-2	E-1	E-3	G-4 T2	G-3	G-2
Tail cement volume [m ³]	21,5	21,5	21,5	16,7	21,5	15,2	15,2	15,2	15,2	15,2
Tail cement density [s.g.]	1,9	1,9	1,9	1,9	1,9	1,9	1,9	1,9	1,9	1,9
Lead cement volume [m ³]	-	-	-	-	-	6,3	6,3	6,3	6,3	6,3
Lead cement density [s.g.]	-	-	-	-	-	1,9	1,9	1,9	1,9	1,9
Spacer volume [m ³]	12,4	12,4	12,4	12,4	22,4	22,4	22,4	20	12,4	12,4
Spacer density [s.g.]	1,55	1,55	1,55	1,55	1,55	1,55	1,55	1,55	1,55	1,55
Low viscosity OBM volume [m ³]	30	30	30	30	30	30	30	30	30	20
Low viscosity OBM density [s.g.]	1,2	1,2	1,25	1,25	1,25	1,25	1,25	1,25	1,25	1,25

Moreover, additives used for the injection wells are equal for all wells: Glass G cement, defoamer, binding agents (anti-gas migration), retarder, fluid loss agents and expansion agent. The exception is G-2, where a dispersant also was added. Even though the additives were the same, different concentration of retarder was used. This was especially critical for the wells with lead and tail cement. Here, a lead cement was added in order to keep hydrostatic pressure on the underlying tail cement (ref. section 3.2.3.1). This was done as an attempt to improve the isolating potential of the cement in the reservoir section, which had shown patchy characteristics for the previous wells.

In addition to lead and tail cement, other alterations were done from E-2 to E-1. The objective of these changes was to apply less pressure on the unset cement. This was achieved by waiting until after logging to pressure test the well, in addition to omit applying pressure against the cement when releasing the liner running tool. Other parameters not related to the cementing process were also altered, namely decreasing the maximum DLS limit in the reservoir and adding more LCM while drilling.

5.1.2 Results

Four of the injection wells lost rotation during cementing, characterized by a rapidly increasing torque until the maximum torque limit was reached and rotation ceased. Table 3 gives an overview of the cement job parameters for the different wells. As one can observe, rotation was lost on F-11, F-14, G-4 T2 and G-3. In addition, F-14 experienced total pack off and went on losses during the cement job. Displacement rates were immediately reduced, except for G-4 T2. A reduction in displacement rate was done as a mitigating action to an increasing stand pipe pressures (SPP). Increasing SPP and lost rotation are solid indicators of an oncoming pack-off. By decreasing the flow rate, SPP will also decrease and consequently lessen the compacting forces on the debris around the liner.

Table 3: Overview of displacement rate and rotation when displacing cement in annulus, including wells with lost rotation during displacement.

	F-11	F-14	F-12	F-13	E-2	E-1	E-3	G-4 T2	G-3	G-2
Initial Rate [liter/min]	1000	1000	1000	1000	1600	1600	1600	1000	1000	1000
Rotation [RPM]	20	20	20	20	20	20	20	20	20	20
Lost rotation [Yes/No]	Yes	Yes	No	No	No	No	No	Yes	Yes	No
Rate after lost rotation [liter/min]	500	500	-	-	-	-	-	1000	500	-

In an attempt to uncover the reasons for these lost rotation incidents, the height of cement at lost rotation was calculated. This was done by finding the amount of pump strokes between shearing the bottom wiper plug until the start of torque increase and converting this value to cubic meters. Calculations are shown in the following equation:

$$N_{strokes} \times 16,7 \frac{l}{stroke} \times \frac{1}{1000} \frac{m^3}{l} = V_{pumped} \quad (6)$$

where,

$N_{strokes}$, number of strokes

V_{pumped} , volume pumped from plug is sheared to rotation is lost, m^3

Then, since the wiper plug lands and shears in the landing collar, the shoe track volume has to be subtracted. Calculations are shown in the following equation:

$$V_{pumped} - V_{shoe track} = V_{ann} \quad (7)$$

where,

V_{pumped} , volume pumped from plug is sheared to rotation is lost, m^3

$V_{shoe track}$, volume of cement inside shoe track, m^3

V_{ann} , volume of cement in annulus at lost rotation, m^3

Finally, the remaining volume is divided by the annular capacity of a 9 5/8'' liner in a 12 1/4'' hole to obtain the length of cement above liner shoe. Calculations are shown in the following equation:

$$\frac{V_{ann}}{C_{ann}} = L_{cement} \quad (8)$$

where,

V_{ann} , volume of cement in annulus at lost rotation, m^3

C_{ann} , capacity of the annulus, $0,0291 m^3/m$

L_{cement} , length of the cement column in the annulus at lost rotation

By subtracting the length of cement with the depth of the liner shoe, one obtains the depth of the top of cement at lost rotation. The results are shown in Table 4.

Table 4: Length of cement and depth of top cement at lost rotation. Including the corresponding formation.

	F-11	F-14	G-4 T2	G-3
Length of cement [m]	240	165	227	232
Depth of top cement at lost rotation [m]	2583	2196	2662	2144
Related formation	Bottom Sola	Top Aasgard	Top Aasgard	Top Aasgard

Interestingly, the cement seems to be located approximately in the Sola/ Aasgard boundary at lost rotation, according to the calculations. As previously mentioned, this is a boundary which is prone to wash outs due to weak formations in Sola and hard stringers in Aasgard.

As mentioned in section 3.3.4.1, rotation during cementing could prove important to achieve a good continuous isolating cement around the borehole, especially in deviated wells. A correlation between the top of good cement on the logs (T_{log}) and the theoretical top of cement at lost rotation ($T_{theoretical}$) was identified, as shown in Figure 26 and Figure 27. From the figures, it is obvious that the difference between the two depths is minimal. Although, one should keep in mind that the calculations were done based on the assumption of an in-gauge borehole, which is not the case in practice. However, this would make the theoretical values overestimate the

height of the cement column, which would render the difference between T_{log} and $T_{theoretical}$ positive. As seen in Figure 27, that is the case for these wells.

This result strengthens the statement that casing rotation is essential for obtaining a good cement job in highly deviated wells. In addition, for G-3, the displacement rate was lowered to 500 LPM long before rotation stopped (displaced 5,3 m³ out of 6,8 m³ with low rate and rotation), which means that the cement was displaced with a very low rate and rotation, and still managed to yield a fully isolating cement.

Since only four of the injection wells experienced lost rotation, the amount of data is somewhat insufficient to conclude these findings as absolute certain. Nevertheless, it should be kept in mind during the cementing of the upcoming injection wells, to see if the trend will continue. Furthermore, in order to uncover the underlying reasons for lost rotation during cementing, it became clear that the drilling, wiper trip and liner running phases should be investigated.

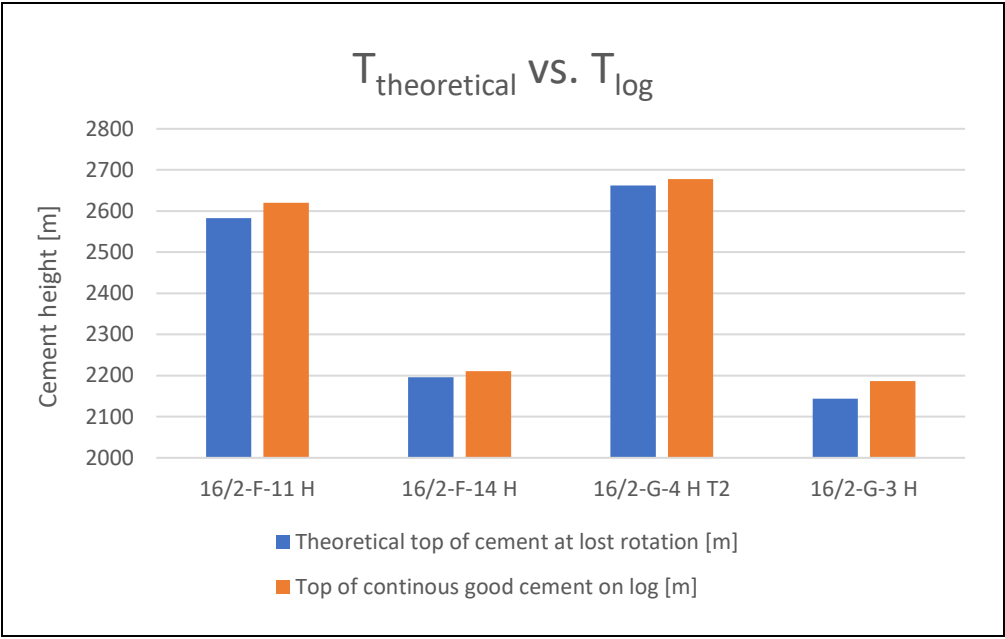


Figure 26: Theoretical top of cement at lost rotation versus the top of continuous cement from the logs.

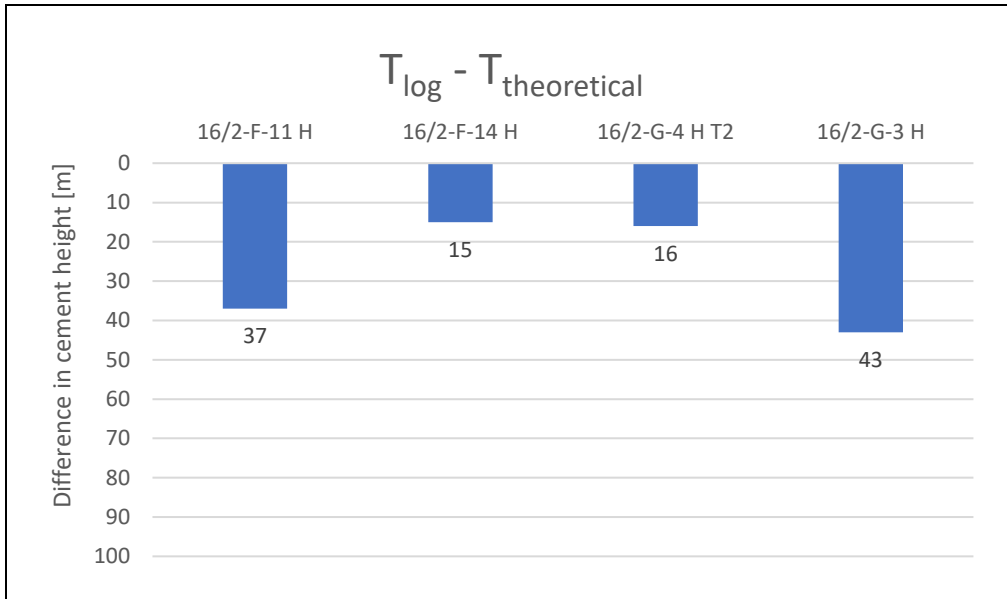


Figure 27: Difference between the top of continuous good cement on the logs and the theoretical top of cement at lost rotation.

As previously mentioned, most of the F-wells in addition to E-2 experienced low to medium bonding cement in the reservoir section (Draupne Fm. 1). After implementing certain changes (see section 5.1.1), the amount of good cement in the reservoir increased drastically for E-1 and E-3. Figure 28 illustrates the length of good cement both below and above the top reservoir (Draupne 2 Fm). For G-4 T2, the deepest 70–130 meters logging interval experienced poor logging quality, most likely due to debris in the well, according to the cement reports. Consequently, rendering the interpretation inaccurate. Also, only a few meters of the reservoir were exposed for G-2, which possessed good quality cement.

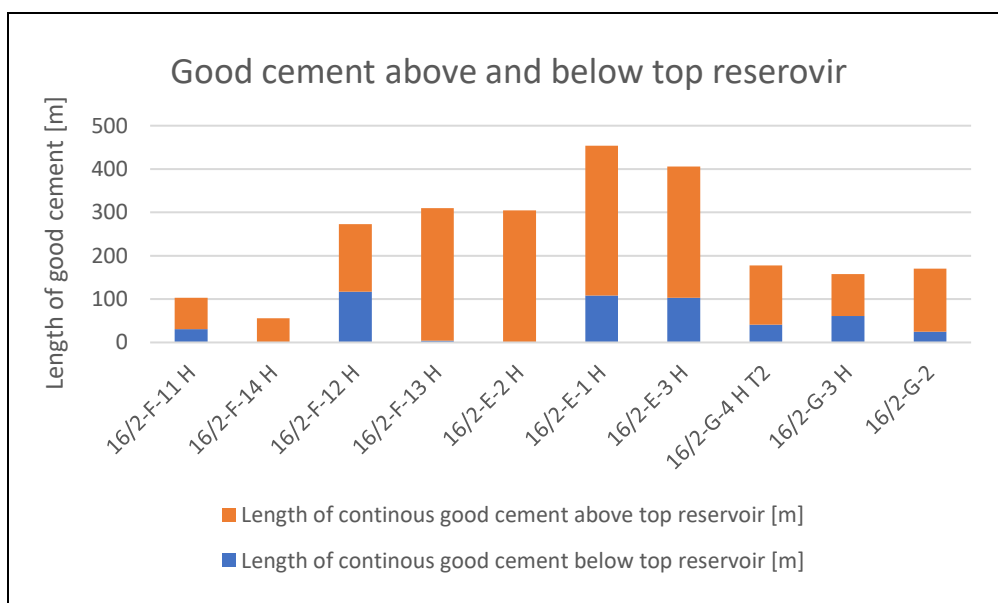


Figure 28: Good, isolating cement above and below top reservoir (top Draupne Fm. 2).

5.2 Drilling

When drilling a well, it is essential to plan towards the cement job. Ideally, this means creating a smooth borehole with a carefully selected mud to maintain well stability. Of course, this is not achievable in practice. There is an abundance of factors that could adversely affect the borehole quality, such as unstable or weak formations, insufficient mud weight, inappropriate BHA, vibrations and undesirable values for WOB, ROP, flow rate and RPM during drilling. These parameters are all contributing to a poor borehole geometry.

During the creation of this thesis, the drilling of all ten injection wells have been studied in detail. Certain values have been extracted from real-time logs for each well, namely ROP, WOB, flow rate, RPM and torque. In addition to lateral vibrations, DLS, inclination and stick slip. The real-time log is pictured in Figure 29. Maximum and minimum values were extracted for the drilling of Sola Fm., Aasgard Fm. and Draupne Fm. 2. These are the formations of interest which will be investigated further in this section.

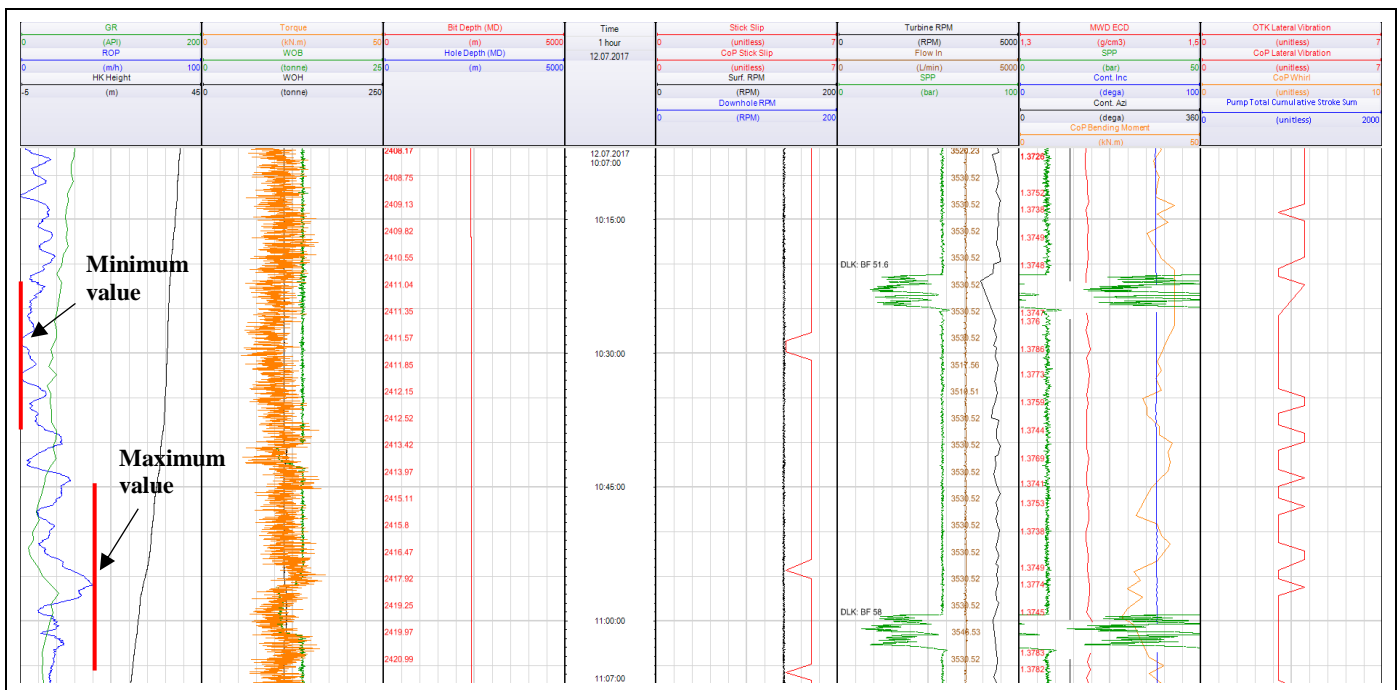


Figure 29: Real-time log for E-1. Illustrating how the different maximum and minimum values were obtained.

5.2.1 Introduction

Some similarities in design between the wells are evident. All wells drilled a 12 ¼” section containing a cemented 9 5/8” liner. The drilling was done with an oil-based mud (OBM) partly due to its friction-lowering and swell-preventing effects, which will prove beneficial when

drilling calcareous and clay-containing formations, respectively. Also, the 12 ¼” section have a relatively similar angle when reaching TD, except for F-13 which was planned to hit the top of the reservoir at a lower angle. This is illustrated in Figure 30.

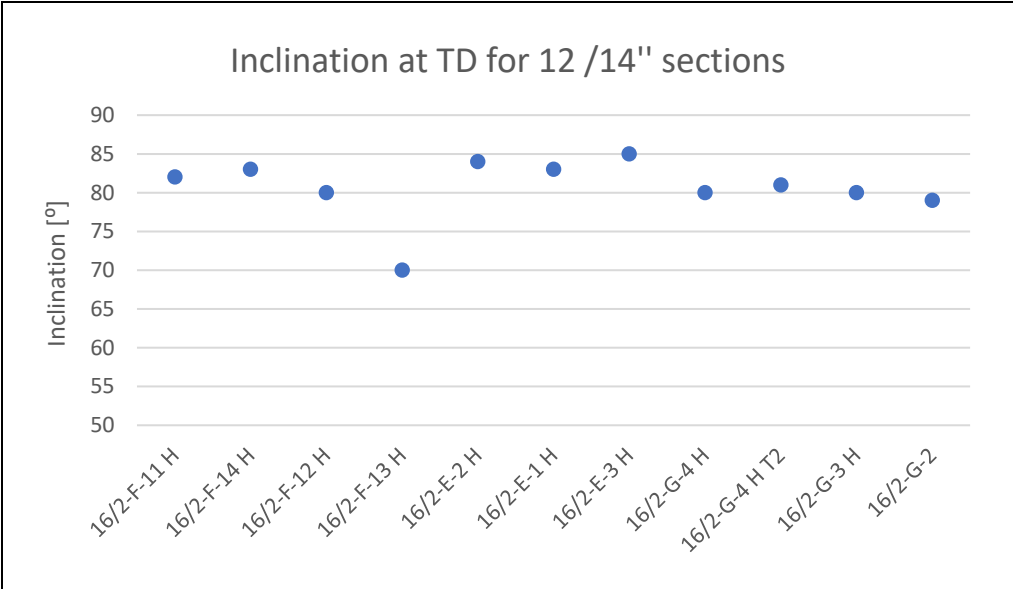


Figure 30: Inclination at TD for the 12 ¼" section of the Johan Sverdrup injector wells.

Not surprisingly, there are also several dissimilarities for the injector wells. Nearly every well was drilled with a PDC bit through the 12 ¼” section, except from F-12, where a hybrid bit was used.

Regarding drilled length, which is critical in terms of affecting the friction in the well. Torque and drag increases with length of the well, where the open hole section possesses the highest friction factor. The 12 ¼” section lengths are shown in Figure 31. The difference in exposed open hole for the wells are obvious, where F-11, F-12, G-4, G-4 T2 and G-2 stands out as the longer sections. A lot of drilling problems are related to increased torque and drag, e.g. stick slip or whirl, which will contribute to increasing irregular geometry.

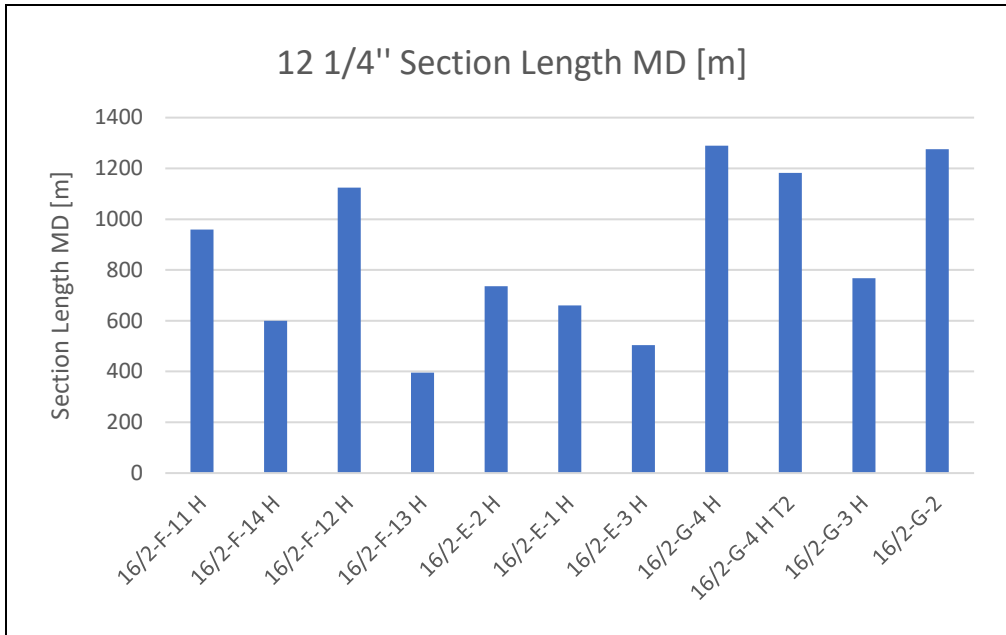


Figure 31: Length of the 12 1/4" sections on the Johan Sverdrup injectors. Lengths are given in measured depth.

Furthermore, mud weight has also been altered. During the first two wells, F-11 and F-14, the mud weight (MW) was 1.33 s.g., which was dictated by a strategy to challenge the theoretical shear failure [60] [61]. Then, for F-12 and F-13, the MW was increased to 1.4 s.g. For the E-wells, identical MW of 1.33 s.g. was maintained. Similarly, the G-wells had a MW of 1.4 s.g. for all wells. Table 5 illustrates the mud properties. For the choice of MW, there is a tradeoff between avoiding losses and mud invasion when drilling into the reservoir (MW too high) and avoiding shear failure of the borehole wall (MW too low).

Table 5: Overview of the mud properties for all injector wells.

	F-11	F-14	F-12	F-13	E-2	E-1	E-3	G-4	G-4 T2	G-3	G-2
Mud weight [s.g.]	1,33	1,33	1,4	1,4	1,33	1,33	1,33	1,4	1,4	1,4	1,4
Mud type	OBM	OBM	OBM	OBM	OBM	OBM	OBM	OBM	OBM	OBM	OBM

As previously mentioned, some of the formations possess different properties and compositions depending on the template. Consequently, caution should be taken when comparing formations between wells. This is explained in section 2.4.2.

5.2.2 Results

The results from the analysis of data will be presented for each of the formations of interest: Sola Fm., Aasgard Fm. and Draupne Fm. 2. The objective is to investigate how the given well conditions occurred, and subsequently try to optimize performance in the related formation. There is no doubt that poor well conditions have a potential to compromise the oncoming cement job.

5.2.2.1 Sola Fm.

The weak Sola formations vary in drilled length for the different templates. As shown in Figure 32, Sola is especially long for the E-wells. Moreover, all wells, except F-12, G-4 and G-4 T2, build an angle through Sola.

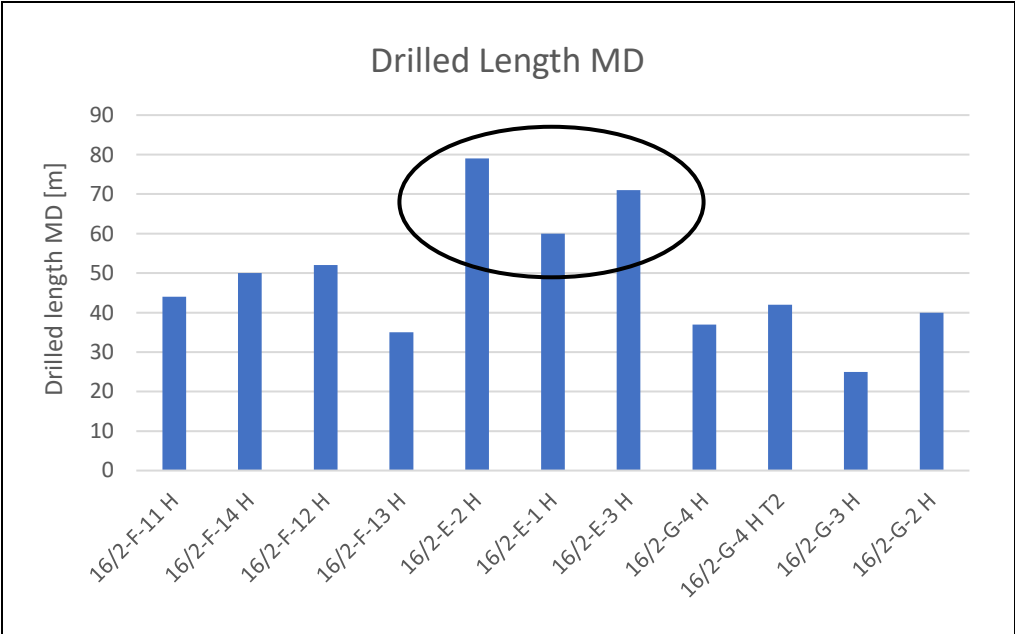


Figure 32: Drilled length of Sola for the different wells on Johan Sverdrup. Length of Sola for the E-wells shown inside circle.

In an attempt to visualize the condition of the borehole, the real-time caliper logs were examined for the different wells. If these logs yield valuable information about the condition of the borehole in real-time, action could be taken immediately to find the optimal drilling parameters. Neither G-2, nor E-1 has a caliper log, due to simplified BHA and tool failure, respectively. Moreover, the real-time caliper logs revealed that most of the wells did not show signs of significant over-gauged sections. However, two of the wells showed some larger-diameter sections towards the Sola/Aasgard interface, namely F-14 and G-4 T2. Figure 33 shows the caliper logs for the two wells, where Sola lies within the dashed squares.

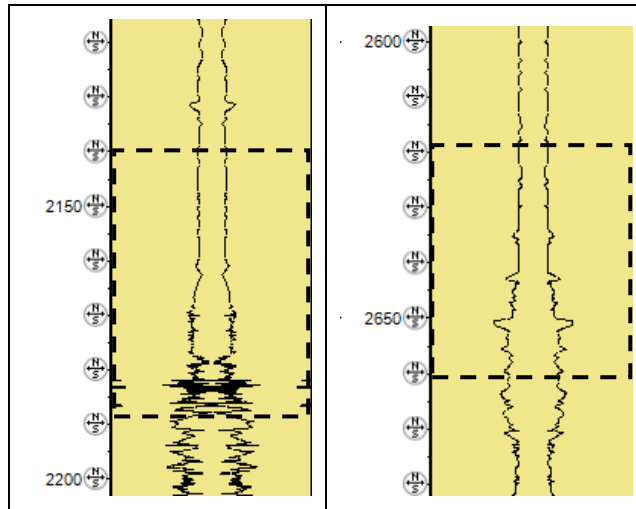


Figure 33: Real-time caliper logs for F-14 (left) and G-4 T2 (right). Sola Fm. is situated within the dashed lines. The left axes are given in meters.

G-4 T2 had a significant reduction in ROP towards the end of Sola, which could indicate a stringer. F-14, on the other hand, maintained constant ROP. As shown in Figure 34, all the G-wells struggled with varying ROP due to hard formations.

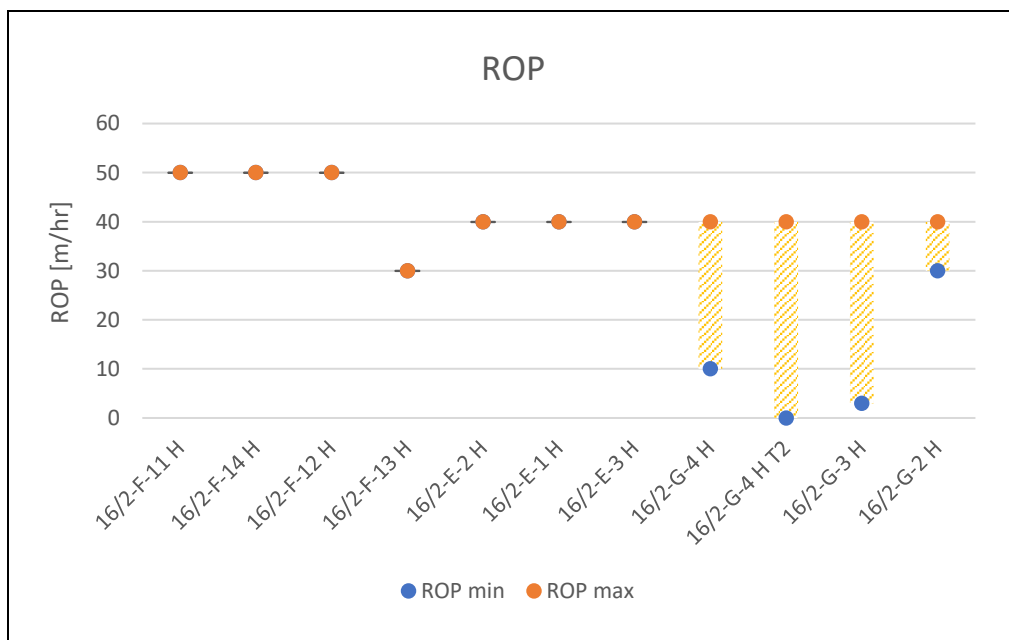


Figure 34: Maximum and minimum ROP for the different injection wells when drilling Sola Fm.

Although F-14 maintained constant ROP, there was some fluctuation in WOB. However, this is not unique for F-14. This can be observed in Figure 35. Furthermore, although the ROP varied for most of the G-wells, their maximum value for WOB were relatively low compared to all other wells. Obviously, insufficient WOB could cause low progress in hard formations.

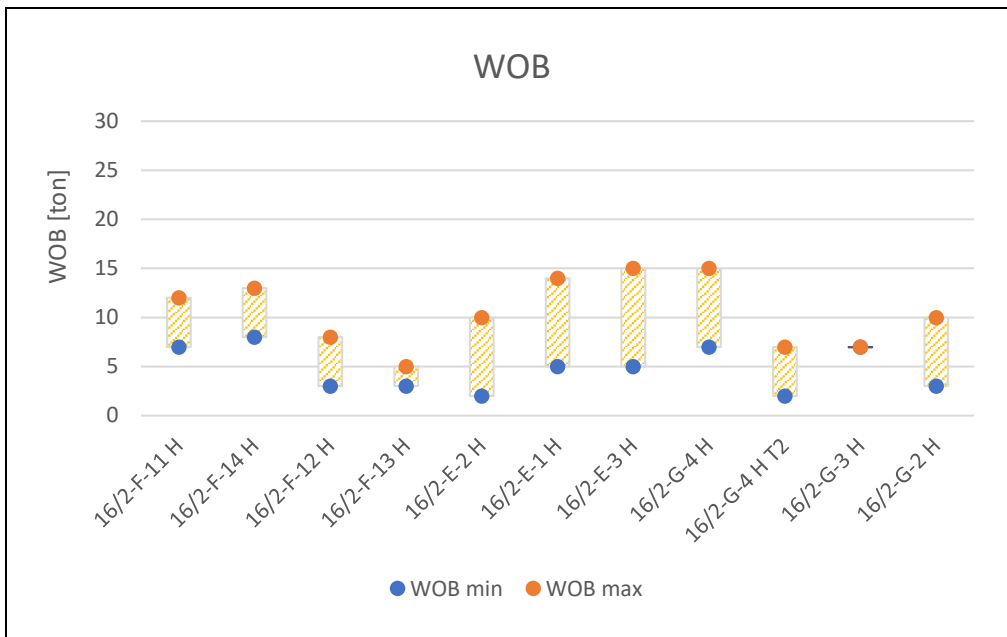


Figure 35: Maximum and minimum WOB for the different injection wells while drilling Sola Fm.

When drilling F-14, the flow rate had to be lowered from 3500 LPM to 3000 LPM when the Sola/Asgard boundary was met. For G-4 T2, the flow rate was maintained at 3500 LPM. This is illustrated in Figure 36. A constant flow rate was maintained for the majority of the wells, except from F-12, F-13 and F-14.

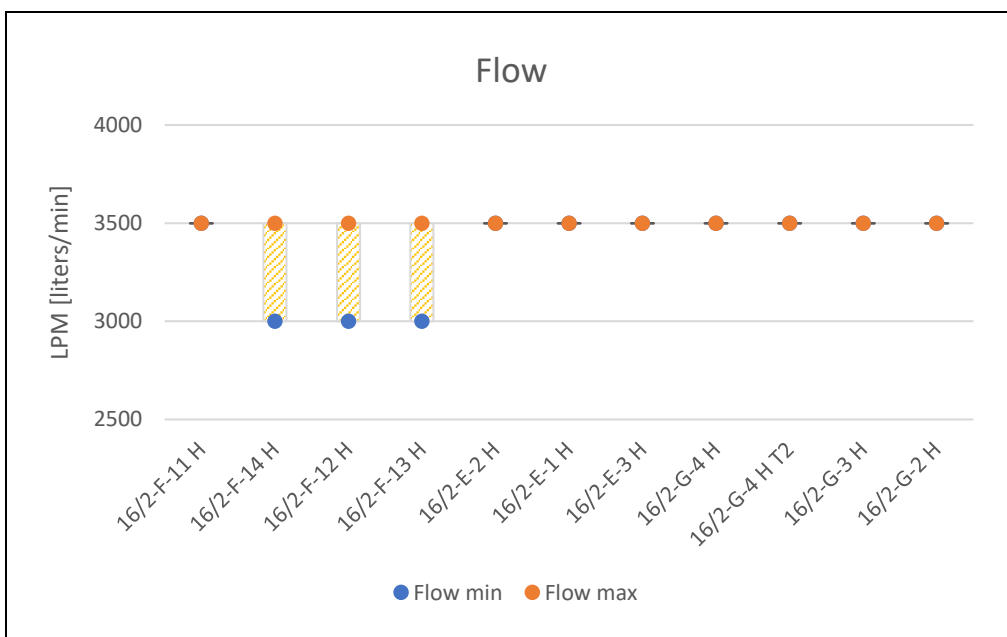


Figure 36: Maximum and minimum flow rate for the different injection wells when drilling Sola Fm.

When examining the rotation values for the different wells through Sola, there is a clear trend showing increasing RPM throughout the drilling of the wells. Starting out at F-11 with low rotation and increasing towards the G-wells. Here, the initial objective was to spare the formation from excessive mechanical impact by drilling with reduced rotation. However, it seemed as if the formation was stronger than expected, according to mostly in-gauge caliper logs recorded when drilling. Therefore, the rotation was increased during the next wells. Figure 34 shows the rotation for the injection wells, including a line indicating the increasing trend in rotation.

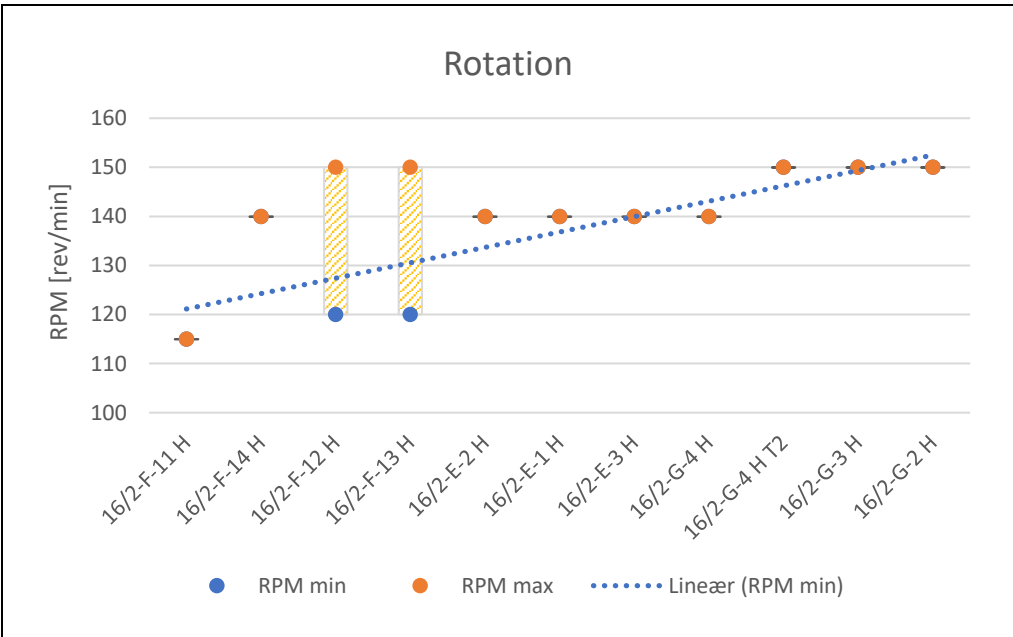


Figure 37: Maximum and minimum rotation for the injection wells when drilling Sola Fm. The blue line shows the linear trend for the RPM min values.

For F-14 and G-4 T2, the reason for the over-gauged section may be caused by the stringers encountered in the lower part of Sola towards Asgard, which is supported by the logs and geological interpretation. As one can tell from the figures above, high rotation and flow rate were maintained throughout the section.

Since the real-time caliper logs only yield a two-dimensional result, the image log was examined to get a better visualization of the borehole geometry. The image logs for F-14 and G-4 T2 are shown in Figure 38 and Figure 39, respectively. First, the log from F-14 shows a relatively smooth and in-gauge borehole through the first half of Sola. As the deviation increases (red line to the left), one can observe that there is a distinct pattern emerging on the PEF log. This pattern is characterized by lines which are slightly deviated from the horizontal,

stacked closely together. Some of these features are marked with red lines in Figure 38. This is a clear indication of a borehole with corkscrew geometry.

Furthermore, the white section from 2180 m MD to 2190 m MD yields a very high reading of PEF, which might be explained by an increased distance between the BHA and the high side of the borehole. Increased length of barite-containing mud will show an increase in PEF values due to the logs sensitivity to heavy minerals. The caliper image log (to the right) supports that the BHA probably was laying on the low side of the borehole at this particular interval. This is seen as an under-gauged (blue) section in the center (low side) and over-gauged sections on both edges of the log (high side). This makes sense as the DLS was very high at this point.

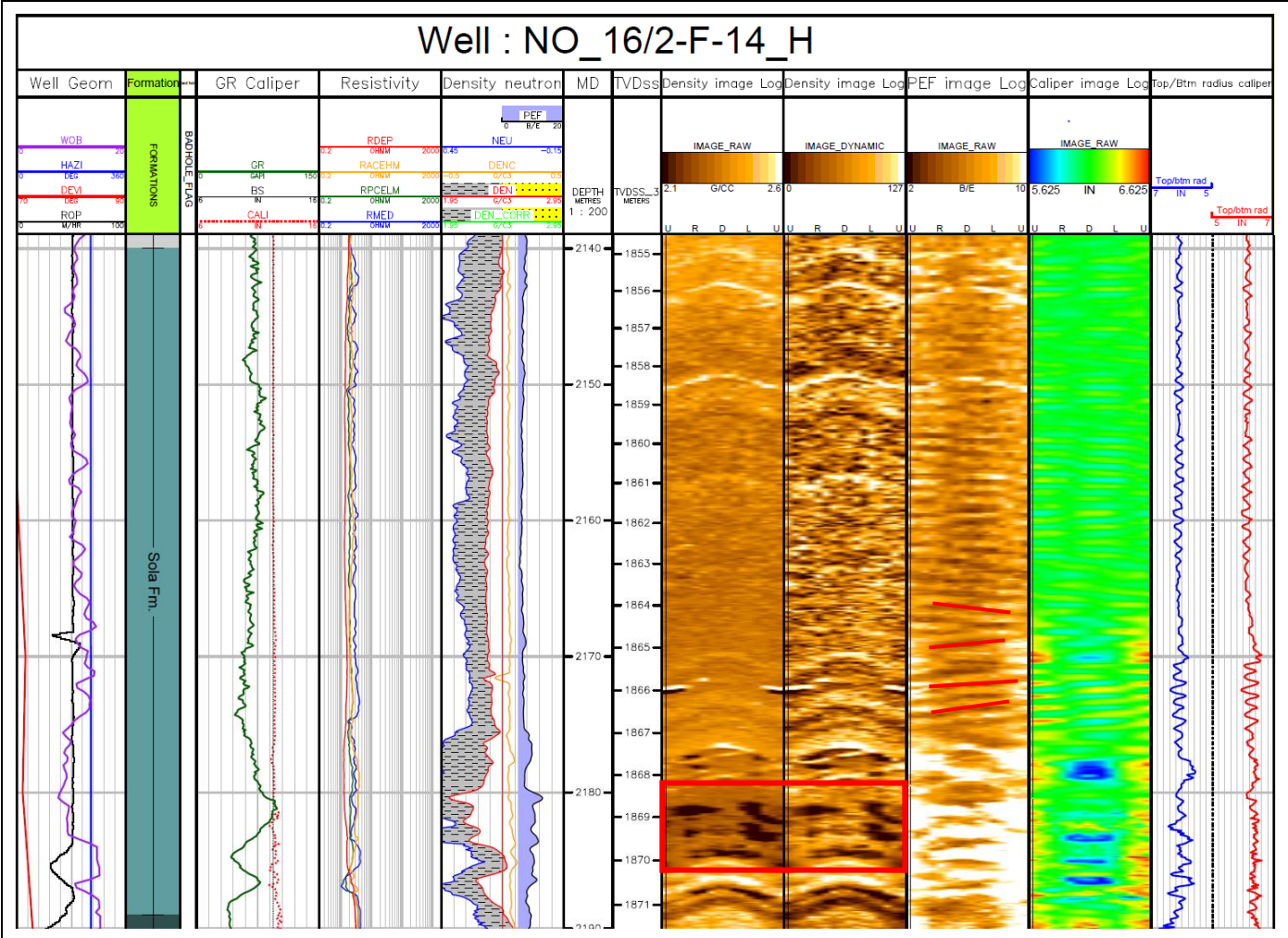


Figure 38: Image log from the drilling of F-14, containing various measurements.

Moreover, the features marked within the red square are particularly interesting. Since the density image log has a depth of investigation of about 2.5–4 inches, these completely dark spots illustrate a relatively deep area of notably low density. What makes these especially interesting, is that the features occur at approximately 90 and 270 degrees (shown as R and L on the top of the density image log), i.e. parallel to the minimal stress direction. This may indicate an early-stage break-out. As previously mentioned, break-outs happen due to insufficient support from the lateral pressures in the well, which may indicate too low mud weight (1.33 s.g.).

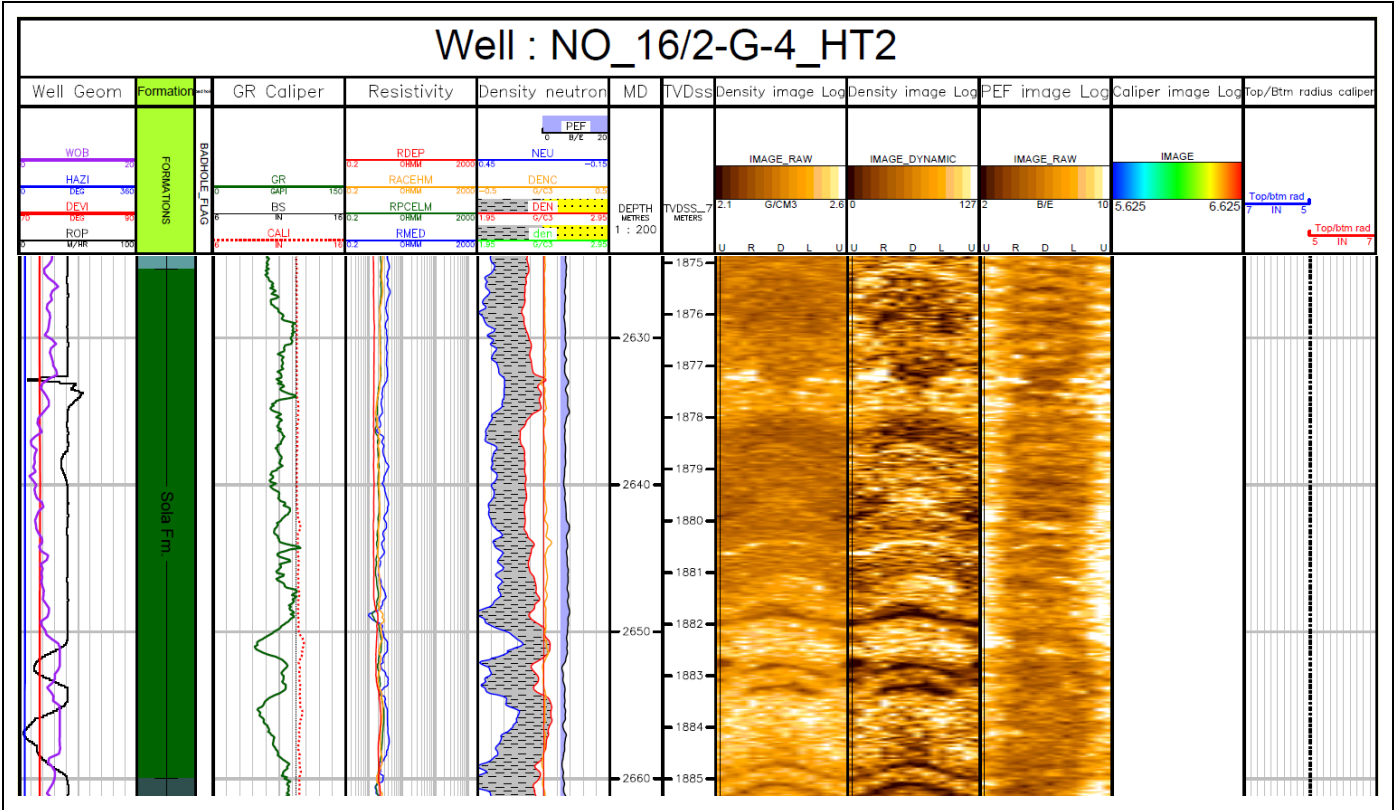


Figure 39: Image log from the drilling of G-4 T2, containing various measurements.

Unfortunately, the caliper image log was not available for G-4 T2. By examining the density and PEF logs, there is no obvious patterns in Sola as there were for F-14. As one can tell from the ROP (black line to the left) and the one-dimensional caliper log (red dotted line), the over-gauged sections have most likely been created when hitting the calcareous stringers. This is also supported by a narrowing of the neutron-density curves and higher density readings, accompanied by a reduction in gamma ray, right before the ROP drops. As stated previously,

for G-4 T2, high values for flow rate and rotation was maintained through these sections in Sola, which may have worsened the deterioration of the borehole wall.

The torque is highly dependent on the length of open hole drilled and would be expected to increase as the open hole section gets longer.

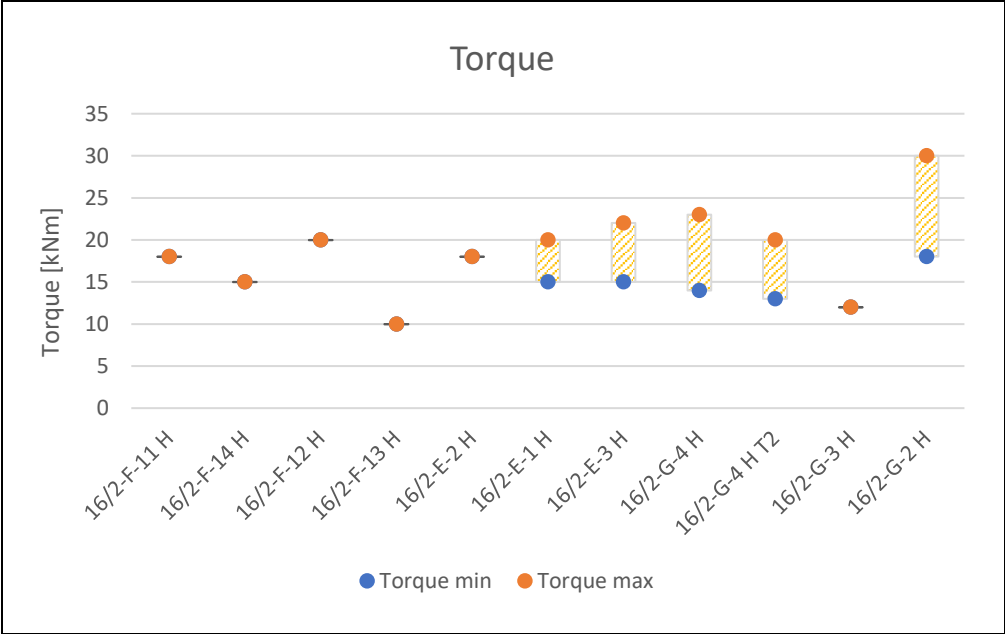


Figure 40: Maximum and minimum torque values for the injection wells when drilling Sola Fm.

Lastly, vibrations and stick slip were examined at for all the wells. High stick slip was encountered for E-1 and G-3. The intervals of high stick slip were correlated to an increase in WOB while drilling harder formation, accompanied with constant high DLS values. Lateral vibrations were low for most wells in Sola, except for E-1. This is illustrated in Figure 41. As previously stated, lateral vibrations are the most destructive in terms of diminishing borehole quality, mainly due to side cutting from the bit.

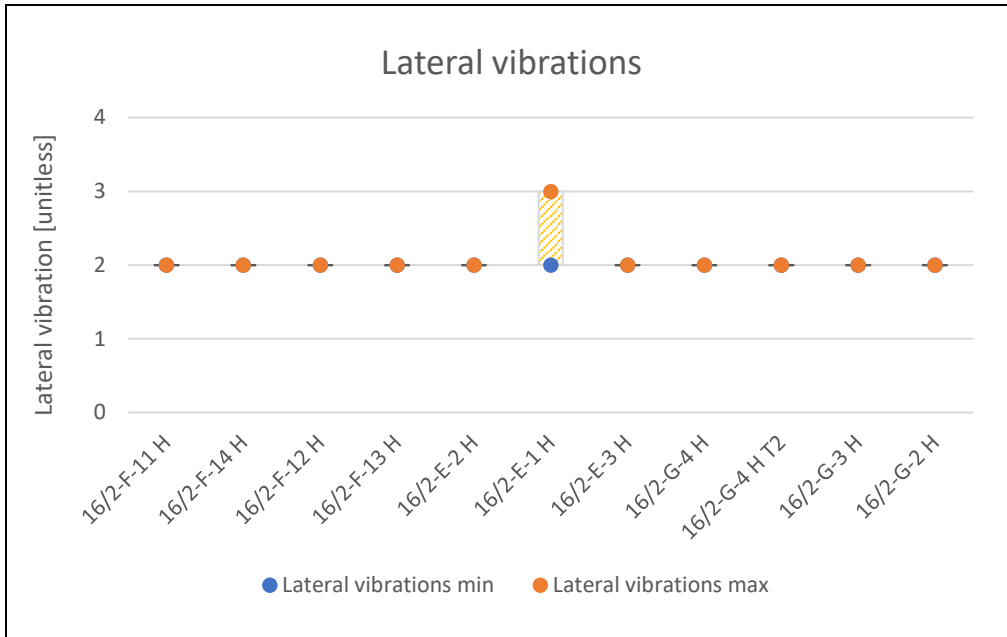


Figure 41: Maximum and minimum values for lateral vibrations for the injection wells when drilling Sola Fm.

5.2.2.2 Aasgard Fm.

An investigation of drilling parameters in Aasgard Fm. was performed for all the wells. Due to interbedded hard formation (stringers), the Aasgard section generally has a lower average ROP. Interestingly, the drilled length of Aasgard Fm. is significantly greater for the G-wells, compared to F and E. This can be observed in Figure 42. Building angle and relatively high DLS values are characteristic when drilling Aasgard, except for G-2.

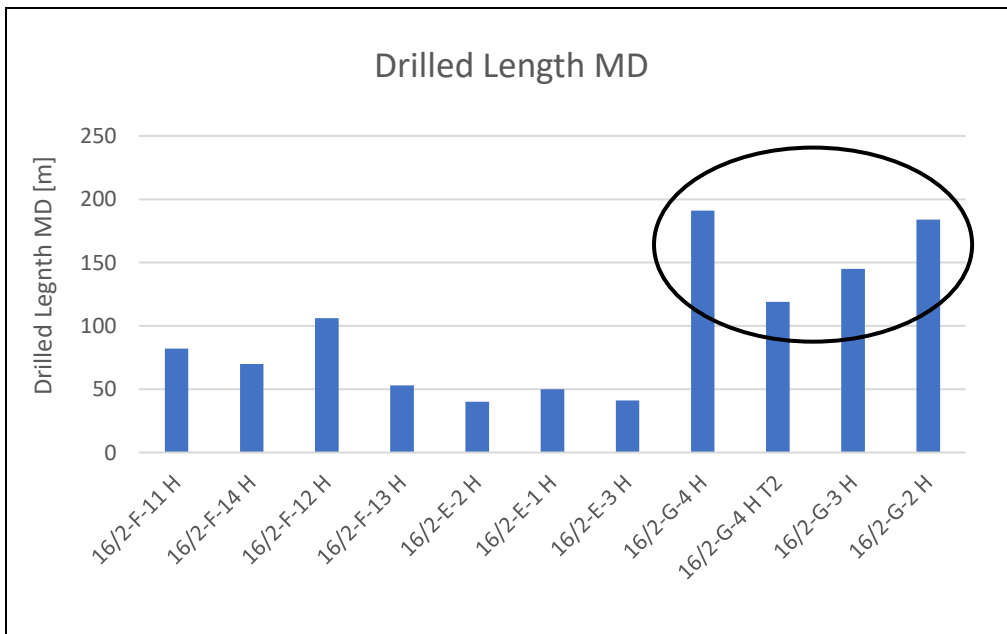


Figure 42: Drilled length of Aasgard for the different injection wells. Length of Aasgard for the G-wells are shown inside the circle.

As for Sola, the real-time caliper logs while drilling Asgard were examined for all the injection wells. One can clearly observe significant over-gauged sections for many of the wells, namely F-14, F-13, E-2, G-4 and G-4 T2 (see Figure 43). In addition, minor over-gauged sections are found in F-12 and G-3. For F-11 and E-3, on the other hand, the caliper log displays a relative continuous and smooth wellbore. Unfortunately, there were no logs available for E-1 and G-2.

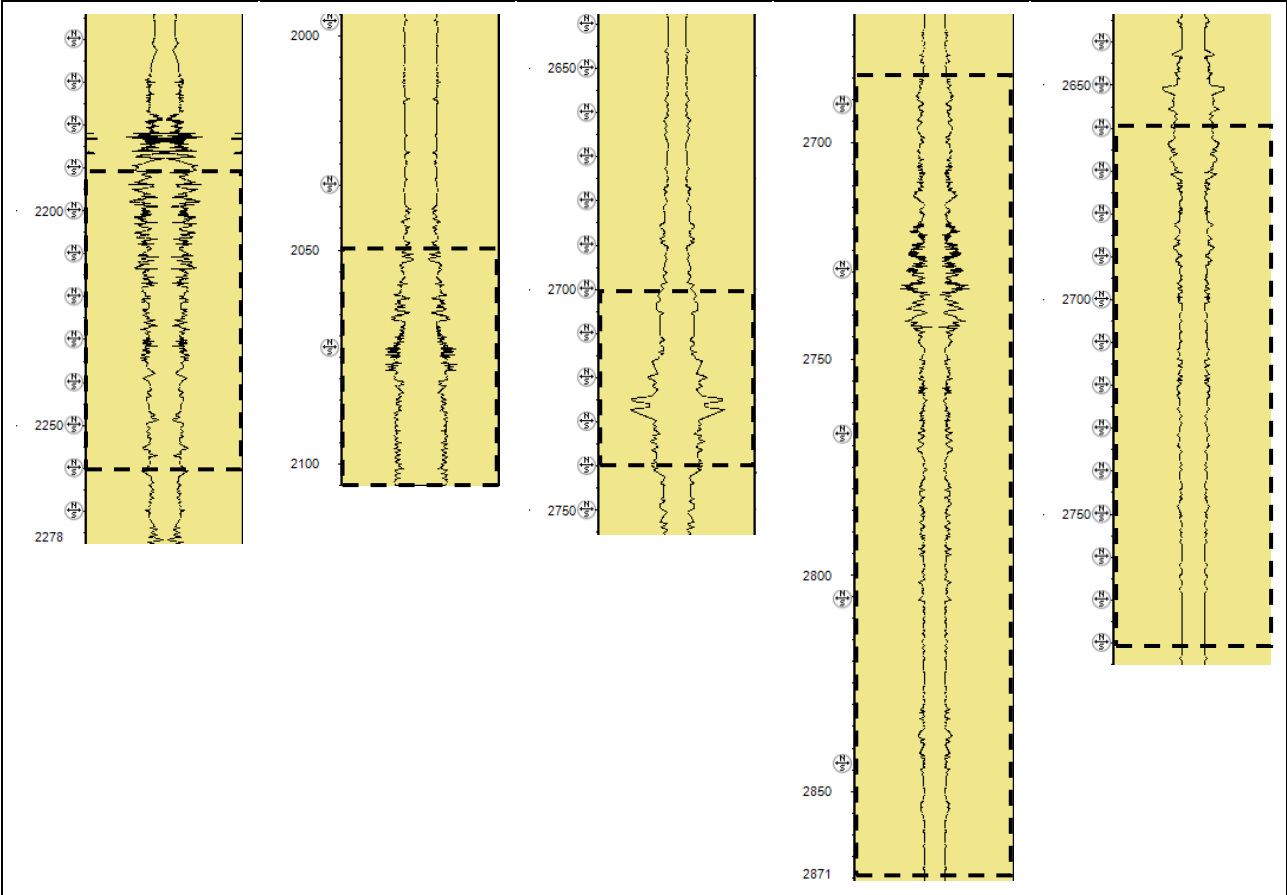


Figure 43: Real-time caliper logs for F-14, F-13, E-2, G-4 and G-4 T2 (from left to right). Asgard Fm. is situated within the dashed lines. The left axes are given in meters.

Moreover, the ROP for the Asgard sections are generally dominated by intervals with low values. As shown in Figure 44, the ROP has a wide range of values for each of the wells, mainly due to interbedded hard formation. F-14 had a particularly low average ROP. In addition, F-12, F-13, E-1, G-4, G-4 T2 and G-3 had intervals with low values (0-5 m/hr).

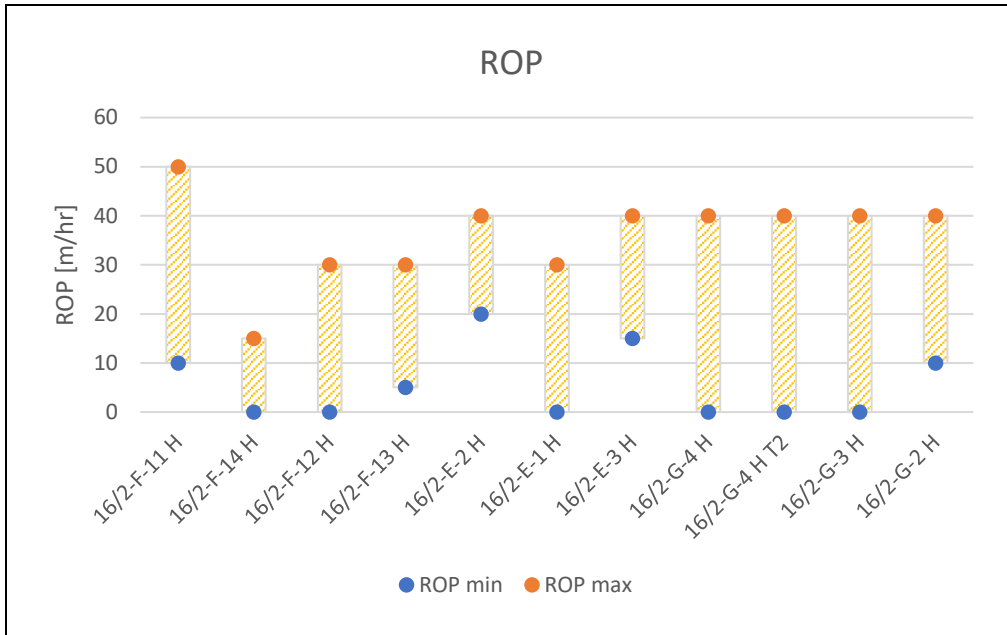


Figure 44: Maximum and minimum ROP for the injection wells when drilling Asgard Fm.

The maximum WOB seems to lie below ~15 tons for most wells, except for F-14, G-4 and G-3 which obtained higher values. The reason for this increase in WOB was to achieve progress in the intervals with hard formation. This increase together with altering the rotation was successfully done to achieve optimal penetration, for G-4 and G-3. Even though high WOB and altering rotation might cause an increase in ROP, other issues may arise, such as increased lateral vibrations and stick slip. This will be discussed later in this subchapter.

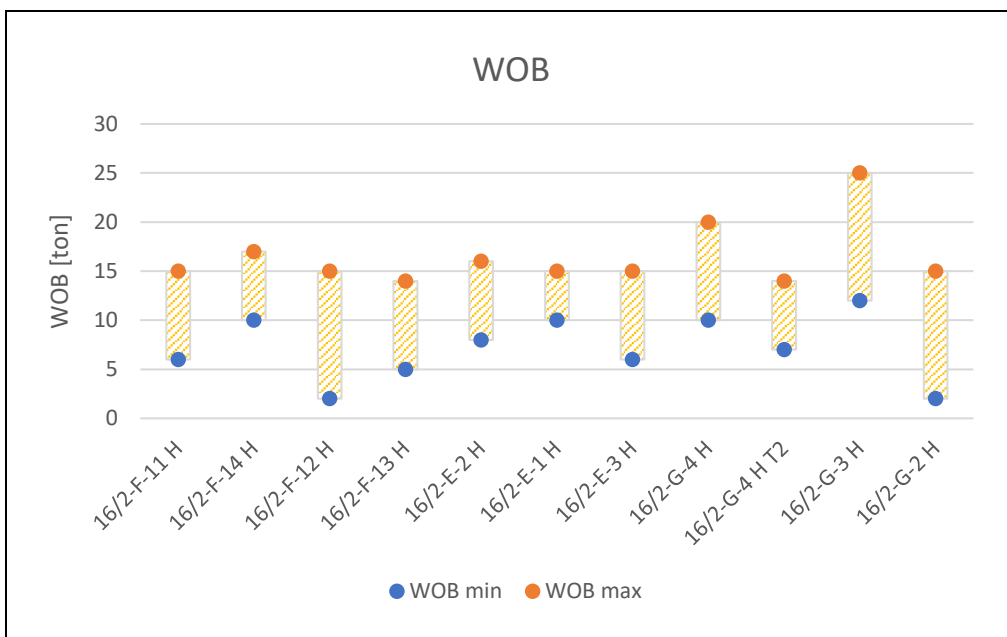


Figure 45: Maximum and minimum WOB for the injection wells when drilling Asgard Fm.

Flow rate and rotation was altered for most wells when drilling Aasgard. This is illustrated in Figure 46 and Figure 47. These parameter changes are to be expected as one tries to optimize ROP, while simultaneously attempting to minimize the probability of washed out intervals. There is a significant reduction in rotation for F-14, F-12, E-1, G-4, G-4 T2 and G-3, which all correlates to low ROP sections and hard formation. Flow was altered for all the beforementioned wells, except G-4 T2 and F-14 which were kept at 3500 and 3000 LPM, respectively. As for Sola, F-11 was drilled with low rotation also through Aasgard.

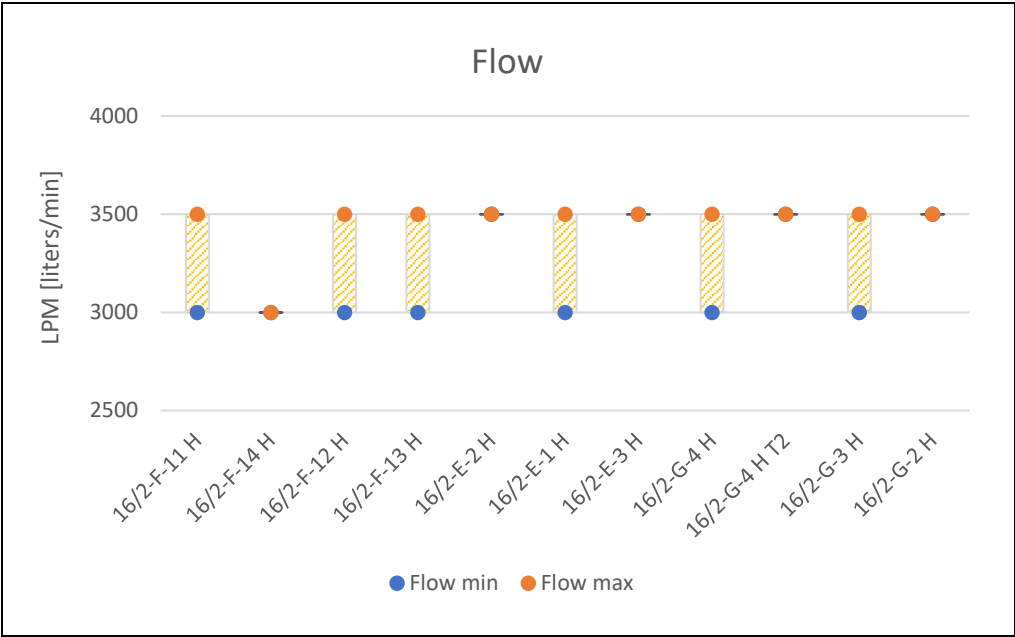


Figure 46: Maximum and minimum flow rate for the injection wells when drilling Aasgard Fm.

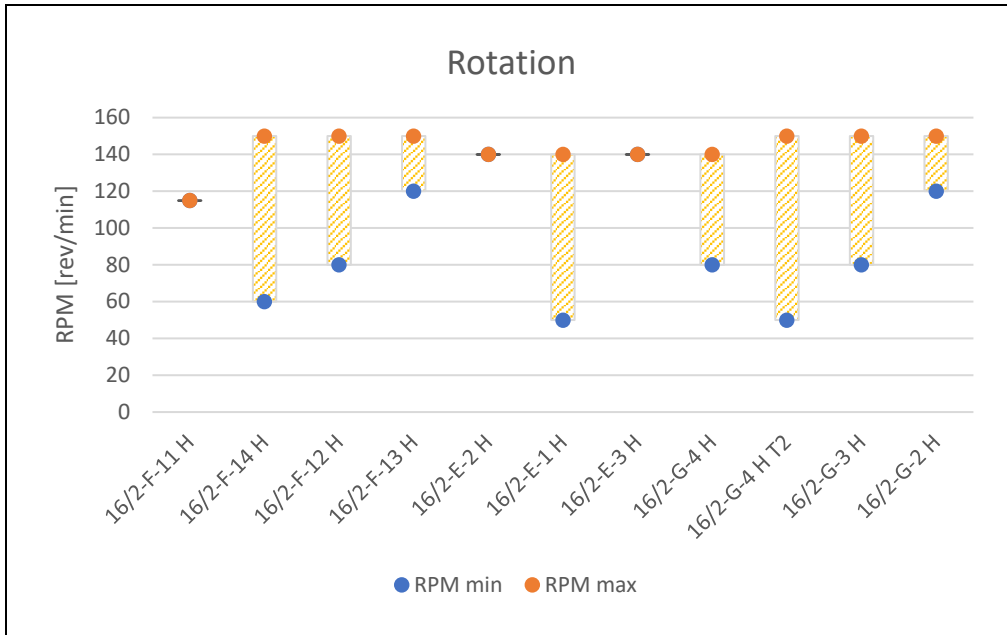


Figure 47: Maximum and minimum rotation for the injection wells when drilling Aasgard Fm.

Image logs for Aasgard were examined in the same manner as for Sola. Since rotation of the liner stopped when the cement was located in top Aasgard for F-11, F-14, G-4 T2 and G-3, as stated in section 5.1, these logs will be presented.

As observed from the real-time caliper log, the wellbore of F-11 seemed relatively smooth and continuous compared to many of the other wells. This is also true for the image log, which is illustrated in Figure 48. Neither the PEF nor caliper image log display any sign of significant borehole irregularities. The light blue line in the center of the image log (approximately 180 degrees) is indicating under-gauge borehole, with the corresponding yellow indicating over-gauge hole at approximately 0 and 360 degrees. This is most likely showing the BHA approaching the low side of the hole due to building angle.

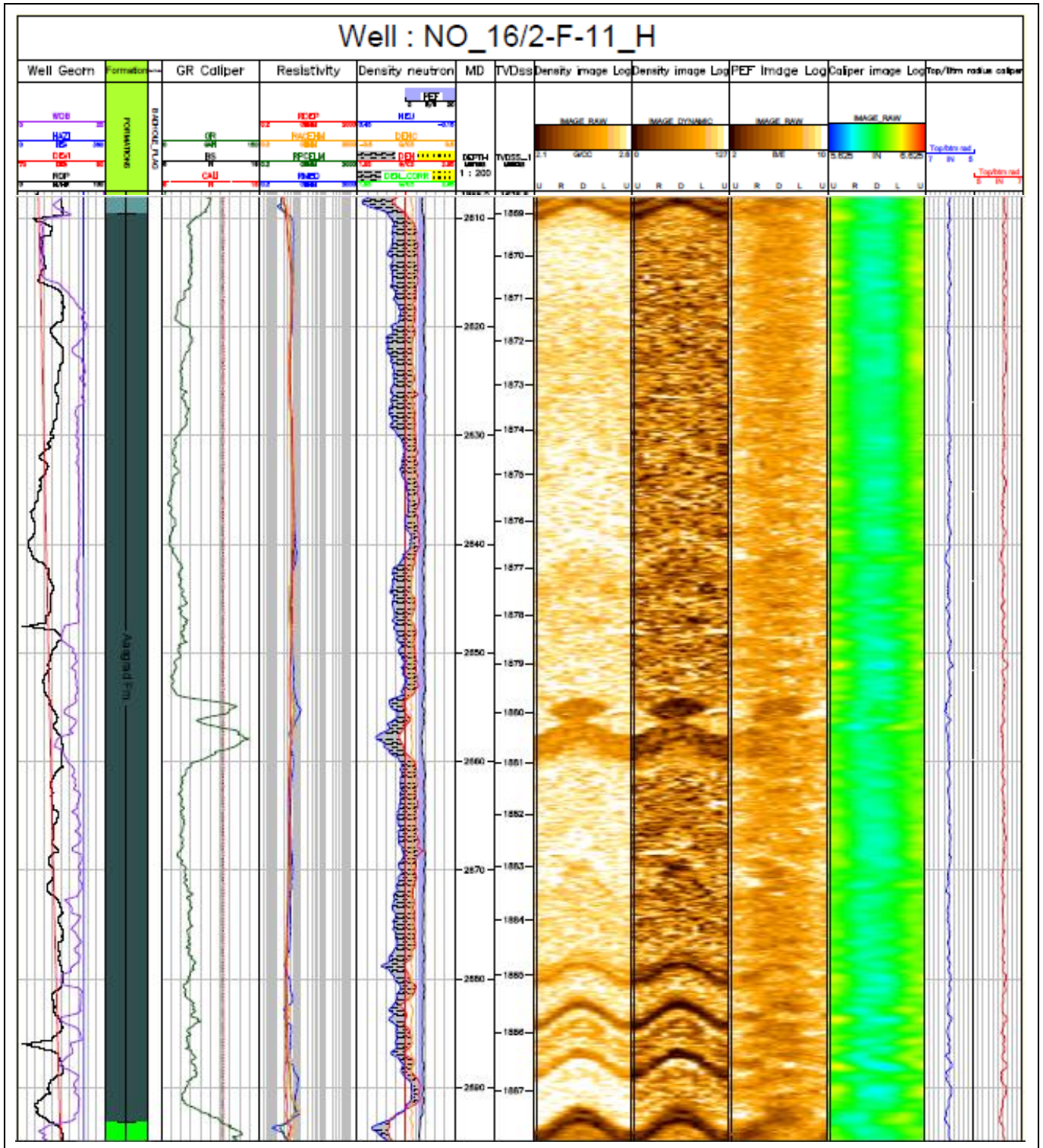


Figure 48: Image log from the drilling of F-11, containing various measurements.

Furthermore, F-14 revealed poor well condition for Aasgard on the real-time caliper log, which is also confirmed by the image log. Significant corkscrew patterns are evident, which could compromise hole cleaning efficiency, increase torque and drag, and possibly cause trouble when re-entering with the liner. This is due to a decrease in effective diameter of the borehole,

which in extreme cases could be less than the liner OD. This was illustrated in subchapter 3.4.3. Moreover, the density-neutron (D-N) and GR indicate some intervals with possible limestone (narrow D-N) and an interval with possible clay-containing formation at the GR peak. The narrowest D-N intervals correlates well with low ROP, indicating that these most likely are hard limestone stringers.

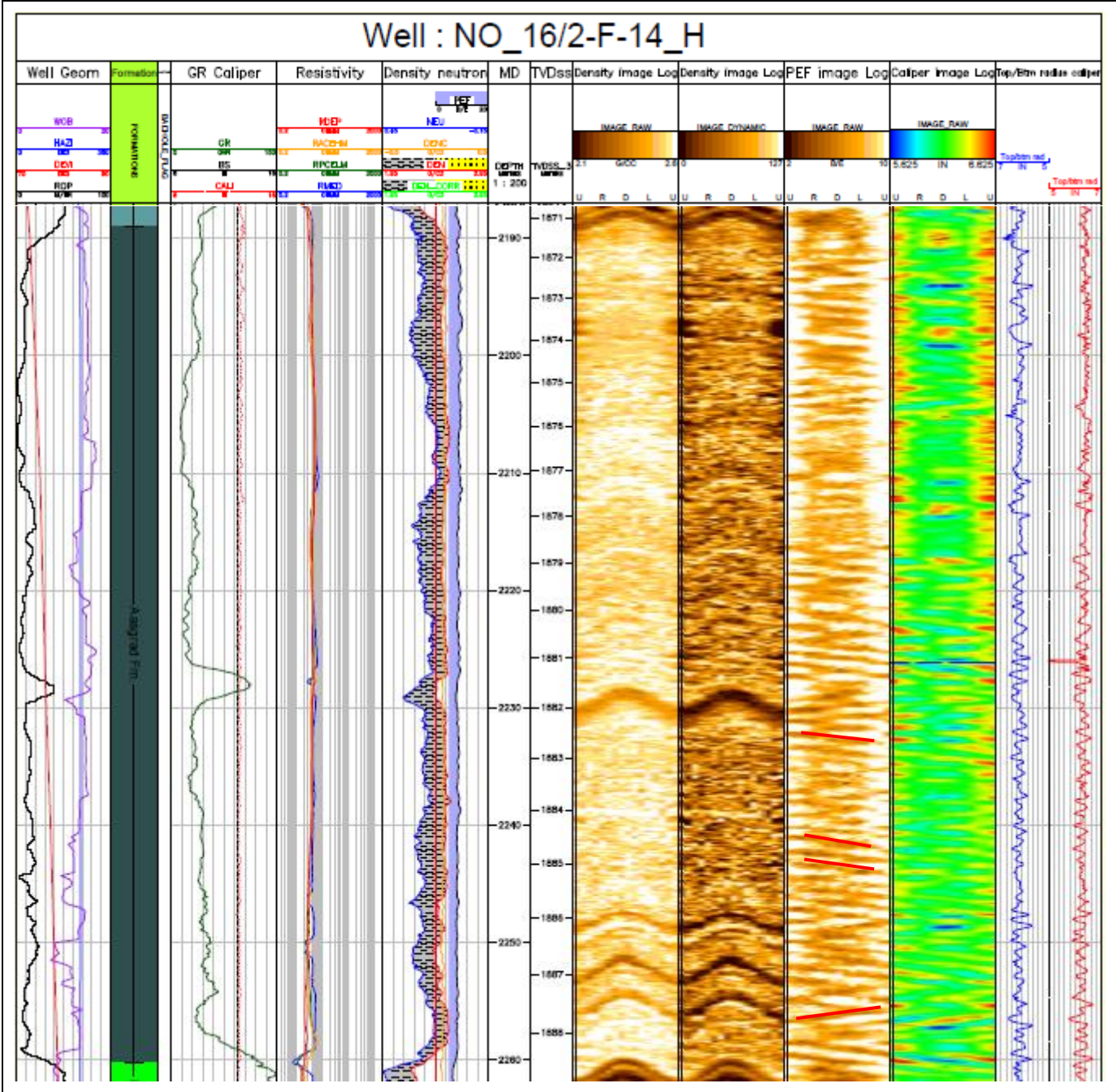


Figure 49: Image log from the drilling of Aasgard for F-14. Features regarding spiral geometry in the borehole are marked with red lines on the PEF log.

As previously mentioned, wells from the G-template have considerably longer Aasgard sections. For these wells, torque is generally higher and have a wider range, except G-4 T2. This is shown in Figure 50. The wide range for G-3 and G-4 are due to very erratic torque, which could indicate significant stick slip and vibrations downhole. This will be shown later. Furthermore, the high torque values could be induced by different factors. In this case, it could be high WOB (see Figure 45), length of exposed open hole, poor borehole geometry or related to the increased friction from chalk and limestone formation (both in overburden and within Aasgard). High WOB seems plausible for G-4 and G-3, but not for G-2. Unfortunately, neither caliper nor image logs are available for G-2 to visualize the borehole conditions.

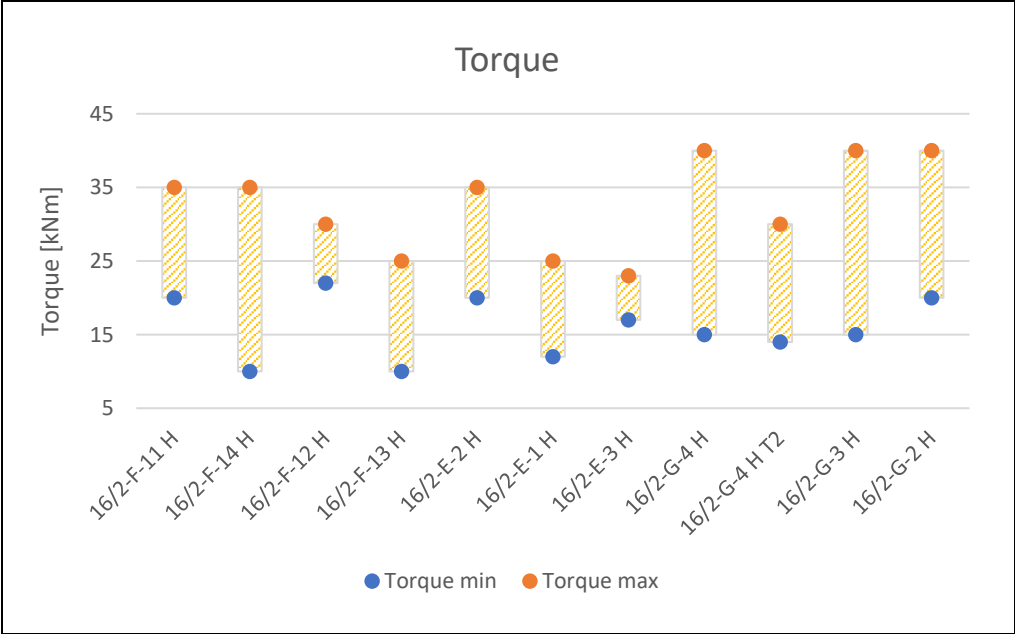


Figure 50: Maximum and minimum torque for the injector wells when drilling Aasgard Fm.

Furthermore, the image log for G-4 T2 are shown in Figure 51. Only a few intervals with minor spiral effect are present. The caliper (dashed red line) indicates over-gauged sections in the top of Aasgard. Very low ROP is observed for the section of over-gauge hole. The reason for this low ROP interval in top Aasgard is most likely due to low WOB (~7 ton), which is not adjusted before reaching 2672 m MD. This results in a ~10 m MD interval of low ROP combined with high flow rate and rotation, which could have been avoided if WOB had been increased when the ROP dropped.

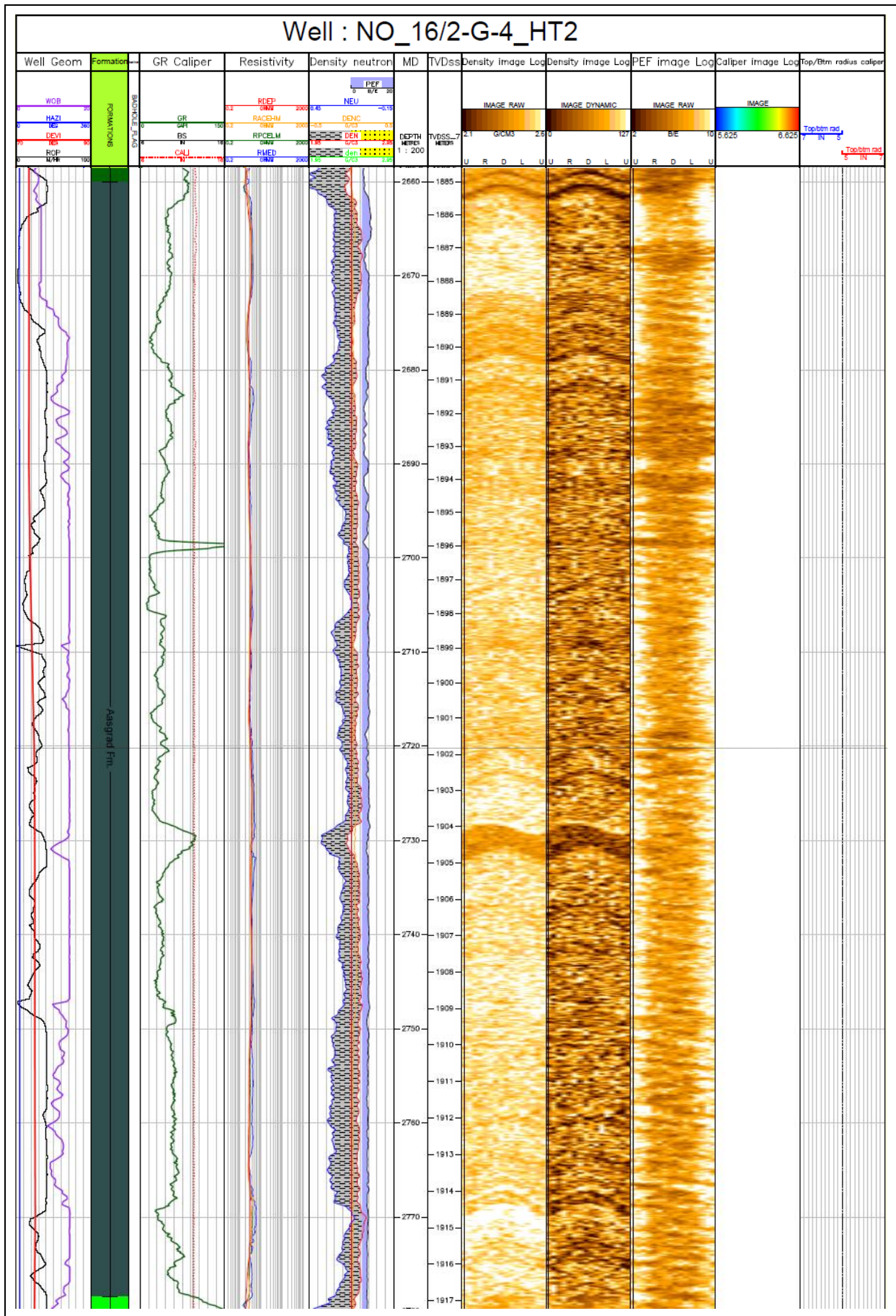


Figure 51: Image log from the drilling of G-4 T2, containing various measurements.

The image log for G-3 is displayed in Figure 52. No sign of considerable spiral geometry is evident on the PEF log. Low ROP intervals are correlating well with a narrowing of the D-N curve, indicating limestone stringers. Also, two noticeable peaks in GR are present, whereas only one of them can be identified on the density image log (~2215 m MD). This is probably indicating the black claystone layer that could occur in Aasgard, which is relatively weak compared to the other rocks present. However, steady progress was achieved beneath the claystone, thus leaving an in-gauge hole. A high WOB (20-25 tons) was maintained when encountering hard formations, which led to an ROP between 10-40 m/hr. Moreover, some short over-gauged sections are observed from the caliper log (dashed red line) during a high DLS interval, namely 2140 to 2225 m MD. Excluding minor over-gauged sections, the wellbore seems to be in relatively good shape despite excessive DLS values.

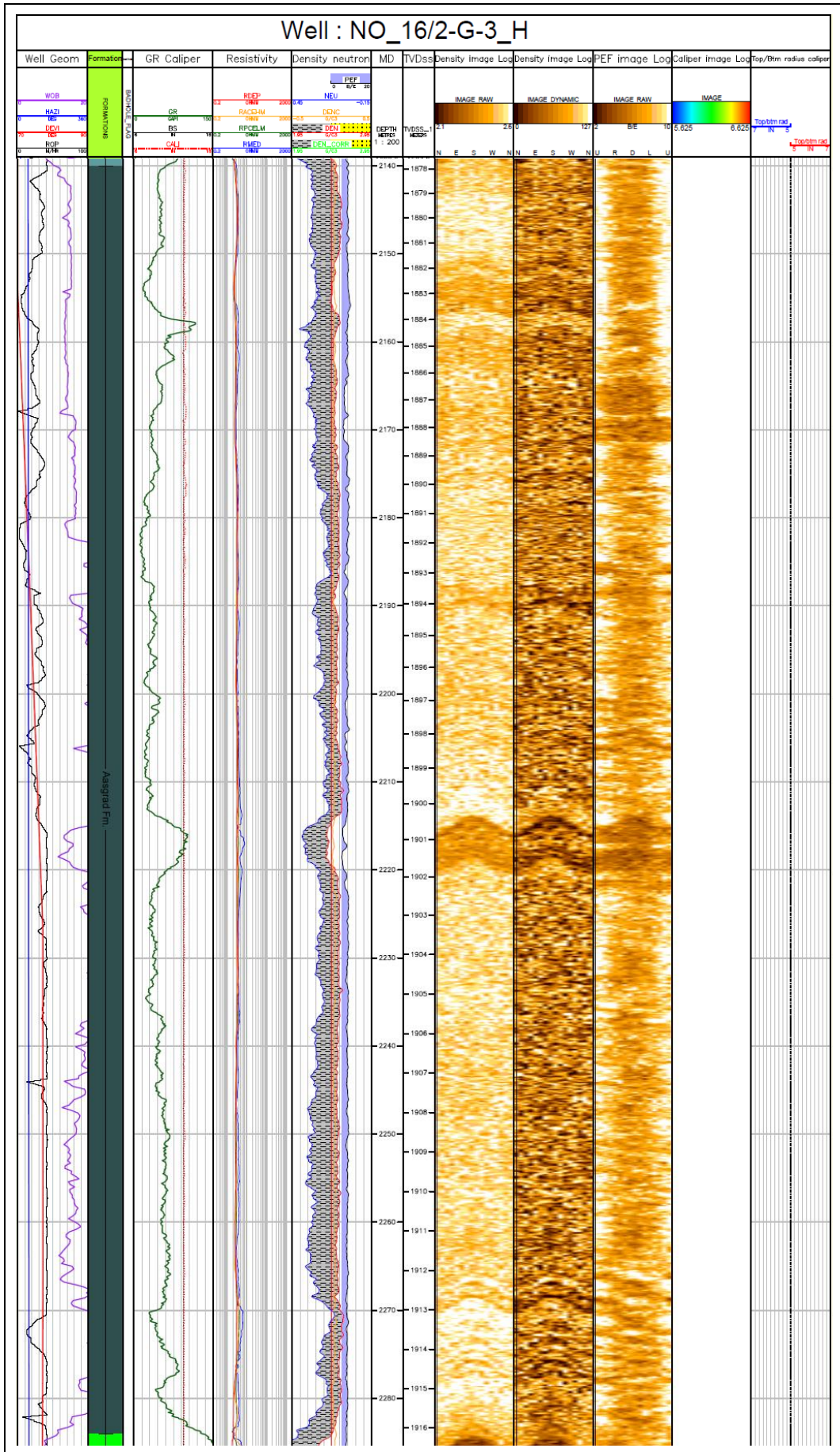


Figure 52: Image log from the drilling of G-3, containing various measurements.

During the investigation of the image logs for Asgard Fm., it became clear that spiral geometry is evident for several wells. F-14 display clear patterns, whereas F-12, G-4 T2, G-4 and E-3 show moderate tendencies. The rest of the wells did not show evidence of such geometry. Although spiral patterns are visible, it must be noted that the PEF log has a shallow depth of investigation. Consequently, the patterns may create an illusion of severe borehole deformation, whereas in practice, these features might be insignificant.

Also, lateral vibrations and stick slip were investigated. Excessive stick slip values were recorded when drilling Asgard Fm. This is illustrated in Figure 53. For F-11, E-2, E-1, G-3 and G-2, stick slip levels were high during all of Asgard. Only E-3 had low stick slip. Through investigation of the intervals experiencing stick slip, the data could suggest that low ROP sections with high WOB in addition to moderate to high DLS could increase the probability of excessive stick slip. According to theory, these are typical parameters for inducing torsional vibrations [39]. In addition, lowering of RPM accompanied by high WOB, could increase risk of high stick slip levels.

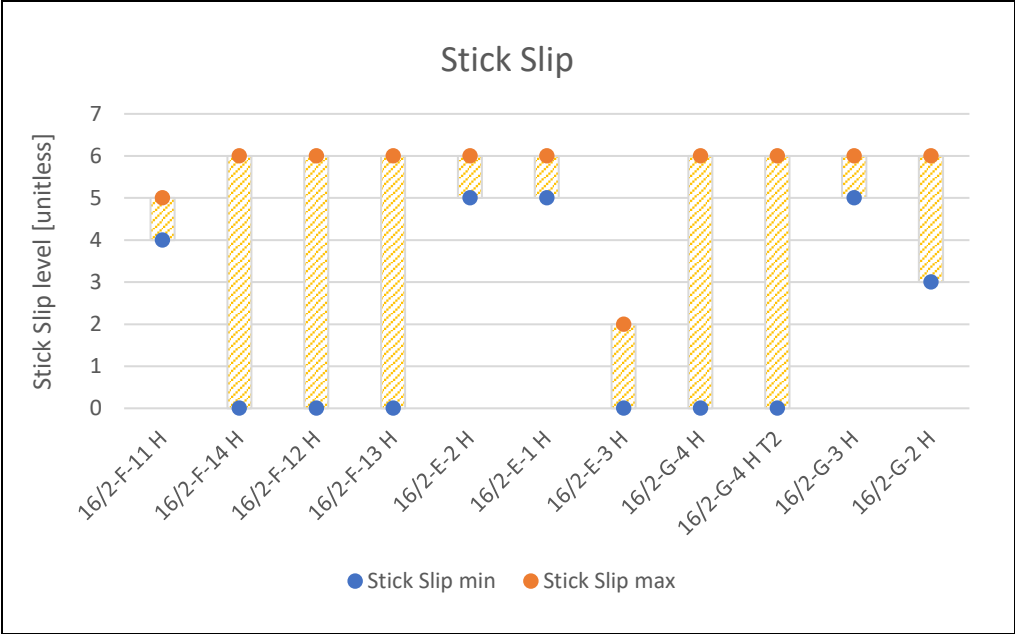


Figure 53: Maximum and minimum stick slip for the injection wells when drilling Asgard Fm.

Furthermore, rather high levels of lateral vibration were recorded, as seen in Figure 54. Especially high values for F-14, E-1 and G-3. Lateral vibrations are related to torsional vibrations, which is the main factor in causing stick slip. Therefore, one would expect to see somewhat elevated lateral vibrations for wells experiencing high stick slip.

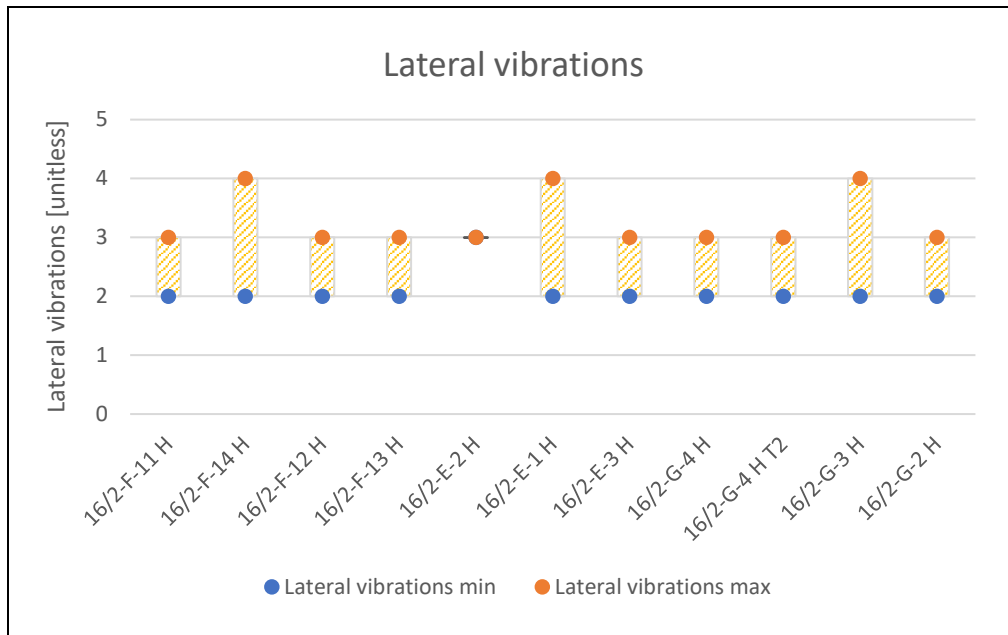


Figure 54: Maximum and minimum lateral vibrations for the injection wells when drilling Aasgard Fm.

5.2.2.3 Draupne Fm. 2

Finally, the drilling of Draupne Fm. 2 was examined. As stated previously, this formation varies significantly from the F- and E-templates to G-template. For the G-wells, Draupne Fm. 2 contain organic rich shale, also called “hot shale”. This formation is particularly troublesome, as its failure is believed to be time-dependent (ref. section 2.4.2.3). Luckily, it is easily detected on the gamma ray real-time log because of its high organic content. Regarding the F- and E-templates, the Draupne 2 contain spiculitic facies dominated by quartz with only a minor fraction of clay minerals. Neither of these variations of Draupne 2 should be particularly problematic regarding the drilling progress. However, the cemented omission zone (transition between Draupne 2 and 1) could yield low ROP values.

Moreover, as presented in Figure 55, the length of Draupne Fm. 2 varies greatly, although fairly short for most wells.

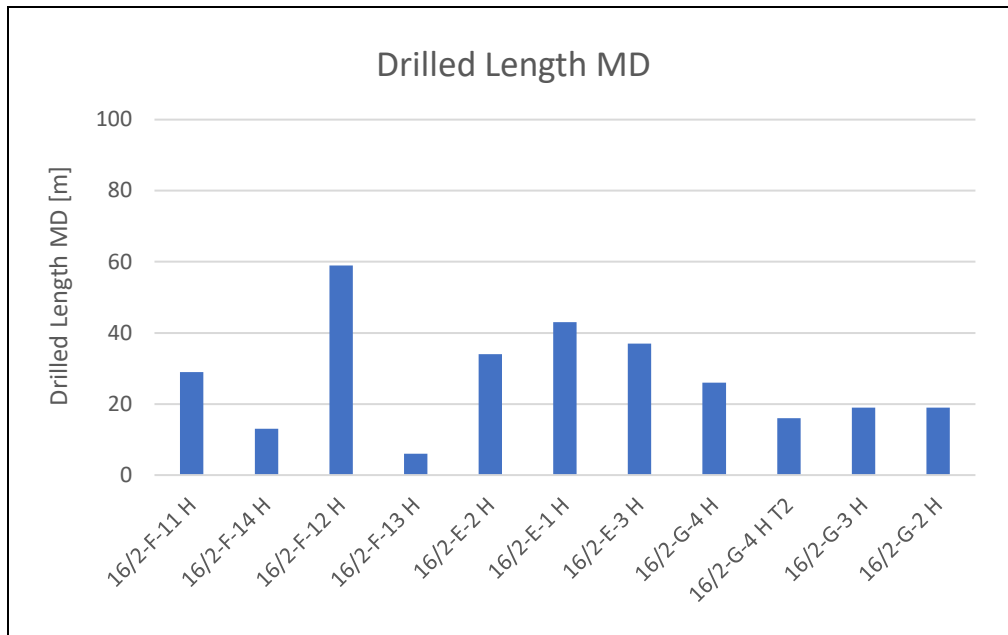


Figure 55: Drilled length of Draupne Fm. 2 for the different injection wells.

The caliper logs for Draupne 2 did not show any signs of severe over-gauged intervals. As previously mentioned, no caliper logs were available for G-2 and E-1. The G-wells appeared to be almost perfectly in-gauge for most of Draupne 2. Although F-11, F-12 and G-4 showed some enlargement-tendencies towards the base of the formation, as illustrated in Figure 56. For F-11, this enlargement was probably caused by making a connection in the interface between Draupne 1 and 2. This interval gave particularly high GR readings (>150), which could indicate softer formation due to high organic content. As progress is stopped during connection, the gravitational forces (in an 80 degree well) are given time to partly submerge the BHA into the soft formation, consequently enlarging the hole.

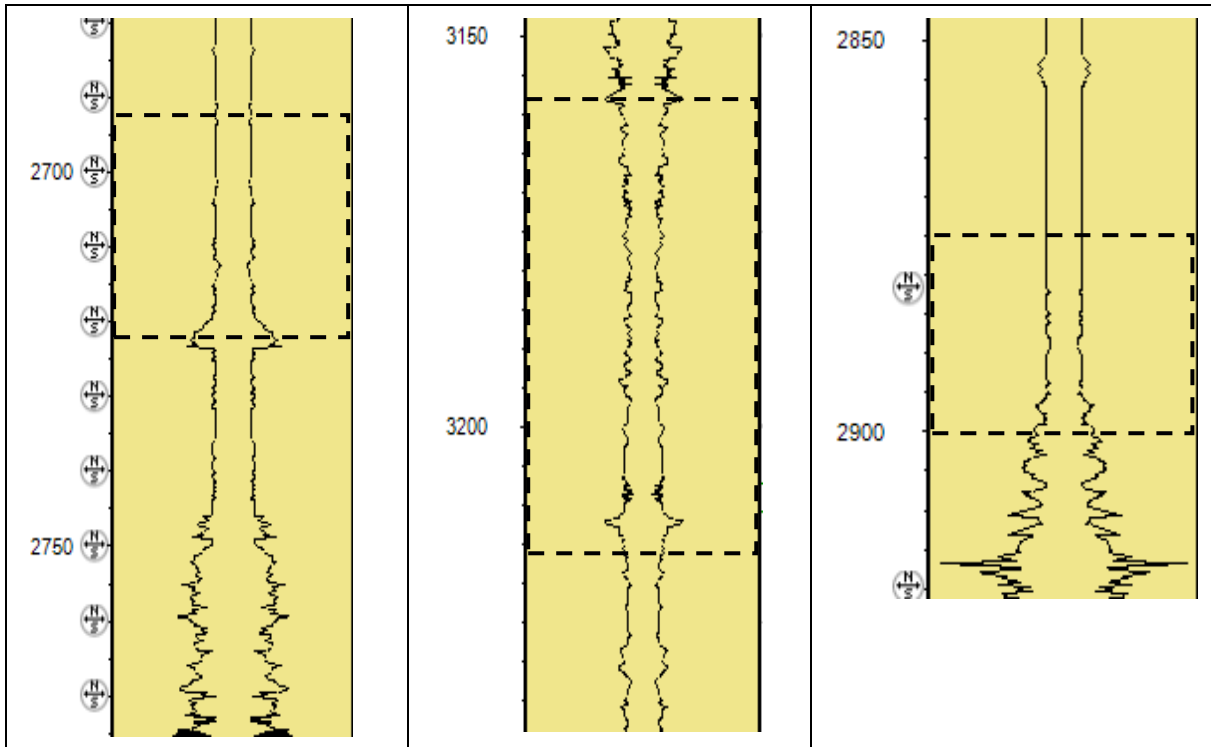


Figure 56: Real-time caliper logs for F-11, F-12 and G-4 (left to right). Draupne Fm. 2 is situated within the dashed lines. The left axes are given in meters.

Furthermore, the drilling parameters through Draupne 2 for the G-wells were mostly stable. This is to be expected as the formation is relatively soft. For many of the other wells, especially the longer Draupne 2 sections, parameters vary significantly. ROP values are shown in Figure 57. Both F-11 and F-12 show a reduction in ROP from the setpoint, because of low progress in the upper parts of Draupne 2. In addition, E-2 and E-1 also had reduced ROP for Draupne 2. For E-2, only minor fluctuation in ROP was observed when trying to maintain 40 m/hr, half way through Draupne 2 the ROP setpoint was dropped to 20 m/hr, hence the interval on Figure 57. E-1, on the other hand, had a drop in ROP in the middle of Draupne 2 in an area which seems to contain harder, spiculite cemented formation.

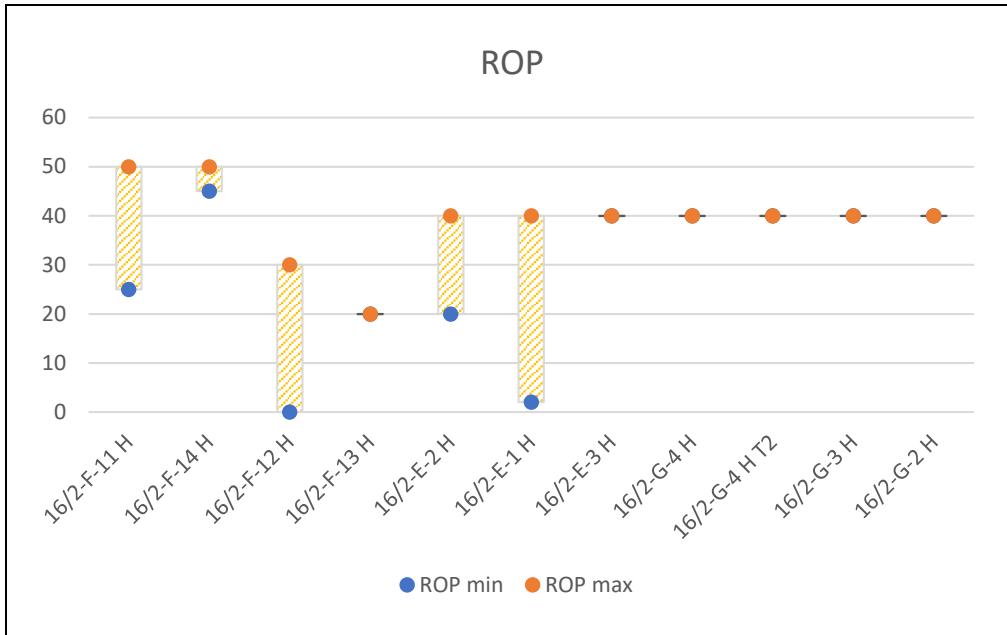


Figure 57: Maximum and minimum ROP for the injection wells when drilling Draupne Fm. 2.

Moreover, the WOB varied for the different wells, as shown in Figure 58. As expected, the wells with fluctuating ROP also possess a fluctuation in WOB. Namely, F-11, F-12, E-2 and E-1. Also, there are some variations for the G-wells, which are related to the interface between Draupne 1 and Draupne 2, namely the omission zone.

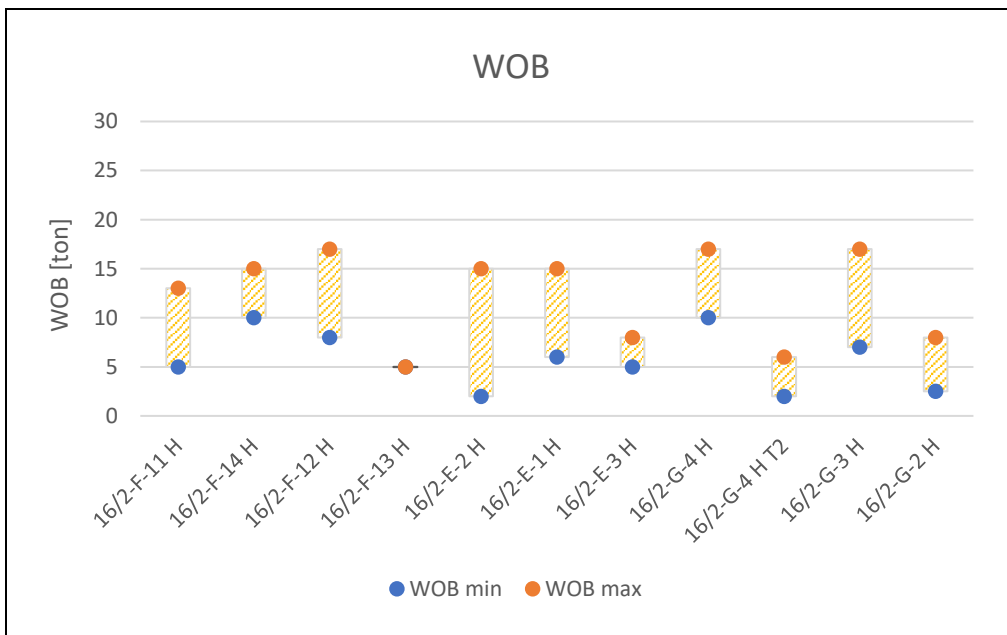


Figure 58: Maximum and minimum WOB for the injection wells when drilling Draupne Fm. 2.

Regarding flow rate and rotation when drilling Draupne 2, the parameters were generally constant, with the exception of F-12. As previously seen, F-12 struggled with low ROP and high WOB through Draupne 2, which led to a decrease in rotation and flow rate for these intervals. The over-gauged interval for F-12, near the base of Draupne 2, was probably due to weak clay formations (high GR) in addition to high flow rate (3500 LPM). This may have been avoided if the flow was adjusted according to indications on the real-time log. Lastly, high rotation and flow was kept through the G-wells, despite the presence of unpredictable Draupne hot shale. According to the caliper logs, this has not been a problem in terms of unwanted borehole geometry caused by drilling.

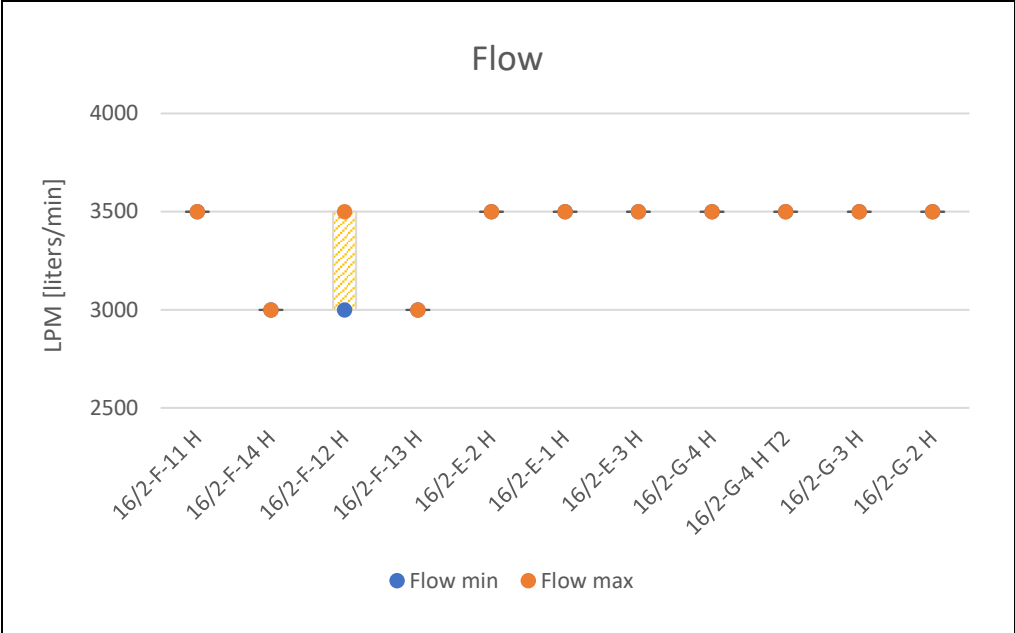


Figure 59: Maximum and minimum flow rate for the injection wells when drilling Draupne Fm. 2.

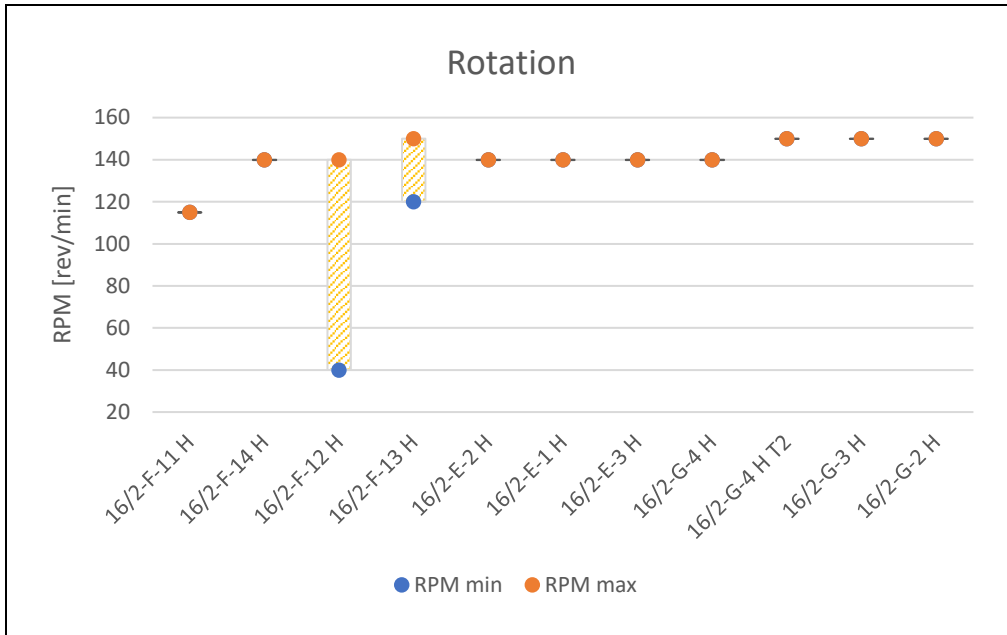


Figure 60: Maximum and minimum rotation for the injection wells when drilling Draupne Fm. 2.

As for both the preceding formations, images logs for Draupne 2 were also investigated. For F-11, as previously mentioned, a connection was taken in the interface between Draupne 1 and Draupne 2. This can be observed in Figure 61 on the caliper image log, which indicates that there is an over-gauged section on the high side of the hole, with a corresponding under-gauge section on the low side. This could illustrate the BHA lying on the low side with a significant distance to the high side of the hole. Moreover, the high GR values at the bottom of Draupne 2 with corresponding high-density values most likely indicate the omission layer. This layer contains glauconite, which will yield high GR values.

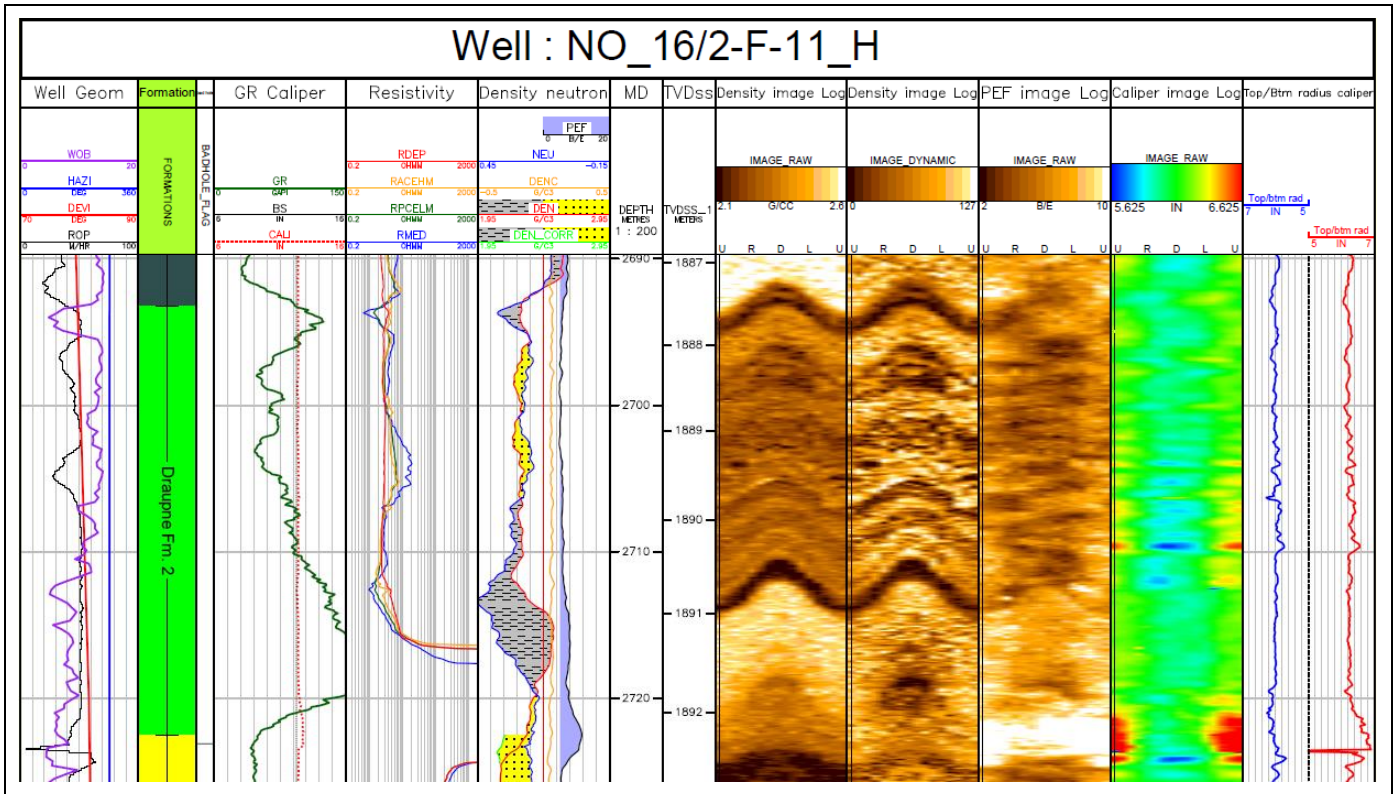


Figure 61: Image log from the drilling of F-11, containing various measurements.

Concerning hole geometry for the rest of the wells, the G-wells seem to be in good condition, apart from minor over-gauge for G-4. However, the time-dependent Draupne hot shale will start deteriorating after a given exposure time, namely between 9–17.5 hours after the hole was drilled (experience from pilot well U-1 B) [62]. From Figure 62 it is clear that after 17.5 hours, the hole is substantially deteriorated. The patterns from the density log could indicate a break-out, with low density values at 90° and 270° phasing (as seen for F-14 lower Sola on a smaller scale). However, as previously mentioned, the mechanisms behind the failure of Draupne hot shale are still debated. Moreover, the hole does not seem to worsen from the first re-log to the second, namely from 17.5 to 30 hours. It should also be noted that it is the upper part of the hot shale which possesses the highest organic content, consequently making it the weakest interval. This can be observed from Figure 62, where the borehole is in-gauge for the lower part of Draupne Fm. 2.

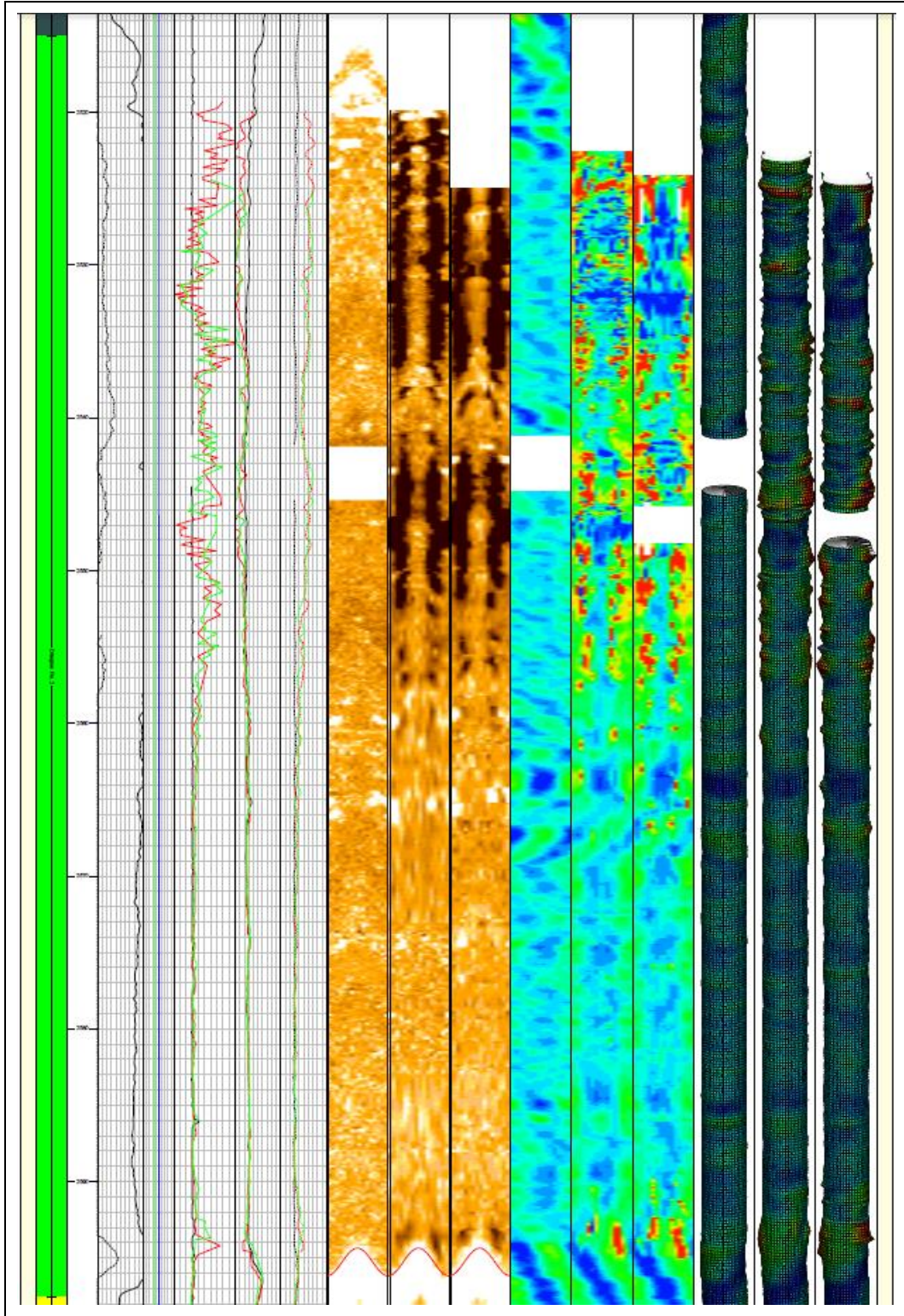


Figure 62: Draupne Fm. 2 hot shale drilled by pilot well U-1 B at 80°. The figure illustrated the gamma ray, resistivity, density image, caliper image and 3D caliper image logs (from left to right) from drilling, first re-log (17.5 hours) and second re-log (30 hours). Deterioration of the borehole after 17.5 hours is evident. However, it does not seem to worsen from 17.5 to 30 hours.

Some minor indications of irregular geometry are indicated for F-12, E-2 and E-1. The strongest indications, although not very pronounced, were two short intervals for E-1 on the PEF log. These features are marked within the dashed black squares in Figure 63. One could also argue

that some irregular shapes are evident for the density log as well, for the same intervals. If so, the spiraling shapes go significantly deeper into the formation, since the depth of investigation (DOI) for the density log is between 2,5–4 inches. Nevertheless, probability of poor hole quality is undoubtedly present.

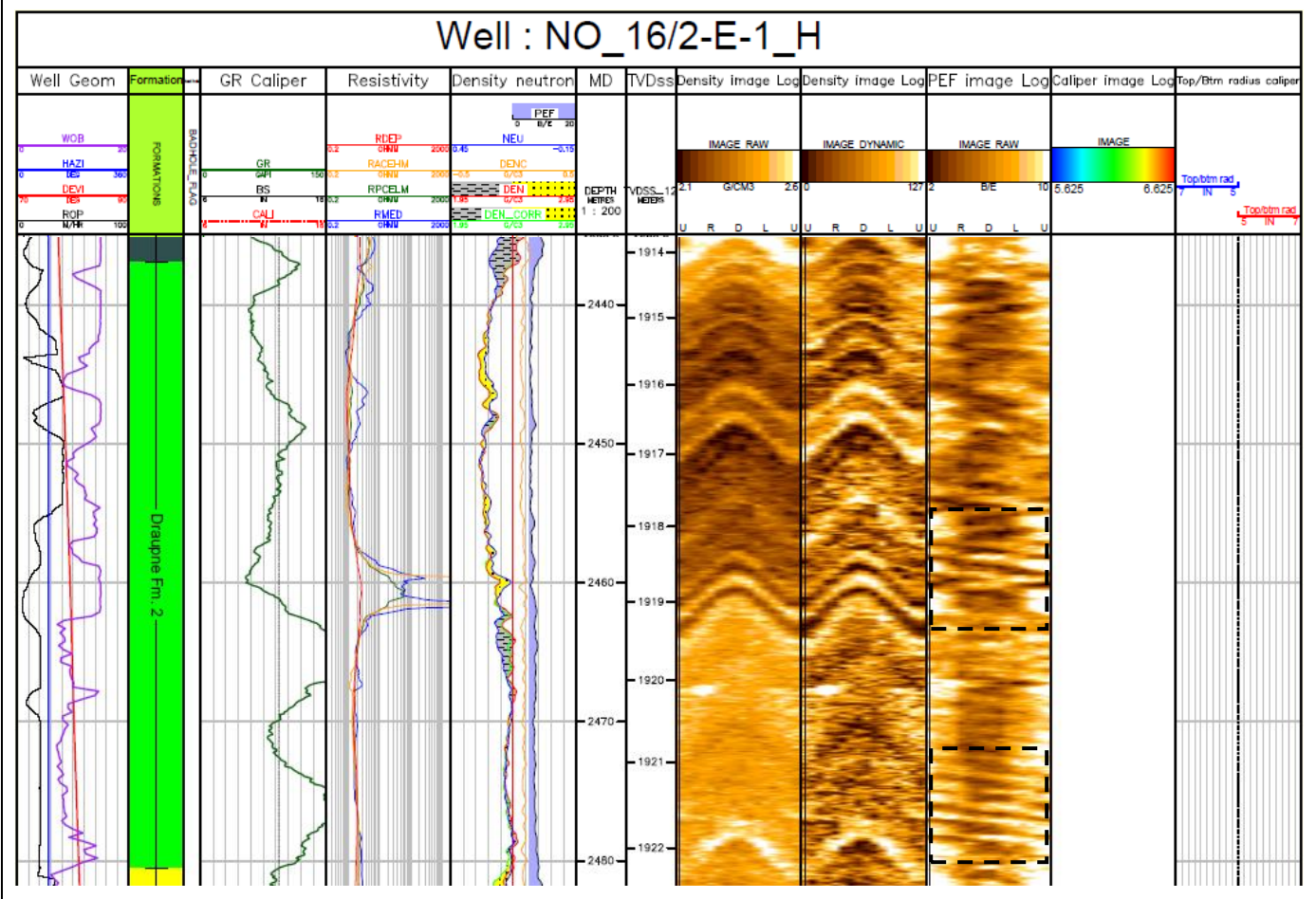


Figure 63: Image log from the drilling of E-1, containing various measurements. Interesting features which may indicate irregular hole geometry are marked within the black squares.

Furthermore, the image log for E-3 shows that the hole is over-gauged with a bit over an inch at ~2235 m MD (see Figure 64). This is not indicated on the real-time caliper log. In addition, the PEF log yield very high readings for the lower part of Draupne 2. This could be because of mud invasion due to lack of sufficient mud cake in this high-permeable reservoir section.

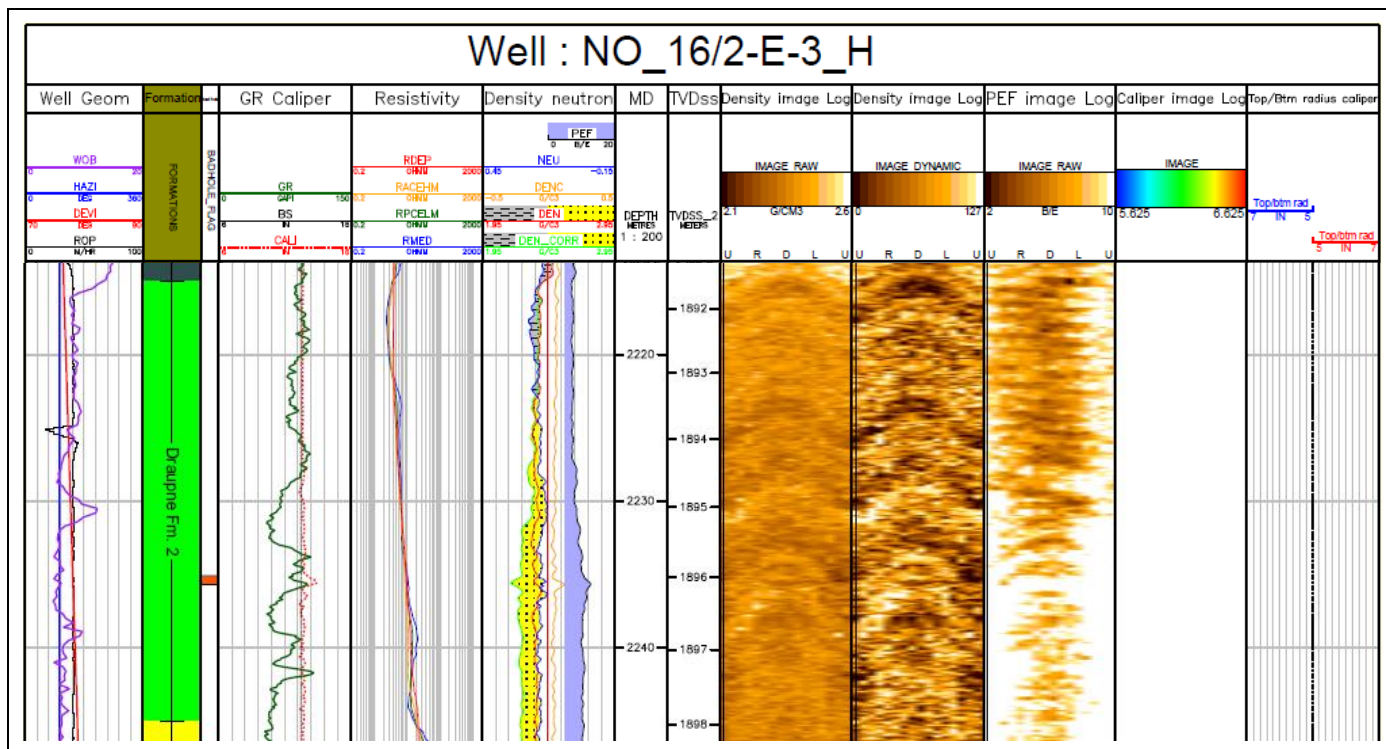


Figure 64: Image log from the drilling of E-3, containing various measurements.

Moreover, the torque values for the different wells were as expected, with relatively high and erratic torque for the wells experiencing low ROP and high WOB. In contrast, the G-wells had low torque values compared to the rest of the wells, most likely due to softer formation in Draupne 2 combined with low DLS (see Figure 65).

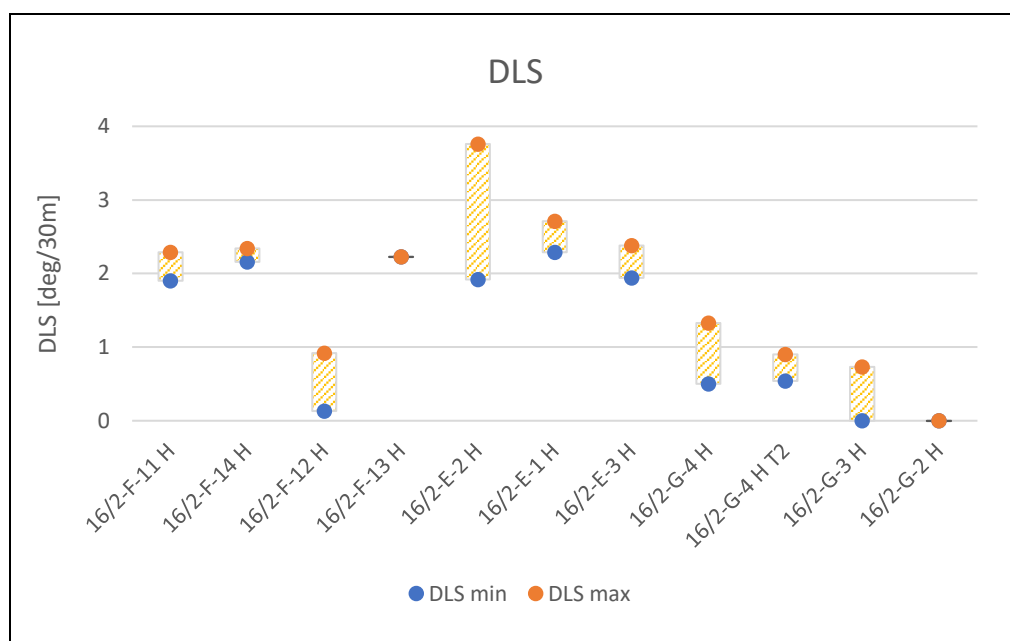


Figure 65: Maximum and minimum DLS for the injection wells when drilling Draupne Fm. 2.

As expected, stick slip was evident for the wells with low ROP values, corresponding to harder formation. Combined with high DLS, considerable probability of stick slip is present. This can be observed in Figure 66. Contrastingly, the G-wells experienced almost no stick slip.

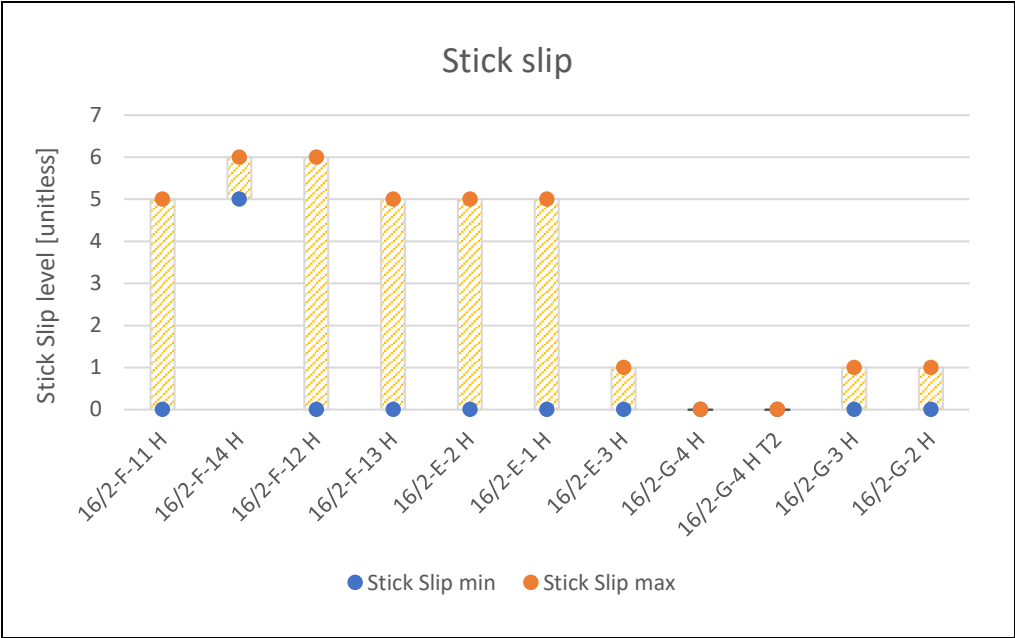


Figure 66: Maximum and minimum stick slip values for the injection wells when drilling Draupne Fm. 2.

5.2.2.4 Hole cleaning

According to best practice, after drilling the section to TD, circulation should be performed to clean the well. At least 3 B/U should be completed with the highest flow and rotation allowed, while stating minimum values of 3000 LPM and 130 RPM for a 12 ¼” hole. Although, for long deviated and/or high ROP sections, the minimum values are not sufficient. Obtaining efficient parameters is especially important for high inclination wells, which tend to accumulate cuttings beds on the low side that are hard to remove.

Figure 67 shows how many B/U circulated for each of the injection wells. A B/U is equal to one annular volume. All wells reciprocated the drillstring during circulation (20-30 meters). Interestingly, F-11, F-14, F-13 and G-2 had considerably lower circulation at TD than the other wells. However, it should be noted that the last few meters of both F-11 and F-14 were drilled with very low ROP (0-5 m/hr) for a longer period of time due to stringers in Draupne Fm. 1. These intervals were drilled with 3000-3500 LPM and 120-140 RPM, and would approximately equal 1,5 - 2 B/U. Nevertheless, fewer B/U at TD were circulated for the two wells compared to the others. F-13 and G-2 were only drilled a few meters into Draupne Fm. 1, which means

that the BHA would be located in Draupne 2 if circulating B/U at TD. Therefore, no circulation was done at TD to spare Draupne 2 for excessive mechanical impact. All circulation for F-13 and G-2 were performed in competent formation above Sola, namely Rødby and Tor.

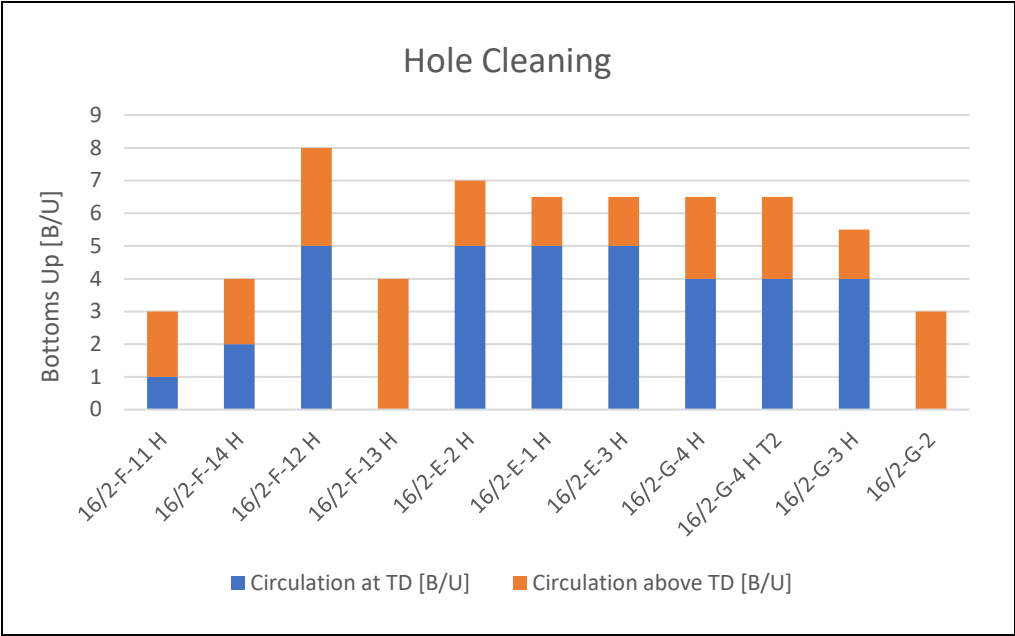


Figure 67: Total amount of B/U circulated for the injection wells.

Furthermore, values for flow rate and rotation during circulation are presented in Figure 68 and Figure 69. Flow rates were kept relatively low for F-11 and F-14, which may have compromised the hole cleaning and consequently the following liner run. As previously stated, a minimum of 130 RPM and 3000 LPM is preferred to be able to clean the hole during drilling, for an in-gauge borehole. In practice, when circulating at TD, one would need more than this due to over-gauged sections and potential cuttings beds, probably yielding the flow rate and rotation for F-11 and F-14 insufficient. However, rotation should not be too high, which could cause weak formation to break loose. Cavings was seen on G-3 during the last B/U, which could signify that 170 RPM may be too high for the G-wells.

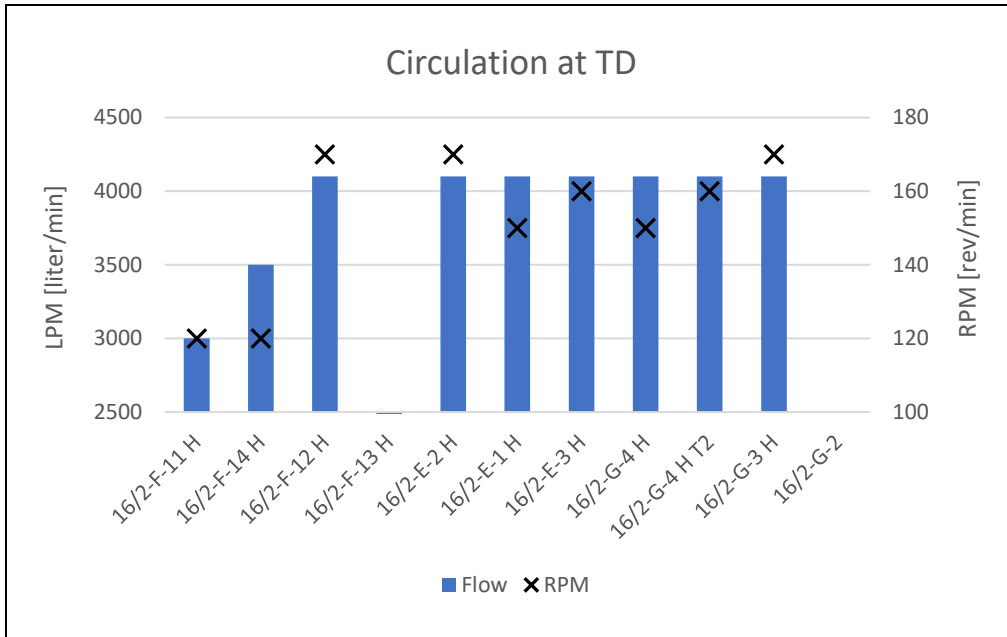


Figure 68: Flow rate and rotation for the injection wells when circulating B/U at TD.

Regarding the rotation above TD, this was performed in a competent formation in the overburden. Either in Rødby, Svarte, Tor or inside the casing. Generally, only a minor amount of cuttings came over the shaker during circulation above TD.

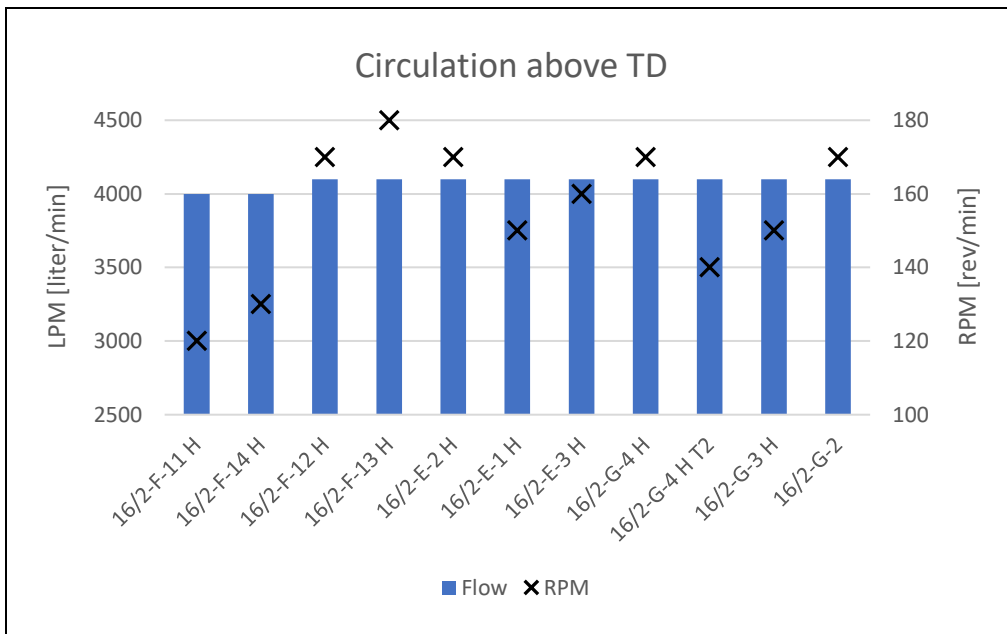


Figure 69: Flow rate and rotation for the injection wells when circulating B/U above TD.

5.2.2.5 Stringer drilling

Stringers are encountered, to some extent, for all the injection wells. However, they have been handled differently. According to best practice [63], stringers should be confirmed by an increase in WOB and torque response. If not torque response is seen, rotation should be decreased for this to be achieved. F-14 struggled with obtaining torque response when drilling stringers, which could be explained by a worn bit.

Furthermore, best practice guidelines also state that flow, along with rotation, should be reduced in order to avoid washout in weak formations above the stringer. However, this was not done for all wells. F-12, F-13, E-1, G-4, G-4 T2, G-3 and G-2 all had intervals where the flow and/or rotation was kept high, although low ROP was evident on the real-time log. The most damaging cases were F-12, G-4 and G-4 T2. These wells will be used as examples.

During the drilling of Asgard for F-12, a low ROP section was drilled with 3500 LPM and 120-140 RPM for an hour, before decreasing the flow. The real-time log is shown in Figure 70. This was an interval at the bottom of Asgard, which corresponds to a washed-out section on the caliper log. It should be noted that this occurred during hand-over at 19:00.

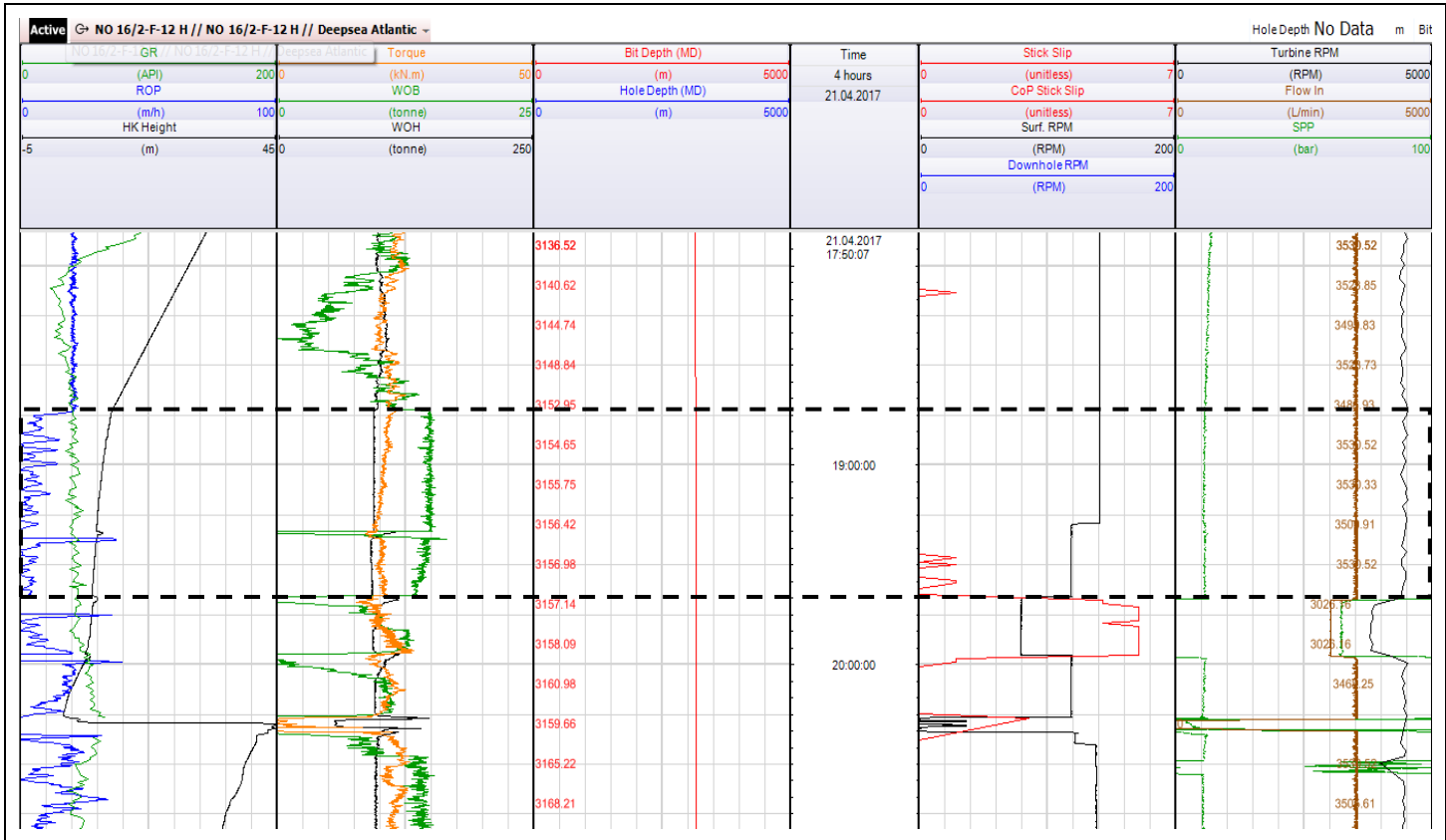


Figure 70: Real-time log for F-12 when drilling stringers in Asgard Fm.

Furthermore, for G-4, an interval with very low ROP was encountered from 2710 m MD to 2770 m MD. Here, flow rate and RPM was not changed before reaching ~2750 m MD. This is illustrated in Figure 71. Significant over-gauged sections from 2710 m MD to 2750 m MD were evident, followed by less over-gauged sections from 2750 m MD to 2770 m MD. This indicates the necessity of altering the parameters according to the real-time values.

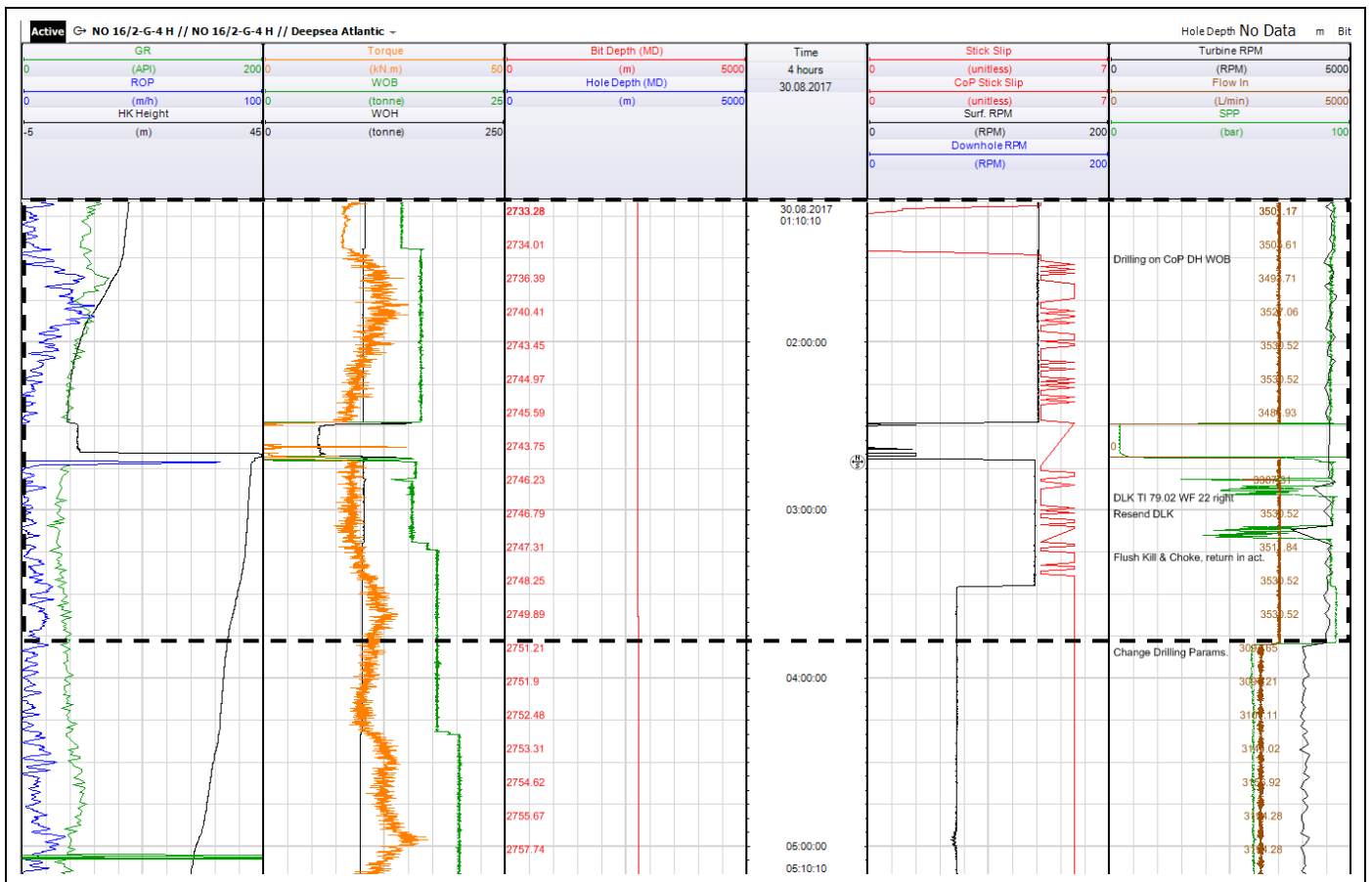


Figure 71: Real-time log for G-4 when drilling stringer in Asgard Fm.

Lastly, G-4 T2 showed very low ROP between 2660 m MD and 2672 m MD (Sola/Aasgard interface), while flow was kept at 3500 LPM and rotation was varied between 100–150 RPM. This is shown in Figure 72. The interval corresponds to significant over-gauged sections on the real-time caliper log. During this interval, the WOB limit was set to 7 tons, which is probably the reason for slow progress. Again, this happened during handover, this time at 07:00.

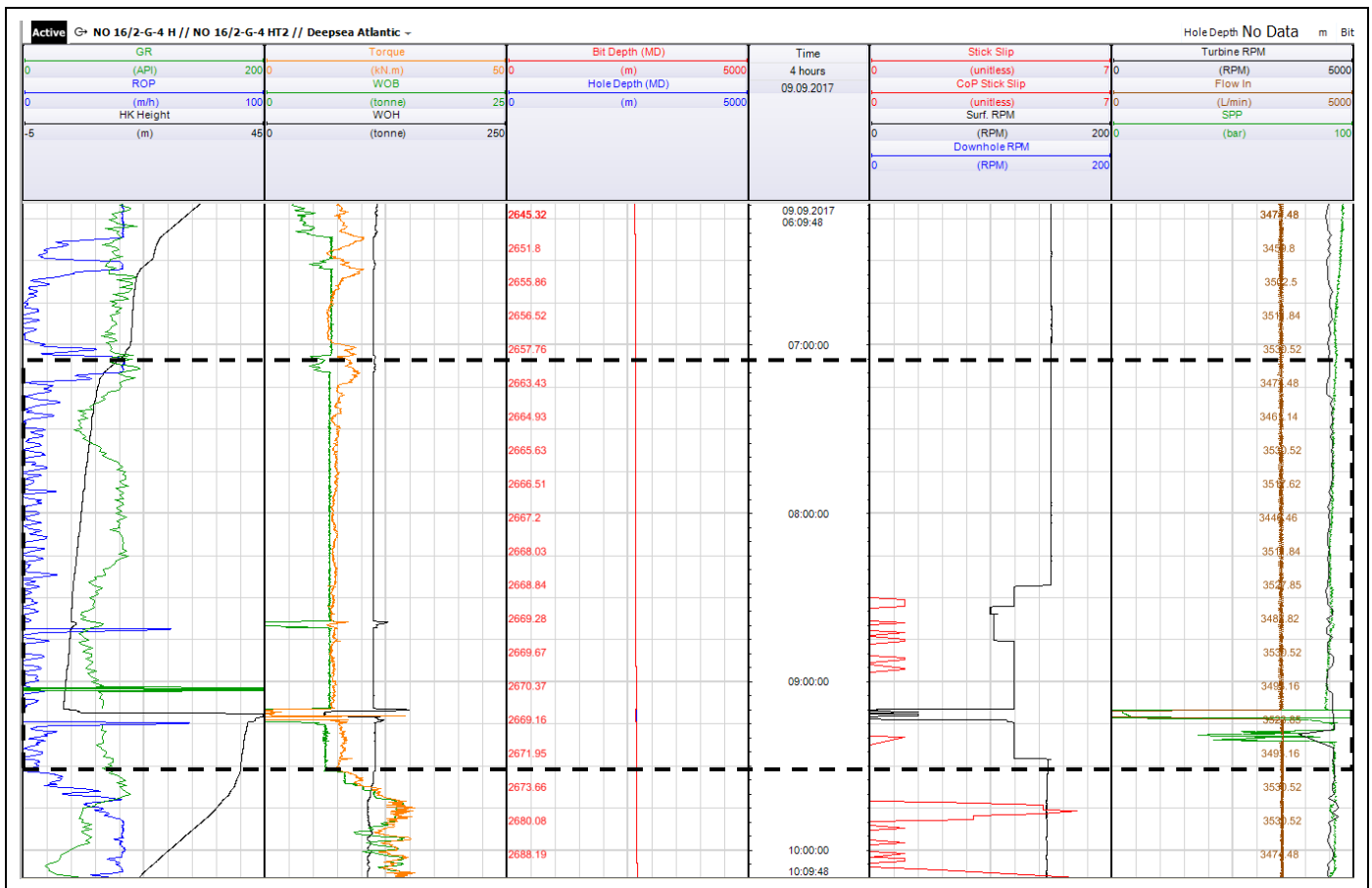


Figure 72: Real-time log for G-4 T2 when drilling stringers in Sola/Aasgard Fm.

5.3 Wiper trip

Several of the liners had to be pulled due to either problems regarding the liner hanger system or inadequate well conditions, where poor hole cleaning was an important factor. Therefore, a wiper trip was performed for some of the wells, namely, F-14, F-12, G-3 and G-2. Subsequently, a second liner run was performed.

Restrictions were met during RIH with the drillstring for all the wells. First, for F-14, there was restriction in Sola Fm. at 2180 m MD. Took 10 tons of weight. Tried several times to wash down past the restriction with different parameters, resulting in fluctuating pressures and pack-offs every time. Eventually, the string was successfully worked down with flow and rotation, where 300 LPM and 25 RPM showed best progress. Also took 15 tons of weight at 2264 m MD, inside Draupne 2. Interestingly, at 2180 m MD there was evidence of a minor breakout on the image log and over-gauged hole was evident on the caliper log during drilling, as discussed previously.

Similarly, for F-12, the bit took 15 tons weight in Sola, at 3019 m MD. No signs of poor hole geometry were evident for the logs. Tried to wash down with different parameters, but eventually had to pull back due to pack off tendencies. Then, circulation was initiated above Sola with 2500 LPM and 50 RPM while reciprocating. During this circulation, the ECD dropped 3 points. After circulating above Sola, the string was washed down with 800 LPM and 50 RPM until the stabilizers were below Sola. Then, slid the drillstring down without flow nor rotation. F-12 also took weight in Draupne 2, at 3200 m MD. After pulling up and starting rotation, no problems were observed when washing down through the rest of Draupne 2. From the D-N log and WOB at this point during drilling, it seems to be a soft and porous formation. Although there is no sign of poor borehole quality on the logs, it may have happened over time or been provoked during the first liner run. Another possibility is that the stabilizers, located at the Aasgard/ Draupne boundary, may have gotten hooked on a ledge at the interface.

For G-3, there were no problems in Sola nor Aasgard. Slid down without any flow or rotation. However, the drillstring took weight inside the Draupne hot shale at 2288 m MD. Pulled above and started circulation with 400 LPM and 20 RPM, but not able to pass restriction when washing back down due to pack off-tendencies. Then, when trying to rotate with 40 RPM, the string was able to pass. Washed through the rest of Draupne 2 with the same parameters.

Lastly, G-2 encountered tight hole in Sola, taking weight three places. Had to wash through with 400 LPM and 20 RPM. Furthermore, the string slid down from Aasgard to TD without

any problems. However, after establishing circulation to 3000 LPM at TD with reciprocation, the string packed off when reaching a rotation of 100 RPM. This is probably because the stabilizers were located in Draupne 2, when circulating. The string was pulled back into Aasgard, and circulation was initiated. Another unsuccessful attempt was done to establish circulation at TD. Eventually, the string was pulled into Aasgard and circulation was performed with 4000 LPM. After circulation was done, RIH to spot an LCM pill at TD and subsequently POOH. LCM was also added to the mud during circulation.

Moreover, Figure 73 shows how many B/U circulated during the wiper trips. The parameters are given in Figure 74. For G-3, the rotation had to be reduced because of cavings on the shaker.

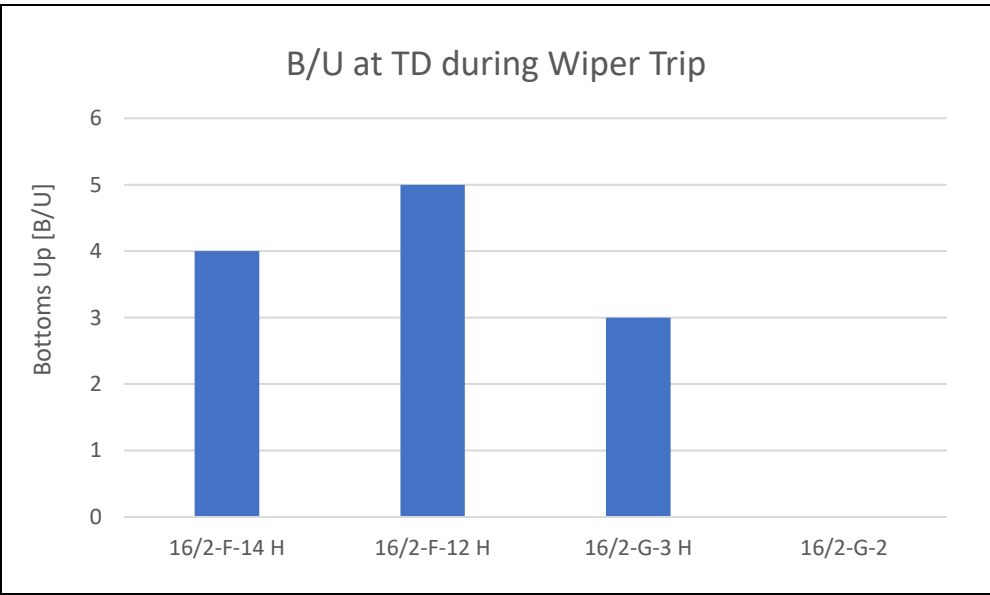


Figure 73: Amount of B/U during wiper trip for the injection wells.

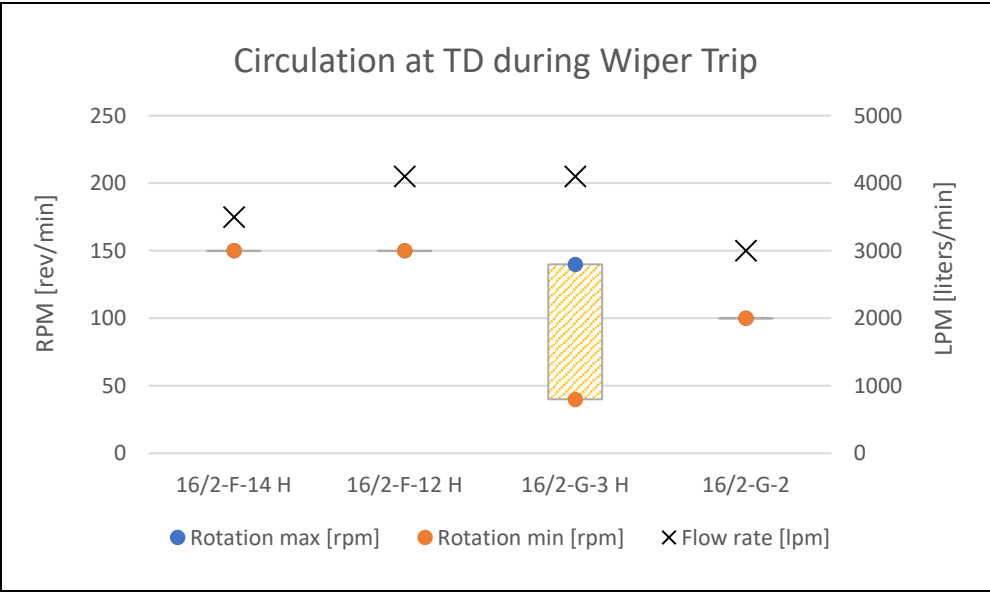


Figure 74: Flow rate and rotation for the injection wells when circulating at TD during wiper trip.

For all the wells a significant amount of cuttings came over the shaker during circulation at TD. For F-12, as much as 3 skips were filled. This is a clear indication that a wiper trip was needed in order to clean the well and leave it suitable for liner running. For G-3 and G-2, cavings were seen on the shakers during circulation. The reasons for this could be that the stabilizers were placed in Draupne 2 during circulation and rotation at TD. For G-3, there had already been shows of cavings during hole cleaning after drilling, making it possible that they were present before the wiper trip.

5.4 Running Liner

The image and caliper logs examined in section 5.2 are a best-case scenario for the state of the borehole when the liner reaches TD. However, the borehole could go through several weakening processes after it has been drilled, both mechanical and chemical.

As for previous sections, the real-time logs were used to obtain useful data for analysis. Maximum and minimum values were collected for Sola Fm., Aasgard Fm. and Draupne Fm. 2.

5.4.1 Introduction

Naturally, longer liners are more difficult to run and cement. Elevated torque and drag values are a key factor to why long liners are incapable of initiating or maintaining rotation at greater depths. From Figure 75, one can observe that F-11, F-12, G-4 T2 and G-2 possess somewhat longer liners than the other wells.

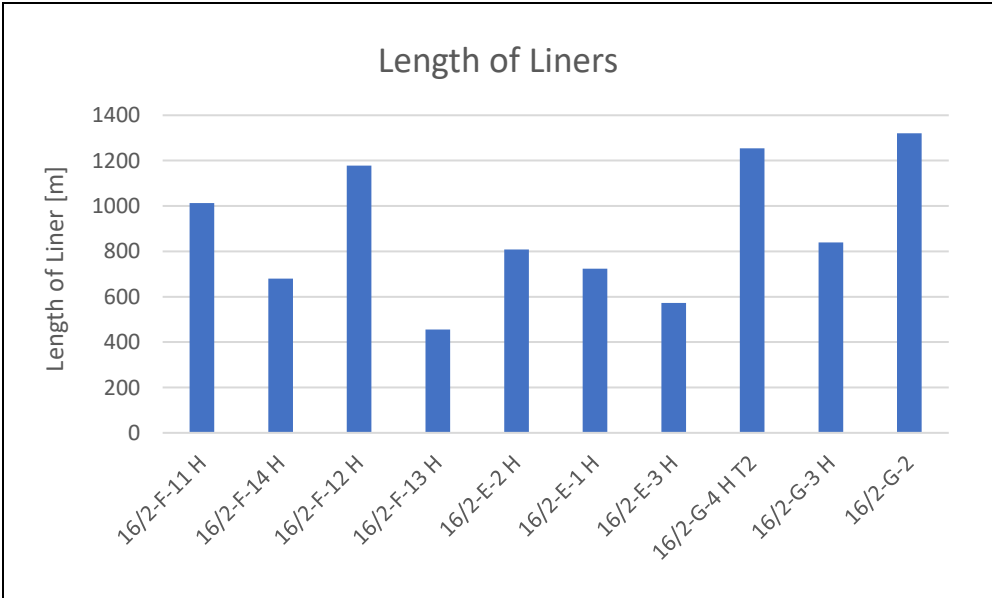


Figure 75: Length of liners used on the different injection wells.

Furthermore, bow spring centralizers were used for all the injection wells. However, there were some alteration to the centralizer density, where the F- and E-templates used 2 centralizers per joint, while 3 centralizers per 2 joints were used for the G-template. Obviously, this would render the stand-off of the liner a bit less for the G-wells, namely 86%. While the other wells obtained a stand-off of about 88%. Nevertheless, both these values are well above the API minimum value of 67% and would yield satisfying centralization.

Also, some changes to the liner hanger system has been done. For F-11 and F-14, a hanger system containing a packer and two sets of slips, one for anchoring the liner to the previous casing and one to be engaged after the packer element is set (hold-down slips). However, for F-14, the hold down slips set prematurely, which caused the liner to get stuck. Consequently, the liner hanger system was altered for the next wells, where the packer was not run as part of the liner but was set subsequently. Thereby excluding the hold-down slips.

Moreover, during liner running on F-12, sufficient circulation could not be established, and rotation was lost after setting the liner hanger slips when circulating at TD. Therefore, the liner had to be cut and pulled. It should be noted that this was due to a destroyed bearing in the liner hanger. There were similar experiences for G-3, although this was not directly linked to a malfunctioning bearing. However, engaged slips is an area of potential pressure drop and cuttings accumulation, which could be the reason for fluctuating pressure after setting the slips (ref. section 3.5). Therefore, an expandable liner hanger system was implemented for G-2 (last well drilled as of June 2018).

Two liner runs were performed for several wells, namely F-14, F-12, G-3 and G-2. The reasons for pulling the liner on F-14, F-12 and G-3 are explained above. For G-2, circulation could not be established at TD due to pack off tendencies, in addition to high loss rates. Eventually, the decision was made to POOH. Since an expandable liner hanger was used, the liner was not anchored to the previous casing and was consequently retrieved with ease. Moreover, for G-4, the liner packed off and got stuck, consequently leading to a side-track.

5.4.2 Results

The results from the analysis of data will be presented for each of the formations of interest: Sola Fm., Aasgard Fm. and Draupne Fm. 2. The objective is to investigate how the given well conditions occurred and observe if there is any correlation between the obstacles encountered during liner running and the intervals of poor borehole quality seen in section 5.2. There is no doubt that well conditions could be significantly worsened when running liner.

5.4.2.1 Sola Fm.

During liner running, Sola were particularly troublesome for the F-wells. Obstructions were met in F-11, F-14 and F-12, where significant time and work was needed to pass. As seen in Figure 76, the liner had to be worked down for relatively long distances, of which the Sola/Aasgard boundary was passed for all the wells.

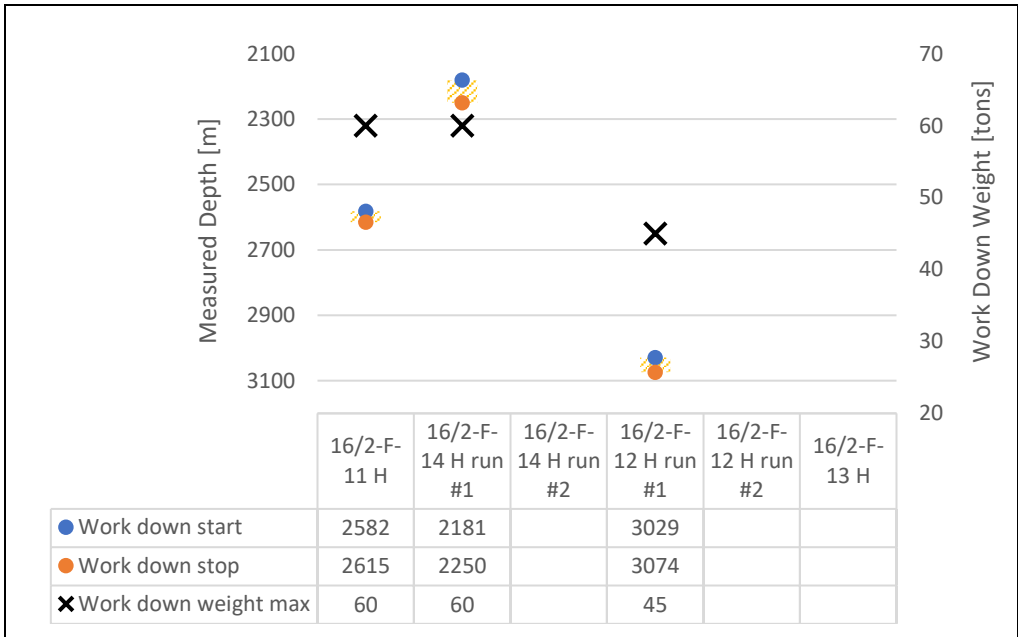


Figure 76: Illustrating the distance the liner was worked down and the corresponding maximum weight applied in Sola for the F-wells.

Washing through Sola with low rotation and flow rate was the primary mitigating action used when meeting restriction for most of the F-wells, except F-14. Here, the liner was worked through the obstruction for ~70 meters over 5 hours. Although washing was the first remedial action, it was not successful for any of the primary liner runs, except for F-13. Fluctuating SPP were experienced when trying to wash with different parameters, indicating a dirty well. Several

attempts with different combinations of flow and rotation was attempted. For F-11, acceptable progress was made with 200 LPM and 20-60 tons of weight. F-14 and F-12 made slow, but steady progress with weight only.

After pulling the liner and performing a wiper trip for F-14 and F-12, no major restrictions were encountered when washing down Sola with steady parameters. However, precautions were taken by making sure a connection was not made in the Sola/ Aasgard interface. In addition, 6 tons weight was taken at this boundary for F-12 during the second liner run. There is no doubt that the Sola/ Aasgard interface has caused time-consuming issues for the F-wells.

Furthermore, there were no obstructions encountered in Sola for the E-wells. All liners slid down without any rotation nor flow on first attempt.

For the G-wells, however, some restriction was seen in Sola (see Figure 77). Especially for G-4 and G-2, where the liner encountered fluctuating pressures while washing. The G-4 liner was pulled back to circulate with moderate rates (1200 LPM), although not successful due to pressure fluctuations. Moreover, both wells eventually had to work down the liner with only rotation. No evidence of poor well geometry on the image nor caliper logs for G-4 in Sola (logs not available for G-2). For G-4 T2, only minor obstruction was observed due to tight hole. Interestingly, obstruction was encountered in the top section of Sola for the G-wells, as opposed to the F-wells where restrictions were seen in lower Sola. Regarding the second liner runs for G-3 and G-2, the liners slid down without problems.

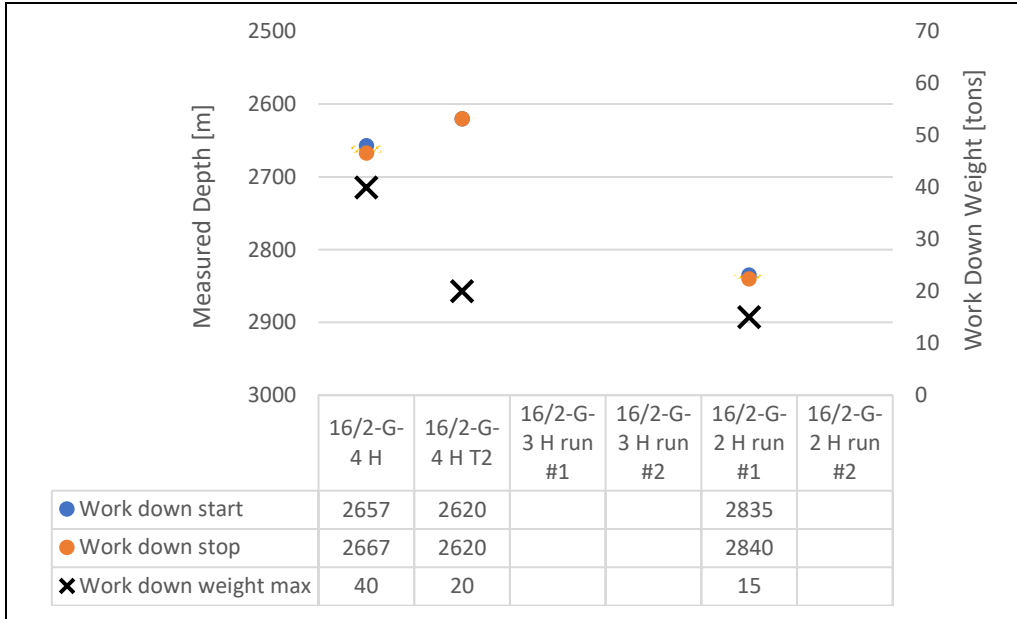


Figure 77: Illustrating the distance the liner was worked down and the corresponding maximum weight applied in Sola for the G-wells.

5.4.2.2 Aasgard Fm.

Restriction in the Sola/Aasgard interface was experienced for the F-wells (illustrated in Figure 77), although no problems in the lower parts of Aasgard. Nearly all wells slid down middle/lower part of Aasgard, without flow or rotation. Except for F-12, which effortlessly washed down with 400 LPM and 20 RPM.

There were no major obstructions when running liner on the E-wells. The liner was slid down without flow or rotation to TD.

All G-wells slid down Aasgard without any major issues. In addition, circulation was established in lower Aasgard before entering Draupne 2. This was done to clean the borehole around the lower part of the liner before running through the hot shale. Thereby mitigating the risk of getting stuck due to debris compacting around the liner. Pack off tendencies occurred during circulation in lower Aasgard for G-4 T2 and G-2 (first run). Interestingly, fluctuating pressures were seen for G-3 during the second liner run, but not the first.

5.4.2.3 Draupne Fm. 2

No restrictions were seen in Draupne 2 for neither F- nor E-wells. Here, F-14 (second run), F-12 and F-13 washed through Draupne with 400 LPM and 20 RPM. The rest of the liner runs on the F- and E-wells slid down without flow nor rotation.

For the G-wells, however, restriction was met in Draupne 2. This may not be surprising due to the presence of the problematic hot shale. Figure 78 illustrates where the liners had to be worked down, including maximum work down weight. For G-4 and G-4 T2, obstructions were met instantly when reaching the interface between Aasgard and Draupne 2. For G-3 and G-2, however, restrictions were experienced when approaching the deeper parts of Draupne 2.

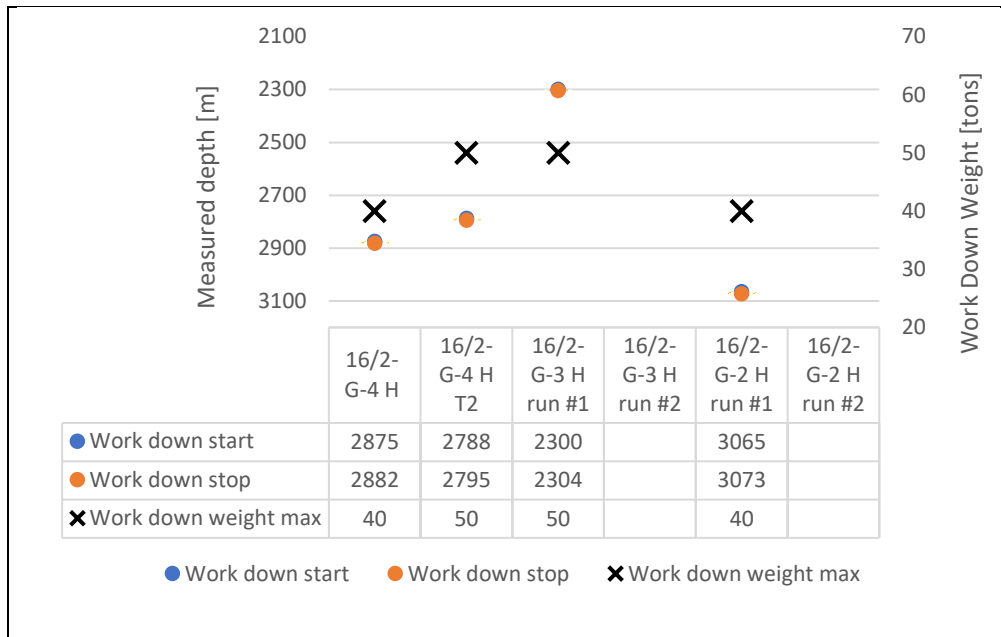


Figure 78: Illustrating the distance the liner was worked down and the corresponding maximum weight applied in Draupne 2 for the G-wells.

For G-4, the liner was worked down with 200 LPM until the pressures fluctuated and the flow had to be stopped. Eventually, the liner was worked down with only rotation the last two meters. Moreover, the liner on G-4 T2 had to be worked with 300 LPM through lower part Draupne 2, causing pressure fluctuations.

Furthermore, for G-3, the liner was worked down when reaching the omission zone (~2300 m MD) with maximum 50 tons for ~1 hour. At this point, a connection was performed, which probably contributed to the slow progress. The casing shoe may have been partly submerged into the soft formation on the low side due to gravitational forces acting over a longer period of time. Also, G-2 encountered problems when approaching the omission zone. First, the liner was worked with 30 tons, before pulling up to bottom Aasgard to circulate. Following the circulation, another unsuccessful attempt was done to wash down into Draupne 2. Eventually, the liner had to be worked down for 9 hours with 30-40 tons weight.

For the G-wells, there was not observed any unwanted hole geometry on the logs that correlates to the abovementioned restrictions. This supports the experiences from the pilot wells, where Draupne 2, especially the hot shale, seems to be almost perfectly in-gauge on the logs during drilling.

5.4.2.4 Circulation and rotation at TD

For most of the wells, a lot of time was spent trying to obtain sufficient flow rates when the liner had reached TD. Especially for F-11, where 52 hours passed before finally achieving 1200 LPM with stable pressures. As mentioned previously, for F-14 and F-12 mechanical failure of the liner hanger system is largely to blame for the difficulty of obtaining wanted parameters at TD. For G-3, however, there were only problems with achieving flow rates after the slips were set. Moreover, G-2 experienced somewhat fluctuating pressures while circulating, including static losses at TD, which is why it was decided to POOH and perform a wiper trip to clean the well and circulate LCM.

For the E-wells, no problems were encountered while bringing up flow at TD. Optimal flow rates of 2000 LPM without rotation and 1600 LPM with rotation were achieved quickly and with stable pressures. F-13 is the only well, excluding E-wells, that did not encounter any problems with circulation during the first liner run.

Furthermore, for G-4 the liner never reached TD because of an obstruction inside Draupne 1. First, the string stalled out and SPP was very fluctuating, in addition to having overpull when trying to pull above trouble zone. Eventually, full losses were experienced when circulating above trouble zone. When trying to run back down, not able to reach former point of obstruction. LCM was pumped with reciprocation above obstruction for 14 hours in an attempt to mitigate losses. Not able to cure losses, in addition to an unbreachable obstruction led to POOH and a side track (G-4 T2).

For all the secondary liner runs, there was no problems achieving the wanted rates, although inferior to the rates obtained for the E-wells. Namely 1200 LPM without rotation and 1000 LPM with 20 RPM.

Furthermore, being capable of performing rotation at TD is vital for the upcoming cement job. For the injection wells, a rotation of 20 RPM was desired. Torque values when rotating the liner at TD were extracted and are illustrated in Figure 79, except for G-4 where the values relates to the rotation just above TD. All values were obtained before the liner hanger slips were set. The torque is expected to increase with section length and the general quality of the borehole. It is evident that F-14 possessed higher torque values relative to section length than any of the other injection wells. Since the aspect of section length is considered, together with eliminating the impact of the liner hanger bearing (which was proven faulty for F-14), this could indicate a poor

well geometry for F-14. Namely, increased frictional forces between the borehole wall and liner.

Moreover, G-4 T2 showed low torque values relative to section length. By comparing these values to the torque values of G-4, which is drilled in formations possessing almost exact same properties, possibly indicating increased hole quality.

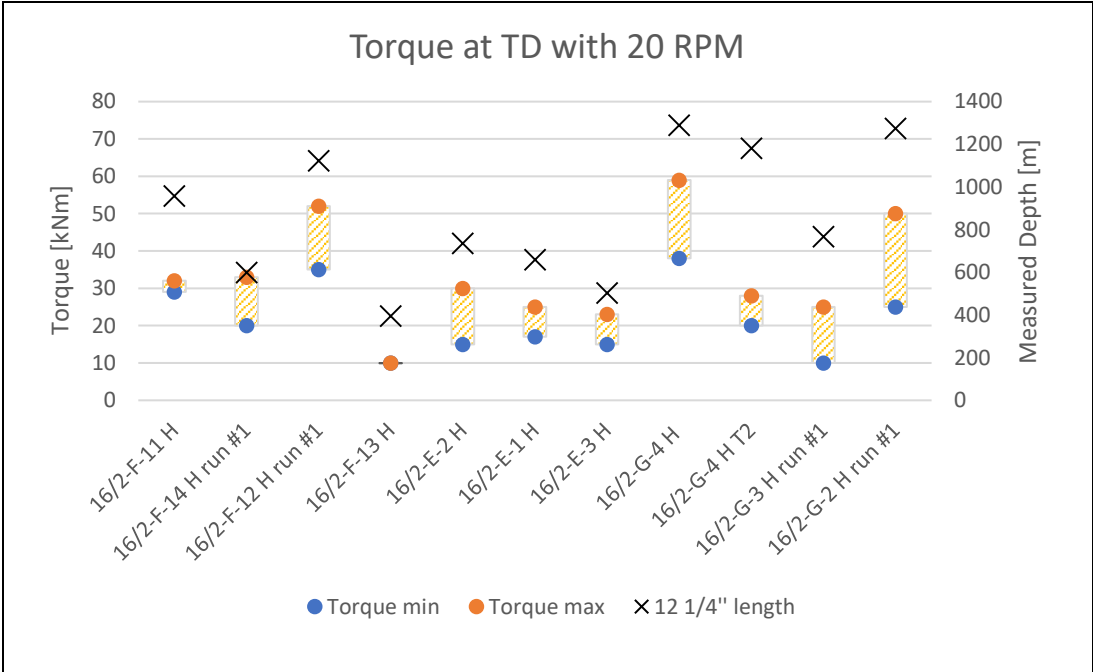


Figure 79: Torque values for rotation of liner at TD with 20 RPM, before setting liner hanger slips.

5.4.2.5 Time from drilling to running liner

In order to investigate if there was any time-dependency on the hole stability for the injection wells, time from drilling to running liner was noted. These can be observed for Sola Fm., Aasgard Fm. and Draupne Fm. 2 in Figure 80, Figure 81 and Figure 82, respectively.

Of course, the time spent from drilling to running liner is dependent on the 12 1/4” section length. This can be seen in Figure 80. However, it seems that the drilling and running went faster for the G-wells.

Furthermore, significant obstructions occurred during the liner run through Sola for the F-wells. Interestingly, longer time went by from drilling to running for the F-wells compared to the other wells, namely above 40 hours. This is excluding F-13, which was the shortest injection well drilled. Due to relatively short sections on the E-template, reduced times are observed. Both G-

4 T2 and G-3 ran the liner though Sola before 40 hours had passed. Similar to the F-wells, G-4 and G-2 also experienced restriction when running through Sola after more than 40 hours after drilling.

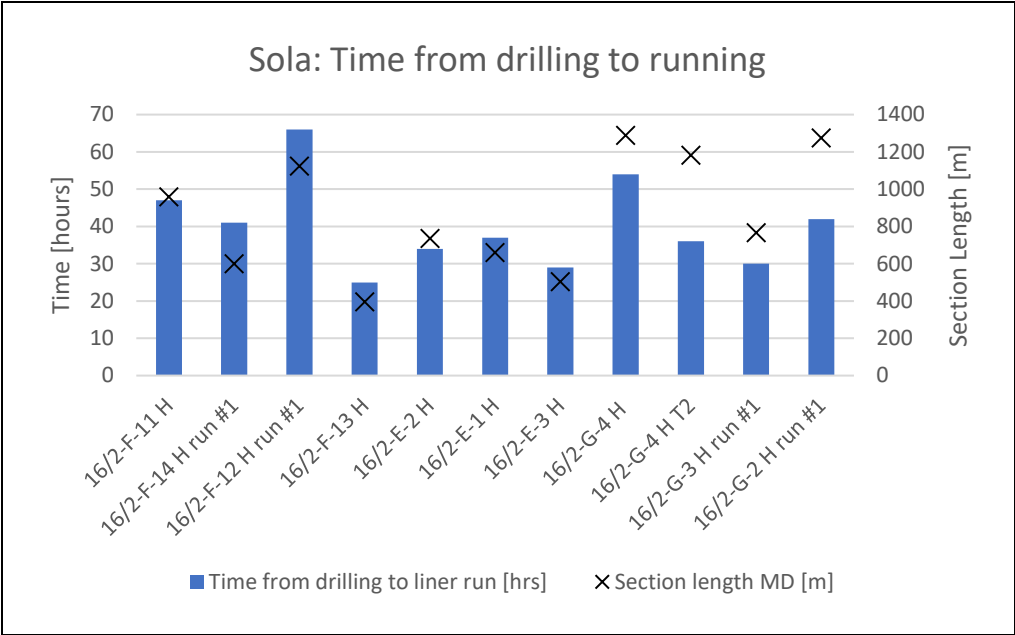


Figure 80: Time from drilling to running liner in Sola Fm. for the injection wells, including the 12 1/4" section lengths.

Time spent from drilling to running for Aasgard and Draupne 2 are fairly similar to those for Sola. However, considerable time was spent drilling the Aasgard section, which renders the drilling-to-running times for Draupne 2 a bit less for almost all the wells.

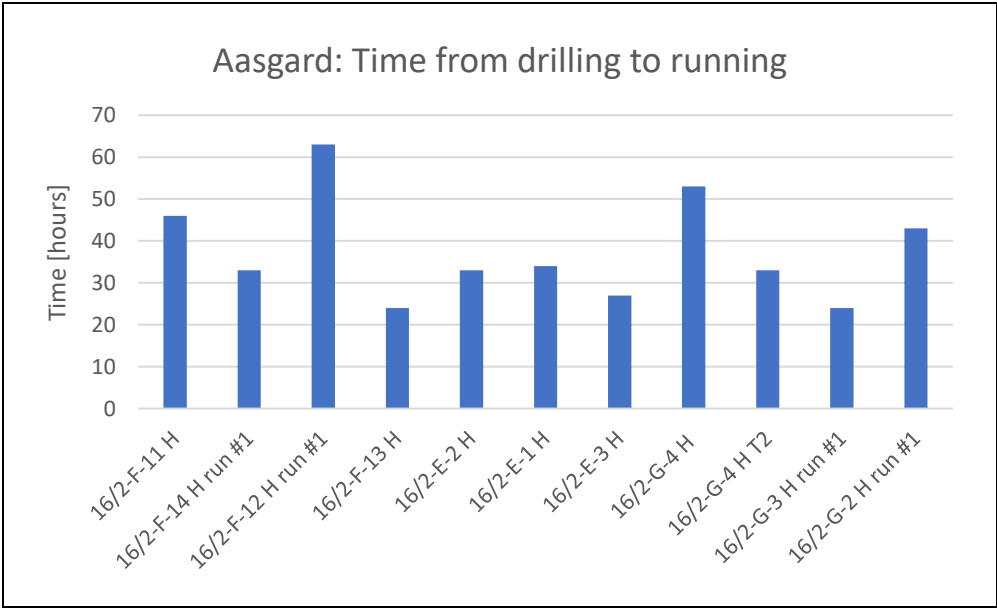


Figure 81: Time from drilling to running liner in Aasgard Fm. for the injection wells.

As previously stated, the time-dependency of Draupne 2 hot shale has been established through the drilling of the pilot well U-1 B. Here, bits of the formation had fallen into the borehole when running in after ~18 hours [14]. All G-wells spent more than 18 hours from drilling to running, consequently meeting a lot of restriction in this formation. In practice, running the liner through Draupne Fm. 2 before 18 hours has passed is nearly unfeasible for long sections. Also, other problems arise when running speed increases (swab/surge effects).

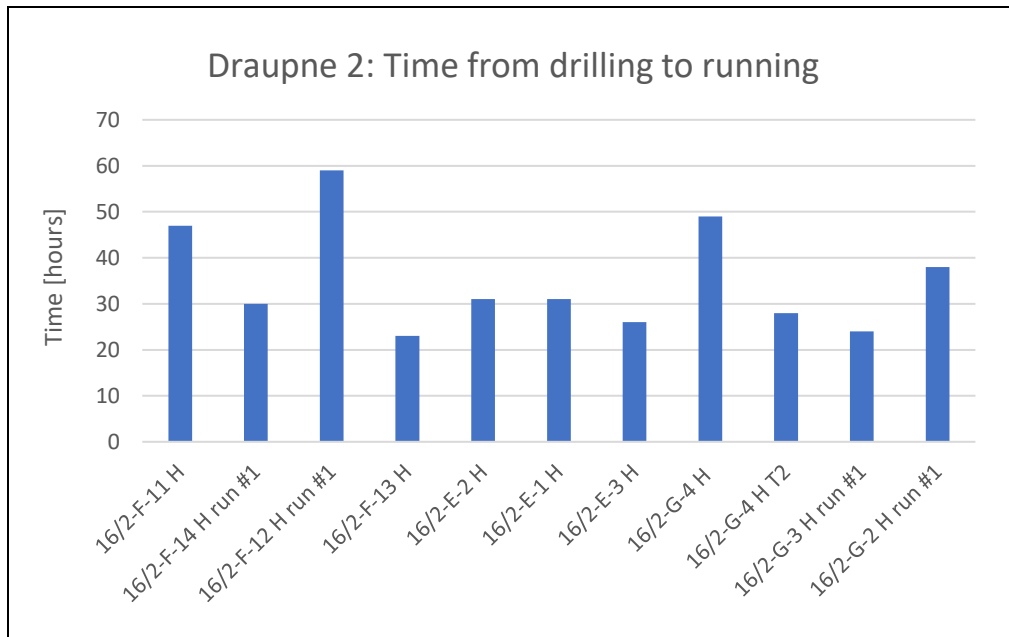


Figure 82: Time from drilling to running liner in Draupne Fm. 2 for the injection wells.

6 Summary and Discussion

During the course of writing this thesis, a lot of data was collected and analyzed. Although some of the data indicates trends and results, one must keep in mind that comparing wells from different templates should be done with great care due to the alteration in the composition of the formations. Nevertheless, some interesting results were obtained.

Regarding the formations, there is a clear trend in the length of the different sections. Generally, the E-wells possess longer sections of Sola Fm., whereas the Aasgard Fm. section is significantly shorter than the other wells. However, for the G-wells, Aasgard Fm. is undoubtedly longer compared to the F- and E-wells. Also, the G-wells encounter the unstable Draupne hot shale.

6.1 Cement

First, the cement jobs were investigated. Interestingly, the theoretical top of cement seemed to correlate well with the top of good cement seen on the logs at rotation stop. Additionally, the top of good cement was located in upper Aasgard for all the wells experiencing a cease in rotation during cement displacement. Namely, F-11, F-14, G-4 T2 and G3. It should be noted that the cement log interpretation for G-3 was only preliminary and should be investigated in greater detail. However, these results clearly demonstrate the importance of rotation during cementing. For G-3, before rotation stopped, a majority of the displacement was performed with only 500 LPM. Even at such low rates, the preliminary cement interpretation revealed a good, continuous, isolating cement (ref. section 5.1.2).

Furthermore, for the majority of the abovementioned wells, stop in rotation could be correlated to over-gauged sections on the caliper logs. A possible explanation could be cuttings accumulating in the washed-out sections and eventually become static. Due to buildup of gel strength, these cuttings will remain static during circulation and hole cleaning. Eventually, when the cement reaches the static cuttings during cementing, they are mobilized due to the increased lifting capacity of the cement (high density and viscosity). When the cuttings get into the wellbore they pack around the liner, increasing the friction forces, which ultimately causes the liner to stop rotating due to exceeding the maximum torque limit. However, it should be noted that there was a bearing-failure in the liner hanger for F-12, where rotation stopped during the first liner run. Although none of the other wells has proven affected by a malfunctioning bearing in the liner hanger, it should be considered as a contributing factor to stopped rotation.

Also, regarding the quality of the cement in the reservoir section, great improvement was evident after changes done from E-2 to E-1 and E-3. No continuous good cement was present in the reservoir for E-2, whereas E-1 and E-3 obtained ~100 m below top Draupne Fm. 2. The following alterations were performed:

- Pressure testing after logging – to let the cement obtain sufficient strength.
- Limiting DLS to $< 2^{\circ}/30\text{m}$ when drilling the reservoir.
- Lead and tail cement – where the lead cement contains more retarder.
- More LCM in mud while drilling the 12 ¼” section, in addition to spotting an LCM pill at TD before POOH.
- No pressure peak against the cement after releasing the liner running tool.

Since all these alterations were done simultaneously, there is no way of knowing if there was a single change or a synergy between the alterations that provided good quality cement in the reservoir section.

6.2 Drilling

Moreover, based on the theory that over-gauged and irregular hole geometry causes cement job failure, a study regarding the drilling of the 12 ¼” sections were conducted. Poor hole quality can occur at any point in a well, although some areas are more exposed than others. Nevertheless, the most critical areas of poor hole geometry are the deepest formations, namely Sola Fm., Aasgard Fm. and Draupne Fm. If irregular geometry causes a rotation stop or pack-off at these depths, it would be a significant threat to the objective of achieving a sufficient barrier during injection.

First, indications of a break-out in lower Sola was observed for F-14 on the image density log, which was drilled with a MW of 1.33 s.g. This could indicate that the MW was too low to provide sufficient pressure support for the borehole wall [36] [34]. However, no indications were seen when drilling F-11, using the same MW. This could be explained by F-14 instantly hitting hard stringers when reaching Aasgard yielding slow progress (0-10 m/hr), whereas F-11 did not. Therefore, since the density logging tool is positioned ~28 meters behind the bit, the lower section in Sola had been exposed for a longer time before being logged (~7 hours), compared to F-11 (~1 hour). Consequently, allowing the break-out to develop before logging.

Parallels could be drawn to the Draupne Fm. 2 hot shale. Although more severe, similar patterns were observed on the image density log (ref. section 5.2.2.3). However, break-out in Sola was only observed for F-14 despite having a lot of trouble when running the liner through the formation, especially for the F-wells. Nevertheless, this should be kept in mind during mud weight design for upcoming wells near the F-template.

Spiral patterns were observed for F-14, which are usually induced by lateral vibrations. These vibrations allow side-cutting of the bit, ultimately causing spiraling shapes [33] [39]. Regarding torque values versus section length, the highest values were seen for F-14, indicating that the friction against the formation was greater (ref. section 5.4.2.4). Due to the decrease in effective borehole diameter when experiencing spiral geometry, this could lead to an increase in contact points for the liner during running and rotating.

Furthermore, high DLS ($> 3 \text{ } \mu\text{m}/30\text{m}$) intervals were seen in Aasgard for F-14, G-4 and G-3. All these wells contained intervals with high WOB ($> 15 \text{ ton}$) and torque values, which in turn led to high stick slip values (5–6). Over-gauged sections were also seen for these intervals.

Drilling stringers in Aasgard is a very critical part for the 12 ¼” section, where parameters need to be optimized in order to gain sufficient progress and not cause washout of the weaker formation in the overburden. Best practice for stringer drilling is found in Appendix A – Equinor’s Internal Guidelines, where it is stated that both flow rate and rotation should be lowered when hitting a stringer. However, this has not been the case for all the injection wells. As one can tell from the examples shown in section 5.2.2.5, there has been a significant time-interval from hitting the stringer to reducing flow and rotation. This has also been correlated to over-gauged sections on both the image caliper and real-time caliper logs.

Throughout the drilling of the injection wells, the hole cleaning parameters have been altered significantly. Where F-11 and F-14 had insufficient parameters in terms for hole cleaning: both with 120 RPM, accompanied by 3000 and 3500 LPM, respectively. According to best practice (see Appendix A – Equinor’s Internal Guidelines), minimum values for cleaning the hole in a 12 ¼” section is 130 RPM and 3000 LPM, however, values should be higher in the case of a highly deviated well or high ROP. Both wells struggled with obtaining necessary circulation at TD during the first liner run due to fluctuating pressures, where F-11 circulated for >52 hours before obtaining stable pressures. Interestingly, F-11 did not show any significant signs of poor borehole quality on neither the real-time caliper nor images logs. Indicating that a dirty hole might have been a major contributing factor for lost rotation during cementing. F-14, which had

both poor hole cleaning and borehole quality, suffered rotation stop and pack-off during cementing followed by full losses.

Furthermore, hole cleaning parameters at TD were consistent after the F-11 and F-14 incidents (4100 LPM and 150-170 RPM), with the exception of F-13 and G-2. Here, the section was drilled only a few meters into the reservoir, and no circulation was performed at TD. This did not cause any problems for F-13, since it was a very short well. For G-2, however, lacking circulation at TD combined with the presence of Draupne hot shale may have rendered a dirty well. In addition to losses during circulation with the liner at TD, the liner was not able to develop sufficient flow rate. Subsequently leading to pulling the liner and performing a wiper trip. Moreover, circulated volumes at TD were also changed after F-11 and F-14 (1 and 2 B/U, respectively), where 4–5 B/U were performed for the succeeding wells (except G-2 and F-13). This was also a strongly contributing factor for the poor cleaning of F-11 and F-14. Illustrations are found in section 5.2.2.4.

Lastly, connections done in Draupne hot shale and in the Sola/Asgard boundary may have led to complications. Due to weak formations, the pipe might have been partly submerged into the soft rock, and restriction is seen when trying to continue running in hole. When running liner on G-3, a connection was performed in lower Draupne Fm. 2. Subsequently, the liner had to be worked down for an hour, with only a few meters of progress.

6.3 Running liner

One of the main purposes for drilling a smooth and clean well, is to make it suitable for running casing or liner. As seen from the results, some obstruction was met when RIH with the liner. Generally, although fairly short sections (30–50 m), Sola caused a lot of trouble for the F-wells. Obstructions were encountered in lower Sola, approaching the Sola/Asgard boundary, where the liner ultimately had to be worked down with a lot of weight. For the G-wells, only minor obstructions were seen, except for G-4, which took weight in the middle of Sola (corresponding to the point where the bit started to build angle) and had to work down for ~10 meters. Furthermore, the E-wells did not experience any trouble when running the liner.

Moreover, the logs indicate that there could be harder formation through Sola for the E-wells compared to the others. A narrow D-N and low GR throughout Sola may indicate fairly homogeneous composition, except from the stringers in E-1. Both F- and G-wells seem to contain weaker clay-containing formation approaching lower Sola. Especially in the

Sola/Aasgard boundary, where there is a peak in GR, accompanied by a decrease in density and a broader D-N. In addition, the time from drilling to running is significantly lower for the E-wells. Actually, all the wells using above ~40 hours from drilling to running liner through Sola, experienced major obstruction. Both the lithological differences and the time-aspect from drilling to running is worth noting for the upcoming wells in Sola.

Except from having to work the liner from Sola down into Aasgard, no restrictions were seen in the lower part Aasgard for any of the F-wells, including G-4 T2. None of the other wells had any problems running through Aasgard.

Furthermore, when running through Draupne 2, restrictions were only encountered for the G-wells. Most of these obstructions are undoubtedly related to the unstable Draupne hot shale. Since the upper part of Draupne 2 hot shale is the most organic-rich, this is consequently regarded as the weakest. Here, obstruction was met for all G-wells, except for G-3 and G-2, which experienced problems when approaching the omission zone.

For F-14, F-12, G-3 and G-2, where a wiper trip was performed, no remarkable obstructions were experienced during the second liner run. Interestingly, after high flow rate and rotation at TD during the wiper trip, Draupne 2 did not seem to worsen in terms of instability. However, rotation stop, pack-off and full losses were experienced for F-14 during cement displacement. As previously mentioned, this was probably due to static cuttings in large washed out areas in Sola/Aasgard, which probably did not get mobilized during the wiper trip. Also, spiral geometry possibly contributed to the stop in rotation.

6.4 Proposed solutions

Through investigation of the drilling, liner running and cementing operations performed on Johan Sverdrup injection wells, the following proposals for improvement were obtained. Suggestions for future work are also included.

- To reduce mechanical friction during drilling, consequently mitigating the risk of irregular hole geometry and tool failure, BHA optimization is required. The following alternatives are not thoroughly discussed in this thesis but should be explored further by Equinor professionals.
 - The use of roller centralizers combined with AST (anti-stall tool) has shown to reduce buildup of mechanical friction, consequently reducing torsional and lateral vibrations [43].
 - Optimized bit will also contribute to reducing friction. An aggressive drillbit with low WOB requirements is preferred for lowering friction. Increased aggressiveness could be efficiently achieved by reducing cutter chamfer angle and cutter back rake angle of the bit [10]. Autonomous depth of cut (DOC) control is also available with TerrAdapt by Baker Hughes, providing a more consistent ROP and reducing vibrations.
 - Automated real-time mitigation of vibrations by the use of software, e.g. to identify stick-slip and subsequently alter rotation in order to cure the torsional vibrations (SoftSpeed II by NOV).
- Since Draupne 2 hot shale has proven to deteriorate between 9-18 hours, it should be considered to perform a planned wiper trip after drilling. This would be done by pulling from TD into the 13 3/8" casing and wait at least 18 hours before re-entering, thereby eliminating the need for two liner runs. This is based on the fact that the hot shale appeared stable after wiper trips on G-3 and G-2, consequently running the liner to TD effortlessly.
- Based on the potential break-out seen for F-14, a mud weight of 1.4 s.g. should be strongly considered for upcoming wells in the F-template area (ref. section 5.2.2.1)
- Utilize the real-time log to make swift decisions for alteration of flow rate and rotation when drilling heterolithic formations typically encountered in Aasgard Fm (ref. section 5.2.2.5). Act based on internal guidelines for stringer drilling found in Appendix A – Equinor's Internal Guidelines.

- Sufficient hole cleaning at TD is essential. A total of 5 B/U at TD with 4100 LPM and 150–170 RPM has proven efficient. In addition, circulation in competent formation in the overburden should be performed with similar parameters.
- Alteration of parameters in relation to improved cement bonding in the reservoir section, from E-2 to E-1 and E-3, should be carried out for future wells. This includes:
 - Lead and tail cement, where the lead cement contains more retarder. This is done so the lead cement can provide hydrostatic pressure on the tail until it is set (ref. section 3.2.3.1).
 - Pressure testing after logging.
 - Limiting DLS to below 2 °/30m when drilling Draupne.
 - More LCM in mud while drilling 12 ¼”, in addition to spotting LCM pill at TD before POOH.
 - No pressure peak against the cement after releasing liner running tool.
- Through literature study of liner hanger systems, it could be argued that an ELH system would be an optimal system for the Johan Sverdrup injectors. Generally, this system has no external mobile components in the hanger area, consequently causing less risk related to pre-setting slips, which occurred for F-14 (using conventional liner hanger). In addition, ELH systems yields a decreased pressure drop past the liner hanger assembly compared to conventional liner hangers. Since the liner is not anchored to the previous casing until after the cement job, ELH eliminates the possibility of bearing-failure during rotation, enables reciprocation during cementing. So far, only one well has employed an expandable system, namely G-2.
- Limit the DLS to a value below 3°/30m in Aasgard, in order to mitigate lateral vibrations, stick slip and severe local dogleg.

7 Conclusion

By investigating cementing, drilling and liner running operations on Johan Sverdrup injection wells, the following conclusions were established:

- There is a clear correlation between over-gauged, irregular borehole sections from the caliper logs and areas of considerable restriction when running liner.
- Action should be taken during planning to ensure a borehole quality suitable for liner running and cementing.
 - Reducing vibrations by optimizing bit and BHA composition should be a primary concern.
 - Optimization of operational procedures to ensure a decrease in unwanted borehole geometry.
- A standardization of parameters and operational procedures for the entire field is not desirable, due to local variations in formation composition in lower Cromer Knoll Gp. and upper Viking Gp.
 - Sola Fm. has proven especially problematic for the F-wells.
 - Draupne Fm. 2 has proven especially problematic for the G-wells.
- Rotation during cementing is indicated to be critical in terms of obtaining good cement behind the 9 5/8" liner.
- Successful alteration of parameters was performed in order to obtain a good cement bond in the reservoir section.

References

- [1] Equinor, "Aldous Presentation," Stavanger, 2011.
- [2] Norwegian Petroleum Directorate, "Factpages NPD," 2017. [Online]. Available: <http://factpages.npd.no/FactPages/default.aspx?nav1=field&nav2=PageView|All&nav3=26376286&culture=en>.
- [3] K. Ramstad et al, "Origin of Sulphate-Rick Formation Water and Impact on Scale Management Strategy," SPE-179895, 2016.
- [4] Equinor, "Equinor.com," 2018. [Online]. Available: <https://www.equinor.com/no/what-we-do/johan-sverdrup.html>.
- [5] B. E. Ludvigsen and H. Le, "DST Matching and Interpretation through Numerical Well Testing on the Johan Sverdrup Field," SPE-175088, 2015.
- [6] Equinor, *Equinor London Conference*, 2018.
- [7] W. Fang, "Evaluation of low salinity injection EOR potential in Johan Sverdrup Field," UiS, Stavanger, 2017.
- [8] Equinor, "Introduction to Johan Sverdrup," Equinor Petech, Stavanger, 2017.
- [9] Norsk Petroleum, "Norsk Petroleum," March 2018. [Online]. Available: <http://www.norskpetroleum.no/en/facts/remaining-reserves/>.
- [10] E. Akutsu, M. Rødsjø, J. Gjertsen, M. Andersen, N. Reimers, M. Granhøy-Lieng, Tomax, E. Strøm and K. A. Horvei, "Faster ROP in hard Chalk: Providing a New Hypothesis for Drilling Dynamics," Det norske, NOV, Halliburton, 2015.
- [11] I. K. Osmundsen, E. R. A. Brodahl, S. B. Verlo, M. Nygård, T. I. Asheim, K. E. Larsen, O. Skjæveland, P. I. Omdal and L. Omdal, "Concept Selection Report Well F-13 H," Equinor, Stavanger, 2017.
- [12] S. Neogi, "Draupne Shale summary U-1 A B," Equinor, Stavanger, 2017.
- [13] E. Andreassen, "Preliminary learnings from high angle Draupne shale drilling," Equinor, 2017.
- [14] K. Bekkeheien, "SSC Input to U-1 B Draupne Test," Equinor, Stavanger, 2018.
- [15] E. B. Nelson and D. Guillot, *Well Cementing 2nd edition*, Schlumberger, 2006.
- [16] B. Piot, "SPE - Society of Petroleum Engineers," 2009. [Online]. Available: <http://www.spe.org/dl/docs/2009/Piot.pdf>.
- [17] Equinor, "Well Cementing - GL3519," Equinor, 2016.
- [18] Baker Hughes, "SealBond Spacer System Enhanced Cement Bonding," Baker Hughes, 2013.
- [19] E. S. Keeling, "Alternative Cement Program for the Surface Casing in the Skarv Field," University of Stavanger, Stavanger, 2011.
- [20] DrillingFormulas, "Drilling Formulas," 19 May 2018. [Online]. Available: <http://www.drillingformulas.com/what-are-lead-and-tail-cement/>.
- [21] I. M. Færgestad, "The defining series: Rheology," Schlumberger.

- [22] I. Azouz, S. Shirazi, A. Pilehvari and J. Azar, "Numerical Simulation Of Laminar Flow Of Newtonian And Non-Newtonian Fluids In Conduits Of Arbitrary Cross-Section," SPE, 1992.
- [23] J. Sanchez, "The effect of drillpipe rotation on hole cleaning during directional well cleaning," SPE Journal, 1999.
- [24] S. Bittlestone and O. Hassenger, "Mud Removal: Research Improves Traditional Cementing Guidelines," Oilfield Review, 1991.
- [25] R. Speers, "Drilling Fluid Shear Stress Overshoot Behaviour," Rheologica Acta, 1987.
- [26] T. Walvekar and J. A.T., "Expandable Liner Hanger System to Improve Reliability of Conventional Liner Hanger System," SPE-99186-MS, 2006.
- [27] Khang Song et al, "Investigating the Benefits of Rotating Liner Cementing and Impact Factors," SPE-180578-MS, Halliburton & ConocoPhillips, 2016.
- [28] C. R. Hyatt and M. H. Partin Jr., "Liner Rotation and Proper Planning Improve Primary Cementing Success," Society of Petroleum Engineers - SPE-12607-MS, Texas, 1984.
- [29] M. A. Arceneaux and R. Smith, "Liner Rotation While Cementing: An Operator's Experience in South Texas," Society of Petroleum Engineers - SPE-13448-PA, Texas, 1986.
- [30] M. Savery, W. Chin and K. B. Yerubandi, "Modeling Cement Placement Using a New 3-D Flow Simulator," Halliburton, 2008.
- [31] J. Brice and B. Holmes, "Engineered Casing Cementing Programs Utilizing Turbulent Flow Techniques," Journal of Petroleum Technology, 1964.
- [32] G. C. Howard and J. Clark, "Factors to be Considered in Obtaining Proper Cementing of Casing," 1948.
- [33] F. Dupriest, W. J. Elks, O. S., P. Pastusek, J. Zook and C. Aphale, "Borehole-Quality Design and Practices To Maximize Drill-Rate Performance," Society of Petroleum Engineers (SPE), 2011.
- [34] B. Pašić, N. Gaurina-Međimurec and D. Matanović, "Wellbore Instability: Causes and Consequences," University of Zagreb, Zagreb, 2007.
- [35] B. Aadnøy, "Modern Well Design," in *Modern Well Design 2nd edition*, 2010.
- [36] M. Tingay and B. Müller, "Borehole breakout and drilling-induced fracture analysis from image logs," ResearchGate, 2008.
- [37] Z. Zheng, "Analysis of Borehole Breakouts," ResearchGate, 1989.
- [38] R. R. Hillis and S. D. Reynolds, "The Australian Stress Map," National Centre for Petroleum Geology and Geophysics, University of Adelaide, Adelaide, 2000.
- [39] L. K. Larsen, "Tools and Techniques to Minimize Shock and Vibration to the Bottom Hole Assembly," University of Stavanger, Stavanger, 2014.
- [40] J. Rajnauth and D. T. Jagai, "Reduce Torsional Vibration and Improve Drilling Operations," Society of Petroleum Engineers, 2003.
- [41] Equinor, "SoftSpeed Presentation," Equinor, Stavanger, 2017.
- [42] S. F. Sowers and F. E. Dupriest, "Use of Roller Reamers Improves Drilling Performance in Wells Limited by Bit and Bottomhole Assembly Vibrations," Society of Petroleum Engineers, Amsterdam, 2009.

- [43] G. Grindhaug and K. S. Selnes, "Hard Rock Drilling performance improvement as result of systematic approach for drill bit and BHA selection," Equinor, Stavanger, 2013.
- [44] Equinor, "Drilling Practice - GL3501," Equinor, 2017.
- [45] SPE, Cameron, Halliburton, "Drilling Fluids Design and Management for ERD - SPE 72290," SPE, Bahrain, 2001.
- [46] M. Mims and T. Krepp, "Drilling Design and Implementation For Extended Reach and Complex Wells," K&M Technology Group, LLC, Texas, 2003.
- [47] Equinor, "016 Onepager - Holecleaning," Equinor - Subsurface Support Center, Stavanger, 2018.
- [48] Oil & Gas Drilling Engineering, "Oil & Gas Drilling Engineering," 10 05 2018. [Online]. Available: <http://www.oilngasdrilling.com/liner-running-procedures.html>.
- [49] A. Stautzenberger, S. Baird and G. Lundgård, "Expandable Liner Hanger Technology Provides Metal-to-Metal Sealing and Improved Anchoring Solution for ERD Wells: Case History in North Sea," SPE - 180012, Bergen, 2016.
- [50] P. J. Gomes, M. Murray and A. Dondale, "Simulated Pressure Drop When Circulating Fluids Past Liner Hanger Equipment In An Annular Configuration: Computational Fluid Dynamics (CFD) Studies and Experimental Validation," SPE - 173106, London, 2015.
- [51] Baker Hughes, "LithoTrack Advanced LWD Porosity," Baker Hughes, 2010.
- [52] Schlumberger, "Imaging: Getting the Picture Downhole," Schlumberger, Texas, 2015.
- [53] J. Klaja and L. Dudek, "Geological Interpretation of Spectral Gamma Ray Logging in Selected Boreholes," Nafta-Gaz, Krakow, 2016.
- [54] D. P. Glover, "The Neutron Log," University of Leeds, Leeds.
- [55] D. P. Glover, "The Density Log," University of Leeds, Leeds.
- [56] O. G. Schlumberger, "Oilfield Glossary," 7 March 2018. [Online]. Available: http://www.glossary.oilfield.slb.com/Terms/w/water_alternating_gas.aspx.
- [57] "Fekete," 2018. [Online]. Available: http://www.fekete.com/SAN/TheoryAndEquations/WellTestTheoryEquations/Fracture_Closure_Pressure.htm.
- [58] Equinor, "Compilation of Rock Mechanical Works for DG3 Johan Sverdrup Phase 2," Equinor, Stavanger, 2018.
- [59] "NORSOK D-010 rev. 4," Standard Norge, 2013.
- [60] Equinor, "Concept Selection Report Well F-14," Equinor, Stavanger, 2016.
- [61] Equinor, "Concept Selection Report Well F-11," Equinor, Stavanger, 2016.
- [62] E. Andreassen, "Preliminary learnings from high angle Draupne shale drilling," Equinor, Stavanger, 2017.
- [63] Equinor, "010 Onepager - Drilling Stringers," Equinor Subsurface Support Centre, Stavanger, 2018.
- [64] C. Sauer, "Mud Displacement During Cementing State of the Art," SPE, 1987.

- [65] EPA, "United States Environmental Protection Agency," 7 March 2018. [Online]. Available: <https://www.epa.gov/uic/general-information-about-injection-wells>.
- [66] Y.-y. Zhang, Y.-w. Liu, Y.-j. Xu and J.-h. Ren, "Drilling Characteristics of Combinations of Different High Pressure Jet Nozzles," China University of Petroleum, Dongying, 2010.
- [67] E. J. S. Ferreira, "Hole Cleaning Performance Monitoring During The Drilling of Directional Wells," University of Lisbon, Lisbon, 2012.
- [68] E. Andreassen, "Draupne Shale test facts and consequences," Equinor, Stavanger, 2017.

Abbreviations

API	American Petroleum Institute
AST	Anti-Stall Tool
BHA	Bottom Hole Assembly
BHP	Bottom Hole Pressure
BPM	Barrels per Minute
B/U	Bottoms Up
CFD	Computational Fluid Dynamics
DOP	Detailed Operational Procedure
ECD	Equivalent Circulating Density
ECP	External Casing Packer
ELH	Expandable Liner Hanger
EMW	Equivalent Mud Weight
FIT	Formation Integrity Test
GR	Gamma Ray
HI	Hydrogen Index
ID	Inner Diameter
LCM	Lost Circulation Material
LOT	Leak Off Test
LPM	Liter Per Minute
mD	Millidarcy
MD	Measured Depth
MW	Mud Weight
D-N	Density–Neutron
OBM	Oil Based Mud
OD	Outer Diameter
OOZI	Out Of Zone Injection

P&A	Plug and Abandonment
PEF	Photo Electric Factor
POOH	Pull Out Of Hole
PWRI	Produced Water Re-Injection
RIH	Run In Hole
ROP	Rate of Penetration
RPM	Revolutions Per Minute
STB	Stock Tank Barrel
TD	Target Depth
TOC	Top of Cement
TVD	True Vertical Depth
WBE	Well Barrier Element
WBS	Well Barrier Schematic
XLOT	Extended Leak Off Test

Appendix A – Equinor’s Internal Guidelines

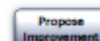
Subsurface Support Centre – OnePager

SSC ID 016

Hole cleaning during drilling operations

Associated GLs: [GL3518](#), [GL3501](#)

Revision: #3.3
Date: 23.02.2018



Purpose: Ensure sufficient hole cleaning without compromising hole quality

no	Operational Recommendations	Comments	Risk
1.	Planning <ul style="list-style-type: none"> High flow rate and high RPM to avoid ROP limitations, ref. table below for recommended parameters Prepare contingency plans for equipment failures <ul style="list-style-type: none"> If pump failure – evaluate to continue with low flow/ ROP 		
2.	Hole cleaning while drilling <ul style="list-style-type: none"> Optimize flow and RPM to clean the hole while drilling Observe for quantity and quality of cuttings on shakers (fines, cavings etc) Use consistent parameters for trend monitoring and effective unloading of cuttings Minimize connection time <p>Optimize ROP while monitoring hole cleaning:</p> <ul style="list-style-type: none"> Observe ECD/ESD/SPP trends Take up/down weights, especially when pushing ROP 	DBR: report cuttings/ cavings trends on shakers Reduced high-end rheology decreases SPP / increases available flow Formation and local DLS can impact the T/D roadmaps	
3.	Not sufficient hole cleaning <ul style="list-style-type: none"> If negative hole cleaning trend, evaluate to: <ul style="list-style-type: none"> Increase flow rate Increase RPM Reduce ROP Last resort: Clean the hole as described in point #4 	Increase low end rheology, if possible	Pack off, high ECD, lost circulation, stuck pipe
4.	Hole cleaning if trip or stop in operations <ul style="list-style-type: none"> Drill hole clean (if possible) with reduced ROP If further cleaning required: <ul style="list-style-type: none"> Circulate/rotate while pulling slowly, avoid reciprocation Rack back 1 stand pr 1.2 BU to avoid hole enlargements If long operational stop/risk of getting stuck: <ul style="list-style-type: none"> Pull into shoe If shorter operational stop in OH: <ul style="list-style-type: none"> Avoid low flow/RPM to maintain gel strength Move/rotate string regularly 	Circulate with bit in competent formations Note off bottom work on trip risk log (cuttings trap/ledges) Stage up pumps carefully when resuming operation	Not able to pass depth of off bottom work with casing/ liner Diff. stuck Sagging mud
5.	Hole cleaning at section TD <ul style="list-style-type: none"> Evaluate to reduce ROP last stand (aim for 1 BU) to drill hole clean. Maximize flow/RPM Reciprocate slowly on last stand with varying stroke length <ul style="list-style-type: none"> If weak rock close to TD, evaluate to pull above and clean hole in competent rock Amount of circulation required at TD is highly dependent on cuttings load up <ul style="list-style-type: none"> High ROP, high inclination and potential high cuttings load up: Max flow/RPM, min 3 BU Low ROP, low inclination and indications of clean hole: Max flow/RPM, min 1.2 BU 	Monitor SPP/ECD for flattening trend, zoom in. Monitor cuttings returns at shakers It takes time to remobilize cuttings into suspension if racking back	Cuttings accum. in incl. build-up zone Tight hole while tripping Unable to install casing/liner/screen Failed cement job

Recom. parameters	17 1/2"	16"	12 1/4"	9 1/2"	8 1/2"	6"
LPM*	> 4500	> 4100	> 3000	> 2100	> 1800	> 900
RPM**	> 150	> 150	> 130	> 130	> 120	> 120

Recommended flow/RPM for hole cleaning.

* Higher flow/RPM needed in long, deviated sections or high ROP.

** Low ECD fluid systems requires higher flow to keep cutting transport efficiency (low 3 rpm).

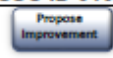
** High RPM is less critical in vertical wells or near vertical wells, typically below 30 deg inclination.

Confirm annular velocity with DP size used. Aim for annular velocity above 1 m/s, min 0.8 m/s for good hole cleaning.

Drilling stringers

Associated GLs:
[GL3501](#)

Revision: #4.4
Date: 12.02.2018



Purpose: Efficient drilling of stringers while avoiding ledges, washouts and losses

no	Main activity / Operational recommendations	Comments	Risk
1.	Planning <ul style="list-style-type: none"> Check offset data for presence of stringers Check local BHA and bit experience <ul style="list-style-type: none"> performance vs. ability to drill stringers Optimize BHA stabilisation, avoid sharp stab-edges and ensure sufficient waterways 	Evaluate to include an anti-vibration tool (e.g. AST)	
2.	Enter/confirm stringer <ul style="list-style-type: none"> Increase WOB to confirm stringer (loss of progress / flat torque) <ul style="list-style-type: none"> reduce RPM (60 - 100) to achieve torque response if low angle of attack (<15°), drill ~0,5 m to avoid deflection prior to adding more weight Reduce flow rate by 20 – 40% to avoid: <ul style="list-style-type: none"> washouts, pump off effects, losses when breaking through 	If UR, repeat steps when UR hits stringer If using auto-driller, avoid aggressive WOB increments	Misinterpreting whirl as hard stringer Deflection -use local experience
3.	Drilling stringer <ul style="list-style-type: none"> Further increase WOB to max in efficient steps Expect stick-slip (torsional oscillations) Adjust parameters to chase progress <ul style="list-style-type: none"> PU string and restart if needed Avoid severe lateral vibrations. If unacceptable: PU string and zero RPM prior to restart drilling Use DHWOB/DHTQ to monitor weight/torque transfer 	If prone to loss, evaluate to set lower max WOB Long intervals with low RPM/ flow can impact hole cleaning	Washout in weak rock above Loss of progress Tool failure Hanging on stabs
4.	Exit stringer <ul style="list-style-type: none"> Monitor for typical "exit torque" response (breaking through) Immediately reduce WOB to avoid: <ul style="list-style-type: none"> high sudden ROP high local doglegs Monitor for deflections, NB INC, bending moment 	Confirm stringers on GR, Res, Density log Unacceptable high local DLS/high bending moment may require reaming	Surge/pack off/losses High local DLS. High total friction. Not able to run casing / liner / screens to TD

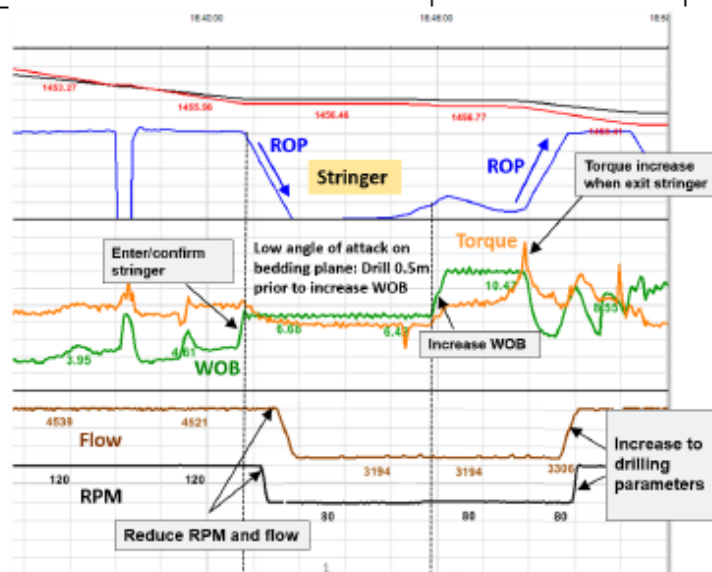


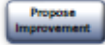
Figure 1, Example of stringer drilling






Drilling weak rock – RIO principles

Associated GLs:
[GL3501](#)

Revision: #1.1
Date: 25.08.2017



Purpose: Efficient drilling of weak rock using RIO (Reduced Impact Operations) principles

no	Main activity / Operational recommendation	Comments	Risk
1.	<p>RIO principles - Speed is your friend</p> <ul style="list-style-type: none"> Reduce mechanical / hydraulic impact <u>and time</u> spent with BHA in weak rock interval 	<p>RIO reduces risk and improves performance in weak rock</p>	
2.	<p>Planning</p> <ul style="list-style-type: none"> Identify potential weak rock Optimise well path. Tangent if possible Maximise angle of attack in weak rock/bedding planes based on field experience Split DOP in steps based on risk and performance. Identify parameters and actions for drilling and tripping for each interval <ul style="list-style-type: none"> Include contingency for unplanned stops Use "Universal connection procedure" (1P) Bit/BHA optimisation <ul style="list-style-type: none"> Simplify BHA and maximise waterways to avoid pack offs and ECD spikes Plan number, shape and size of stabs Avoid aggressive side-cutting bits Avoid/minimise formation pressure points with BHA in weak rock. Evaluate to perform while POOH 	<p>If high risk of losses- See "Lost circulation" (1P)</p> <p>Avoid use of under-reamer (UR) if possible</p> <p>Involve the directional driller and plan how to avoid high local doglegs</p> <p>If experience of BHA dropping inclination in weak rock, plan well path accordingly</p>	<p>Poor hole geometry / quality</p> <p>Bit / BHA not optimised for weak rock</p>
3.	<p>Drilling weak rock</p> <ul style="list-style-type: none"> Reduce RPM (use 120-140) Reduce flow rate, but not below minimum hole cleaning rate Efficient drilling while monitoring returns on shakers <ul style="list-style-type: none"> Avoid drilling with high ROP over long distance with reduced flow Avoid "zero" WOB Gradually increase WOB if needed Maintain consistent parameters for trending <ul style="list-style-type: none"> Change one parameter at a time for early risk detection Ensure progress in stringers, use "Drilling stringers" (1P) <ul style="list-style-type: none"> Avoid washing out weak rock above Avoid high lateral vibrations Increase parameters when BHA through weak zone <p>Minimise and optimise off bottom work in weak rock</p> <ul style="list-style-type: none"> Avoid reciprocation. Pull and rack back if needed Use trip risk log to place BHA in competent rock Know position of BHA components vs weak rock Evaluate lubrication through weak rock intervals when POOH/RIH <p>Hole cleaning at section TD & POOH</p> <ul style="list-style-type: none"> Use "Hole cleaning" (1P) – Ensure good hole cleaning parameters are used at TD Use "POOH" (1P) 	<p>Note: In 17 1/2" hole, 120 rpm may not clean the hole. Use reduced RPM for shorter intervals</p> <p>Monitor cuttings return and hole cleaning parameters and adjust flow rate/RPM/ROP if necessary</p> <p>Typical WOB for 8 1/2" hole in weak rock 2-8 ton. Do not use Auto-driller with high/aggressive WOB settings</p> <p>A weak zone could potentially be a loss zone. If prone to loss, adjust ROP to clean the hole prior to drilling through loss zone (Reduced ECD)</p>	<p>Long time spent with BHA in weak rock</p> <p>Hole enlargement / poor wellbore geometry</p> <p>Pack off and losses</p> <p>Stuck pipe</p>
			



Run casing/liner

Associated GLs:
[GL3501](#)

Revision: 4.2
Date: 12.02.2018

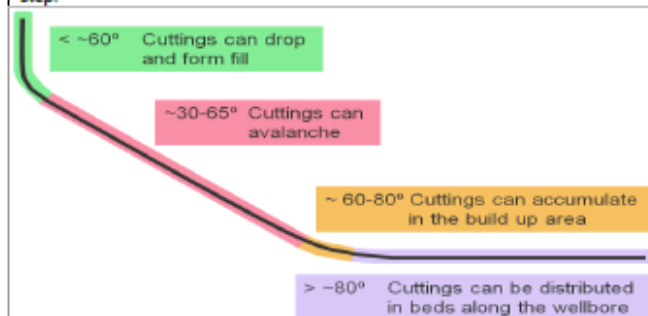


Purpose: Run casing/liner to TD handling possible restrictions to achieve an optimum cement job

	Main Activity / Operational recommendations	Comments	Risk								
1	<p>Strategy</p> <ul style="list-style-type: none"> Include mitigating actions in DOP Update trip risk log and highlight specific risk areas*. Prepare roadmap Typical max down weights prior to taking action: <table border="1"> <tr> <td>17 1/2"</td> <td>12 1/4"</td> <td>8 1/2"</td> <td>6"</td> </tr> <tr> <td>15-20 t</td> <td>10-15 t</td> <td>8-12 t</td> <td>6-10 t</td> </tr> </table> <ul style="list-style-type: none"> Consider lubricate through risk areas* to avoid compacting debris Limit down weight in known weak rock areas (paleosols/coal) 	17 1/2"	12 1/4"	8 1/2"	6"	15-20 t	10-15 t	8-12 t	6-10 t	<p>* Specific risk areas: washouts, paleosols, coals, off bottom work intervals, high doglegs, stringer areas, build up section</p>	<p>Running into cuttings accumulations</p> <p>Evaluate to condition mud in previous shoe if high risk of losses</p>
17 1/2"	12 1/4"	8 1/2"	6"								
15-20 t	10-15 t	8-12 t	6-10 t								
2	<p>RIH</p> <ul style="list-style-type: none"> Focus on weight response <ul style="list-style-type: none"> Use trip risk log, road map and start up friction trend Taking weight and/or deviating road map trend: <ul style="list-style-type: none"> Gradual weight: indicates debris <ul style="list-style-type: none"> Avoid compacting possible debris, limit down weight Sudden weight: indicates a ledge If unsure: lubricate through area (ref. table), rotate if possible <ul style="list-style-type: none"> Erratic pressure indicates debris 	<p>Sudden weight could also be caused by debris</p> <p>Lubrication: monitoring downhole conditions (SPP, torque)</p>	<p>Increased start-up friction w/ increased stationary time - indication of sticky environment</p> <p>Washing down longer length with low flow - risk of pack off/ losses</p>								
3	<p>Debris confirmed</p> <ul style="list-style-type: none"> Pull 10-30m above first point taking weight Establish accept. hole cleaning rate in steps (1), ref. table. Rotate if possible Wash down with hole cleaning rate dictated by stable pump pressure <ul style="list-style-type: none"> Reduce speed to avoid sudden cuttings mobilization/loss <p>Ledge confirmed</p> <ul style="list-style-type: none"> Pull above ledge RIH while evaluating weight response Pull up and orient casing or start rotating liner if no progress <ul style="list-style-type: none"> Evaluate to lubricate to avoid compacting potential debris around ledge If not able to pass, max weight/speed might be needed <p>Continue to RIH with no flow when acceptable down weight</p>	<p>Do not exceed MU torque if working string to achieve rotation</p>	<p>Pack off / lost circulation if starting circulation inside debris area. Pull above</p> <p>Pack off due to washing down with too high running speed</p> <p>Rig heave causing high surge and losses</p>								
4	<p>If taking weight in weak rock areas- or known problem area (paleosols/coal/fractured zones)</p> <ul style="list-style-type: none"> Establish lubrication parameters and 20-30 RPM above weak rock area Lubricate through interval with reduced/low running speed. Be patient If increasing torque and/or pack off tendency, pick up string slightly to regain stable torque/SPP prior to continuing with further reduction in speed <ul style="list-style-type: none"> Evaluate to increase RPM to 40 	<p>Use electronic pop off ramping down flow, if available</p> <p>1-2 m progress/hrs is not unusual in challenging paleosols</p>	<p>Pack off and losses because of too high running speed</p>								
5	<p>~30 m above TD</p> <p>Establish hole cleaning rate (ref. table) stepwise (1) to string out potential fill near TD</p> <ul style="list-style-type: none"> Wash down carefully dictated by stable pump pressure Reduce flow to lubrication flow 2-5 m prior to land/tag TD Casing at TD: Stepwise (1) increase flow to cement displacement rate /loss free rate while conditioning mud for cement job, min 1 x BU Liner at TD: ref one pager "Liner at TD" 	<p>Low risk of fill: evaluate to run closer to TD (dry WH, no circ. device, low inclination)</p>	<p>Lost circ. at TD due to:</p> <ul style="list-style-type: none"> Rig heave Static/Cold mud Pack off due to reduced flow area when hanger/ RT in BOP / WH 								

(1) Stepwise flow increase:

Increase flow in steps of 200 LPM, while monitoring SPP/ECD. Maintain rate until stable / slowly decreasing SPP trend. When approaching hole cleaning rate, increase flow in steps of ± 50 LPM. Erratic pressure indicates mobilisation of cuttings/debris. Let cuttings string out / pressure level out prior to next step.

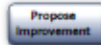


Csg/Hole size	Acceptable hole cleaning flow rate	Typical lubrication flow rates
13 3/8" Csg / 17 1/2" OH	2100 lpm (Same annular velocity as drilling w/ 4500 lpm, 5 1/2" DP)	400-500 lpm
9 5/8" Csg / 12 1/4" OH	1400 lpm	300-400 lpm
7" liner / 8 1/2" OH	600 lpm	200-300 lpm
4 1/2" liner / 6" OH	400 lpm	100-200 lpm

Liner at TD

Associated GLs:
[GL3501](#), [GL 3519](#)

Revision: #5.1
Date: 12.02.2018



Purpose: Avoid losses and optimise for a good cement job

	Main activity / Operational recommendation	Comments	Risk
1.	Circulate at TD <ul style="list-style-type: none"> Minimum 2 x OH with planned cement displacement rate <ul style="list-style-type: none"> If losses, reduce flow to loss free rate immediately 	Start stroke counter when reaching planned rate	Hole not properly cleaned Pack-off in hanger area. Be prepared to cut pumps
2.	Start rotation of liner <ul style="list-style-type: none"> Cut back flow to 200 LPM prior to start rotating to reduce pack-off probability Establish rotation: 20-30 RPM Reciprocate with torque in string if problems achieving rotation <ul style="list-style-type: none"> Do not exceed MU torque when working string 	Be aware of torque limitations in string	Twist-off / over torqued connections due to working too high torque into string
3.	Circulate and condition mud <ul style="list-style-type: none"> Stepwise increase flow (1) to planned cement displacement rate, 20-30 RPM <ul style="list-style-type: none"> Wait for stable SPP/active volume before staging pumps to next step, be patient Reduce flow if increasing SPP (ref. figure), evaluate to reciprocate Circulate min 1xBU in total, ensure mud in spec for cement job 	If losses observed, reduce flow to loss free rate Cut pumps immediately if pack-off occurs	Pack-off in hanger area Losses Possible gas at BU
4.	Set liner hanger <ul style="list-style-type: none"> Stop rotation and flow Set liner hanger 	Expandable liner hanger is set after the cement job	Debris falling down in hanger area if not sufficiently clean
5.	Regain rotation and flow <ul style="list-style-type: none"> 20-30 RPM Stepwise (1) increase flow to cement displacement rate / loss free rate while preparing for cement job 	Be aware that the SPP could increase after setting hanger	Pack-off in hanger area when establishing rate Not achieving rotation Losses

(1) Stepwise flow increase:

Increase flow in steps of 200 LPM, while monitoring SPP/ECD. Maintain rate until stable or slowly decreasing SPP trend. When approaching hole cleaning rate, increase flow in steps of ±50 LPM. Erratic pump pressure indicates mobilisation of cuttings/debris. Let cuttings string out / pressure level out prior to next step.

